ELSEVIER

Earth-Science Reviews 52 (2000) 1–81

EARTH-SCIENCE REVIEWS

www.elsevier.com/locate/earscirev

Dolomite: occurrence, evolution and economically important associations

John Warren

Department Petroleum Geosciences, University Brunei Darussalam, Tungku Link, Bandar Seri Begawan, Brunei

Received 14 October 1999; accepted 7 July 2000

Abstract

Dolomite is not a simple mineral; it can form as a primary precipitate, a diagenetic replacement, or as a hydrothermal/metamorphic phase, all that it requires is permeability, a mechanism that facilitates fluid flow, and a sufficient supply of magnesium. Dolomite can form in lakes, on or beneath the shallow seafloor, in zones of brine reflux, and in early to late burial settings. It may form from seawater, from continental waters, from the mixing of basinal brines, the mixing of hypersaline brine with seawater, or the mixing of seawater with meteoric water, or via the cooling of basinal brines. Bacterial metabolism may aid the process of precipitation in settings where sulfate-reducing species flourish and microbial action may control primary precipitation in some hypersaline anoxic lake settings.

Dolomite is a metastable mineral, early formed crystals can be replaced by later more stable phases with such replacements repeated a number of times during burial and metamorphism. Each new phase is formed by the partial or complete dissolution of an earlier dolomite. This continual re-equilibration during burial detracts from the ability of trace elements to indicate depositional conditions and resets the oxygen isotope signature of the dolomite at progressively higher temperatures.

Because subsurface dolomite evolves via dissolution and reprecipitation, a bed of dolomite can retain or create porosity and permeability to much greater burial depths and into higher temperature realms than a limestone counterpart. Dolomitization also creates new crystals, with new rhomb growth following the dissolution of less stable precursors. Repetition of this process, without complete pore cementation, can generate intercrystalline porosity a number of times in the rock's burial history. Intercrystalline porosity is a highly interconnected style of porosity that gives dolomite reservoirs their good fluid storage capacity and efficient drainage. The fact that many dolomite reservoirs formed via brine reflux means that they sit beneath an evaporite seal in both platform and basinwide evaporite settings. The same association of evaporites (sulfate source) and entrained hydrocarbons means that burial conditions are also suitable for thermochemical sulfate reduction and the precipitation of base metals. This tends to occur at higher temperatures ($>60°C$–$80°C$) and so the resulting dolomites tend to be ferroan and consist of saddle-shaped crystals. © 2000 Elsevier Science B.V. All rights reserved.

Keywords: dolomite; brine; models; porosity; permeability; oil and gas; base metal

E-mail address: jwarren@brunet.bn (J. Warren).

0012-8252/00/$ - see front matter © 2000 Elsevier Science B.V. All rights reserved.
PII: S0012-8252(00)00022-2

1. The dolomite problem — an introduction

What is dolomite? For more than 150 years geologists have addressed this question using both field and laboratory based approaches (Von Morlot, 1847; Skeats, 1905; Van Tuyl, 1918; Steidtmann, 1926; Hewett, 1928; Young, 1933; Riviere, 1939; Landes, 1946; Behre, 1947; Chave, 1952; Graf and Goldsmith, 1956; Fairbridge, 1957; Strakhov, 1958; Medlin, 1959; Baron, 1960; Wells, 1962; Alderman and von der Borch, 1963; Friedman and Sanders, 1967; and the other numerous papers discussed in this review).

About 80% of the oil and gas reservoirs in North American carbonate rocks are in dolomites and up to 50% of the world's carbonate reservoirs are dolomites (Zenger et al., 1980). Most Mississippi Valley-type (MVT) deposits, with their economic accumulations of Pb and Zn, are hosted in dolomite, as are many skarn ore bodies (Warren, 1999). The imperatives for understanding dolomite in its various forms are obvious; why then, is its origin so poorly understood?

Dolomite is an unusual carbonate mineral. It is common in ancient platform carbonates, yet it is rare in Holocene sediments and, without bacterial mediation, is near impossible to precipitate in the laboratory at earth surface temperatures. Some argue that widespread dolomite forms mostly in association with hypersaline brines, others that it can form from schizohaline waters, or that the time required to form large volumes of dolomite means that the process must be predominantly subsurface and perhaps tied to the long-term circulation of seawater through platform sediments (Land, 1985; Hardie, 1987).

Dolomitizing solutions include marine brines (Behrens and Land, 1972; Mackenzie, 1981), continental brines (Clayton et al., 1968; Von der Borch et al., 1975), essentially normal seawater (Saller, 1984; Carballo et al., 1987; Mazzullo et al., 1995), seawater modified by extensive sulfate reduction (Baker and Kastner, 1981; Kelts and Mackenzie, 1982), seawater mixed with meteoric water (Land, 1973; Magaritz et al., 1980; Cander, 1994), and seawater mixed with hypersaline brines (Meyers et al., 1997).

Most modern dolomite occurrences are penecontemporaneous, patchy and micritic. Holocene dolomites comprises units that, at most, are a meter or so thick, dolomite (the mineral) makes up less than 50% of the unit's mineralogy and forms in patches across areas that are no more than tens of kilometers wide. In contrast, most ancient dolomite entrains dolomite (the mineral) that makes up more than 90% of the rock volume, is secondary, extensive and often sparry. It has overprinted whole limestone platforms as diagenetic units that are typically some hundreds of meters thick and extend across areas that may be hundreds of kilometers wide. Possible reasons for the disparity between modern and ancient modes of occurrence are many, and related to dolomite's unique mineralogy and chemistry. The most important control on distribution is possibly kinetics; there has not been enough time in the Holocene to form extensive areas of secondary dolomite (Land 1985, 1998; Chai et al., 1995).

Then there is the problem of parity, do variations in seawater chemistry influence dolomite volumes in carbonate platforms, or are changes in the volume of dolomite influencing seawater chemistry? Some would argue that seawater chemistry has changed from the Archean till now (especially the proportions of Mg/Ca and pCO_2). Were times of widespread platform growth also times of widespread dolomitization (Given and Wilkinson, 1987)? Spencer and Hardie (1990) and Hardie (1996) have argued that the level of Mg in the oceans has been relatively constant, but changes in the rate of seafloor spreading have changed the levels of Ca in seawater and so influenced the dominant mineralogies of marine carbonate and evaporite precipitates. In contrast, Holland et al. (1996) proposed that the preponderance of $MgSO_4$-depleted evaporites in the Cretaceous might reflect a substantial episode of dolomitization and carbonate platform growth. In this case, the formation of dolomite changed seawater chemistry, the opposite of the argument of Hardie (1996). Using micro-inclusion studies of halites of varying ages Zimmermann (2000) has concluded that the evolving chemistry of the Phanerozoic ocean is more indicative of changing volumes of dolomite that it is of changes in the rates of seafloor spreading. In contrast, Burns et al. (2000) argue that the relative level of Mg/Ca and pCO_2 in the dolomite precipitating fluid is far less important in precipitating the varying volumes of dolomite than the levels of oceanic oxygen, which controlled the intensity of anaerobic bacterial metabolism.

And so we can simply state of the dolomite problem. At the current state of our understanding we simply do not know: (1) why there is so little modern dolomite, (2) why there is so much ancient dolomite, and (3) how the chemistry of ancient dolomite forming settings has evolved over time. In other words, we do not know the relative importance of kinetics versus parity in dolomite precipitation, and we do not yet have a good understanding of how the volume of dolomite precipitation has varied through time. Is it controlled by seawater chemistry or does it control seawater chemistry, and what is the effect of bacterial mediation?

2. Dolomite the mineral

The original mineral name *dolomie* was given by N.T. Saussare, in 1792, in honor of the French geologist Deodat Guy de Dolomieu (1750–1801) and was first applied to rocks in the Tyrolean Alps (Bourrouilh-Le Jan, 2000). Dolomite, the rock, contains a large proportion of dolomite the mineral. Ideal dolomite has a crystal lattice consisting of alternating layers of Ca and Mg, separated by layers of CO_3 and is typically represented by a stoichiometric chemical composition of $CaMg(CO_3)_2$ where calcium and magnesium are present in equal proportions (Fig. 1A).

2.1. Equilibrium and kinetics in dolomite precipitation

Seawater is the only abundant source of Mg^{2+} capable of forming large and widespread volumes of sedimentary dolomite, at or near the earth's surface (Land, 1980, 1985). It contains 1290 ppm Mg (0.052 mol l^{-1}), and 411 ppm Ca (0.01 mol l^{-1}) giving a Mg/Ca ratio of 3.14 by weight or a molar ratio of 5.2. Meteoric water entrains lower and more variable concentrations of both Mg and Ca; a typical river water has a Mg/Ca molar ratio of 0.44 (4 ppm Mg

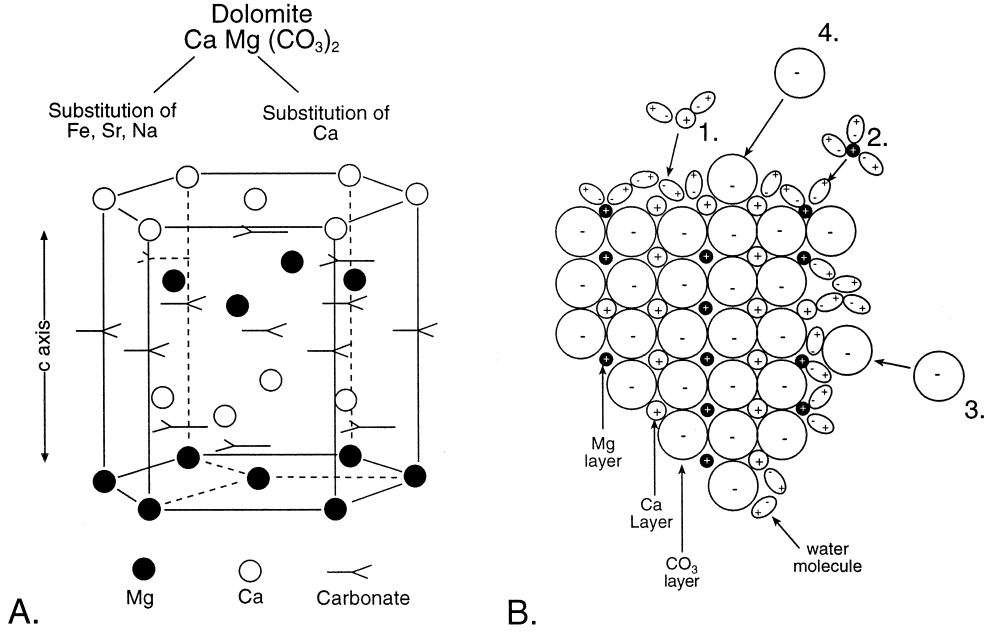

Fig. 1. Dolomite lattice. (A) Ideal structure of stoichiometric dolomite consisting of layers of carbonate separated by alternating layers of calcium and magnesium ions (after Land, 1985; Warren, 1989). (B) Schematic of non-ideal lattice structure showing how water molecules are preferentially bonded to cations on the surface of the growing crystallite. Because Ca ions are not as strongly hydrated as the Mg ions they tend to be incorporated in the magnesium layer creating a typical calcian dolomite. Carbonate ions are unhydrated but must have sufficient energy to displace water molecules adjacent to the cation layer (after Lippman, 1973).

and 15 ppm Ca). Depending on the degree of water–rock interaction, typical subsurface or formation waters also show a wide range in Mg and Ca concentrations, as well as in total ionic strength. The Mg/Ca ratios of these are typically lower than that of seawater, usually in the range 0.04 to 1.8 (Folk and Land, 1975).

Precipitating primary dolomite from any of these waters requires the following reaction:

$$Ca^{2+} + Mg^{2+} + 2\left(CO_3^{2-}\right) = CaMg(CO_3)_2$$

This gives an equilibrium constant K defined by:

$$K = \left(\left[Ca^{2+}\right]\left[Mg^{2+}\right]\left[CO_3^{2-}\right]_2\right)/\left[CaMg(CO_3)_2\right]$$

where the parentheses $[x]$ indicate activities of the dissolved and solid species. Because of the difficulties in synthesizing dolomite at low temperatures in the lab, the value of K is not known with any precision. Arguing from several lines of evidence, Hsu (1967) estimated $K \approx 10^{-17}$, while, based on modern metastable dolomites, Hardie (1987) estimated it to be $\approx 10^{-16.5}$. Knowing the approximate activities of Ca^{2+}, Mg^{2+} and CO_3 in seawater gives an ion activity product of the order of $10^{-15.01}$. It would appear that modern seawater is supersaturated by one to two orders of magnitude with respect to dolomite, yet dolomite is a rare precipitate. This underlines the likelihood that reaction kinetics are a major control in the formation of dolomite from modern seawater.

A similar argument can be made for dolomitization of a limestone by modern seawater (Hsu, 1967) where the reaction is:

$$2CaCO_3 + Mg^{2+} = CaMg(CO_3)_2 + Ca^{2+}$$

Taking the activity of the solid phases as unity reduces the equilibrium constant to:

$$K = \left[Mg^{2+}\right]/\left[Ca^{2+}\right] = 0.67$$

The reaction should go to the right when the $[Mg^{2+}]/[Ca^{2+}]$ ratio is greater than 0.67. As modern seawater has a Mg/Ca molar value of around 5.2, it should not only precipitate dolomite but should also be capable of dolomitizing limestones. Again, the reasons for this not happening over much of the modern seafloor are probably in large part kinetic.

Lippmann (1973, 1982) showed that supersaturation in seawater with respect to dolomite can persist for long periods without dolomite being precipitated. He argued that this reflects the relative strength of the electrostatic bond of the magnesium ion for water (some 20% greater than that for Ca and much greater than for CO_3). Thus, although there is a theoretical saturation in seawater, in practice the carbonate ions cannot overcome the hydration shell to bond with the Mg^+ (Fig. 1B). With magnesium effectively excluded from further reaction, the main carbonate precipitate from modern seawater is aragonite. The higher Mg concentrations of hypersaline waters means that the hydration barrier is more easily overcome, but it is still difficult for calcium and magnesium to segregate into the monolayers necessary to precipitate ideal or stoichiometric dolomite. Lippmann (1973) argues that this is why highly disordered calcian-dolomite is the dominant form in most Holocene hypersaline settings. In order to overcome the kinetic barrier, seawater may need to be concentrated, heated, cooled, diluted, have its levels of sulfate lowered, or its levels of activated CO_3^{2-} increased (see models). After running an experiment for 32 years that unsuccessfully attempted to precipitate dolomite at 25°C, Land (1998) came to the same conclusion, "...we all (?) now agree that 'The Dolomite Problem' is one of kinetics."

2.2. Composition and lattice evolution

Dolomite comprises a group of minerals with similar but not identical Mg/Ca ratios, and with differing ideal chemical and lattice compositions. When used to describe a mineral, the term dolomite indicates a compositional series in much the same way that feldspar does (Land, 1985). Just as there are many kinds of feldspar, so dolomite exhibits variation not only in chemical composition but also in subtle atomic arrangements (Reeder, 1981; Hardie, 1987). Very few, if any, sedimentary dolomites are truly stoichiometric $[CaMg(CO_3)_2]$ and are better represented as: $Ca_{(1+x)}Mg_{(1-x)}(CO_3)_2$. Documented compositions range from $Ca_{1.16}Mg_{0.94}(CO_3)_2$ to $Ca_{0.96}Mg_{1.04}(CO_3)_2$, encompassing the spectrum from calcian to magnesian dolomites. Most ancient dolomites are calcian-rich; they formed slowly and, once formed, are less soluble than their undolomitized limestone equivalents.

Holocene dolomite precipitates or crystallizes as a metastable phase, but is a true dolomite in that it possesses at least partial ordering of the lattice structure. It differs from older sedimentary dolomites in that much higher densities of defects, and greater variations in the degree of ordering and/or calcium enrichment, characterize the lattice across domains tens to hundreds of angstroms wide. Transmission electron microscopy (TEM) shows that ancient post-Paleozoic sedimentary dolomites tend to have much more regular lamellar or modulated structures than Holocene dolomite. They typically possess a pervasive modulated microstructure (wavelengths ≈ 200 Å) that is generally parallel to {1014} (Reeder and Sheppard, 1982; Wenk et al. 1983; Mitchell et al. 1987; Miser et al. 1987). This modulated structure, like the disordered structure of Holocene dolomite, is metastable.

There is no reliable information as to the thermodynamic and kinetic properties of Ca-dolomites with modulated structure, so their persistence in the diagenetic realm is poorly understood. Even "nearly stoichiometric" ancient Paleozoic dolomite still contains numerous defects, mostly fault-like phenomena. Although defect density is typically less than that of other types of sedimentary dolomite and its crystals are better ordered, it is still less stable than structurally and compositionally ideal dolomite. The latter is only commonplace as widespread stratiform units in metamorphic carbonates and skarns (Land, 1985).

Reeder (1981, 1983) interpreted the modulated microstructure of sedimentary dolomite in terms of compositional variations characterized by the incorporation of excess calcium in the B sites (which should be occupied by Mg) in the dolomite structure. Wenk et al. (1983) hypothesized that the modulations are introduced during crystal growth and possibly indicate stabilization through dissolution–reprecipitation. Reeder and Prosky (1986) and Miser et al. (1987) showed that modulated microstructures reflect growth defects and do not necessarily require replacement.

Thus, the term dolomite describes a mineral series that encompasses a range of chemical variation and lattice structures. It encapsulates an array of natural Ca–Mg carbonates with chemical compositions close to ideal dolomite, but with weak or diffuse X-ray reflections that indicate varying degrees of cation disorder (Hardie, 1987). There is not one single dolomite mineral, but many, each with different thermochemical properties depending on the degree of lattice ordering and nonstoichiometry. The free energy differences due to order–disorder are sizeable: there may be more than 1.3 kcal/mol difference in ΔG_f (25°C, 1 atm) between "ordered" and "disordered" dolomite. This is equivalent to a range of one and a half orders of magnitude in solubility constants for the two forms of dolomite. Completely disordered phases (sometimes termed protodolomites) are the most soluble and least stable phases in the dolomite spectrum; they are also the easiest to precipitate at earth-surface temperatures. Variations in free energy and solubility also mean that surface-formed dolomite has a built-in potential to recrystallize over time as it reorganizes structurally and compositionally to more stable forms (Land, 1980, 1985; Hardie, 1987). Thus, because all nonstoichiometric dolomite is metastable, there must be a burial trend towards stoichiometry, so resetting isotopic values and trace element levels during recrystallization (Morse and Mackenzie, 1990).

Many workers now agree that sedimentary dolomite ripens or ages as it follows a chemical paradigm known as the Ostwald step rule or Ostwald ripening, first stated some 100 years ago (Gregg et al., 1992; Nordeng and Sibley, 1994). Ostwald's rule states that the transformation of an unstable to a stable mineral phase (at earth surface conditions) requires one or more intermediate phases. The process is driven by the surface energy of the various crystals and typically describes a recrystallization process whereby large crystals typically grow at the expense of smaller ones (Morse and Casey, 1988). In any supersaturated solution undergoing crystallization, crystallites are continuously forming. Those particles that attain critical radii become critical nuclei and continue to grow. Those with radii less than the critical radii dissolve back into the solution. The size of the critical radius is controlled by the activation energy for nucleation, which is a function of the degree of supersaturation and the free surface energy of the nuclei. Ostwald ripening begins near the end of the initial nucleation and growth process (Gregg and Sibley, 1992). Near equilibrium, the critical radius increases as the degree of supersaturation decreases. Crystals with radii less than critical dis-

solve as the solute reprecipitates on the surface of crystals with radii larger than critical. During this process there is no gain or loss of volume, but the number of individual crystals per unit volume decreases until the system reaches theoretical equilibrium with all crystals of the same size.

Ostwald ripening has been shown to operate during dolomite formation by Sibley et al. (1994) who found in laboratory-based high temperature experiments that the rate of dolomitization increases with temperature, reactant surface area, reactant solubility, ionic strength (salinity) and the Mg/Ca ratio of the solution. In a related paper, Nordeng and Sibley (1994) developed the kinetic theory that relates the Ostwald step rule to dolomite stoichiometry. They show that the surface free energy of high magnesian calcite is less than that of more stoichiometric dolomite (see below) and so the calcite to dolomite transformations observed in the laboratory are consistent with surface free energy controlled nucleation kinetics whereby $CaCO_3$ is replaced by dolomite or very high Mg calcite.

Sibley et al. (1994) showed that dolomite precipitated in the laboratory at elevated temperatures (150°C–300°C) is the result of a three-step reaction beginning with the precipitation of a very high-Mg calcite crystallites followed by its rapid replacement. The stages are the following (Fig. 2):

(1) Nucleation: Nucleation of very high-Mg calcite (35–40 mol% $MgCO_3$-VHMC) or nonstoichiometric dolomite, followed by nucleation of more stoichiometric dolomite on the $CaCO_3$ substrate.

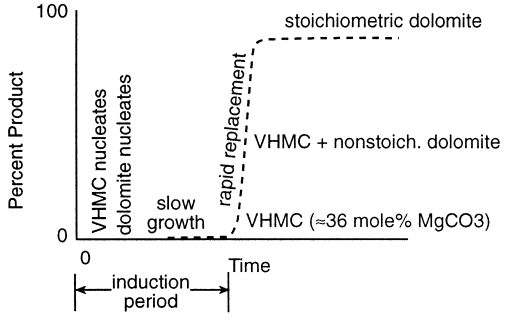

Fig. 2. Three-stage sigmoidal reaction curve for dolomitization of $CaCO_3$, based on hydrothermal bomb experiments (after Sibley et al., 1994). Precipitation of dolomite occurs via Ostwald ripening.

During nucleation, the composition of the VHMC or nonstoichiometric dolomite is a function of Mg/Ca of the solution. Other variables, such as dissolved Fe, can affect the composition of the nuclei.

(2) Induction period: Nucleation continues during induction but most of this period is taken up by the post-nucleation growth of VHMC, nonstoichiometric and stoichiometric dolomite. Changes in the composition of the solution and substrate surface area affect the duration of the period.

(3) Replacement period: (a) $CaCO_3$ is replaced by VHMC or nonstoichiometric dolomite. VHMC nucleates faster than stoichiometric dolomite and therefore begins to replace the substrate first. (b) $CaCO_3$ and VHMC and/or nonstoichiometric dolomite are rapidly replaced by stoichiometric dolomite. This phase of the reaction is sensitive to solution variables such as Mg/Ca and ionic strength.

This three-phase model is consistent the Ostwald ripening and with many characteristics of natural dolomites, including: (1) the fact that very Ca-rich dolomite is common only in modern dolomites; (2) there is a direct relationship between the Mg/Ca in solution and the Mg/Ca ratio in the dolomite; (3) the stoichiometry of dolomites in some ancient rocks is directly related to the percentage of dolomite in the rock; (4) the suppression of stoichiometric dolomite nucleation allows the persistence of metastable $Ca–Mg–CO_3$ phases; (5) dolomite–limestone contacts are often sharp; (6) dolomite selectively replaces fine-grained $CaCO_3$; (7) dolomite crystals often have cloudy centers and clear rims; (8) dolomite textures are mainly determined by the crystal size of the substrate (Sibley et al., 1994). Other key laboratory observations of Sibley et al. (1994), suggesting that the presence of SO_4 may slow the rate of dolomitization, that lithium may increases the rate, and that the induction period required for dolomitization is long, were not predicted from kinetic theory.

In summary, laboratory work in the last two decades, since the publication of Land (1980), has clearly shown that sedimentary dolomites are metastable. Older examples, and those associated with evaporites, tend to be better ordered and "more stoichiometric" than more recent examples. Dolomite follows a ripening or aging paradigm first outlined in the Ostwald step rule more than 100 years ago;

dolomite crystals are modified extensively during diagenesis as earlier phases are replaced by less-soluble phases, in a "stepwise" or interactive fashion. The intermediate stages are more disordered than the ultimate product, a pure stoichiometric dolomite mineral in equilibrium with its pore fluids. Most Phanerozoic sedimentary dolomites have not attained this ideal stoichiometric chemistry. We must conclude that the chemistry of dolomitization is an iterative dissolution–reprecipitation process, as long as sedimentary dolomite retains some degree of permeability, and there is a supply of Mg ions, new dolomitization can occur. On a larger scale, metastable phases can dissolve in one area and reprecipitate in another, locally causing porosity enhancement or porosity occlusion.

This understanding that dolomite ripens with the passage of time adds another level of complication to the dolomite problem. It means that geochemical data (trace element and isotopic) are likely to be reset numerous times during diagenetic evolution (Land, 1980). When we look at such data, we are looking at evidence of the passage of dolomitizing fluids with chemistries that are likely to be dominated by later "resetting" events.

3. Dolomite the rock

Ancient carbonate rocks are mostly composed of two minerals; calcite or dolomite, with any noncarbonate phases usually dominated by terrigenous components or evaporites (Fig. 3A). When a carbonate is dominated by calcite, it is called limestone, when it is dominated by dolomite (the mineral), it is called dolomite (the rock). In North America, the term dolostone is sometimes used to describe such a rock. Carbonate rocks tend to be composed either mostly of calcite or mostly of dolomite (Fig. 3B; Blatt, 1992). Whatever the conditions that favor dolomite or limestone formation the tendency is to form either one or the other end member, subequal mixtures of calcite and dolomite in a carbonate rock are unusual.

In a refinement of this analysis and using other unpublished work as well as their own data, Sperber et al. (1984) found a bimodal distribution in the percentage of dolomite in carbonate rocks (Fig. 4A), with modes at 97% (dolomite/dolostone) and at 20% (dolomitic limestones). Sperber et al. (1984) went on to suggest that dolomitic limestones, which tend to contain rhombs of calcian dolomite (hatchured histogram in Fig. 4A), originate in relatively closed diagenetic systems whereby high Mg-calcite was deposited and then dissolved to reprecipitate within the same rock as calcite and dolomite. In contrast, the pure dolomites (dolostones), composed of more nearly stoichiometric dolomite (open histogram in Fig. 4A), tend to form in more open systems characterized by greater volumes of fluid throughput and continuing dissolution–reprecipitation. Dolomite (the

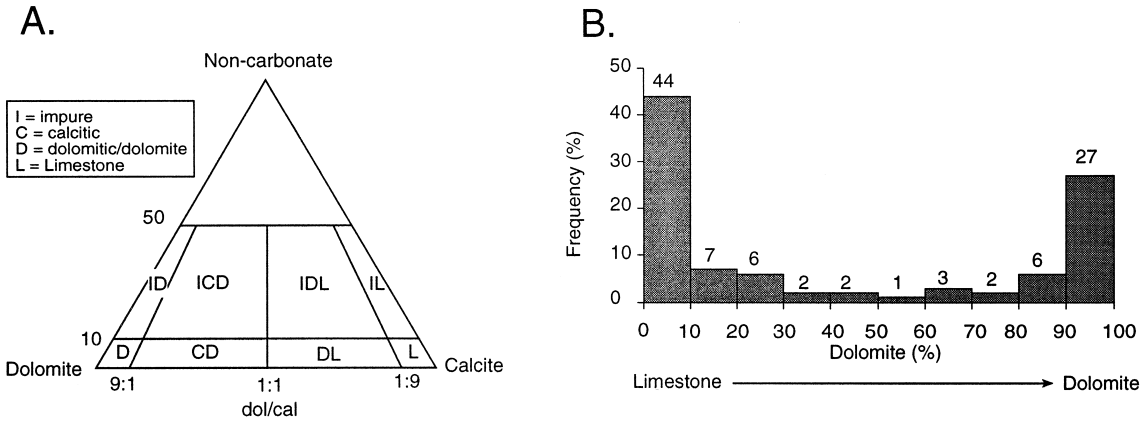

Fig. 3. Dolomite classification. (A) General carbonate classification according to mineralogy of components (after Leighton and Pendexter, 1962). (B) Computed percentages of calcite and dolomite for 1148 modal analyses of North American carbonates (after Steidtmann, 1926; Blatt, 1992).

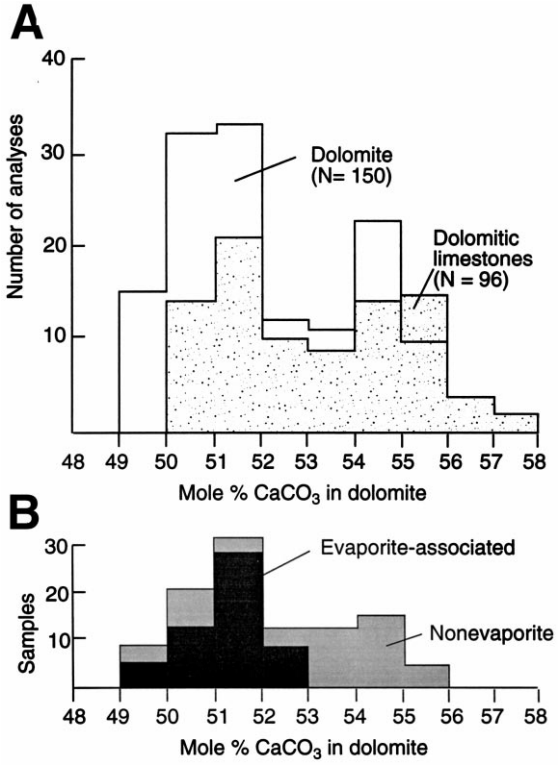

Fig. 4. Phanerozoic dolomite chemistry. (A) Dolomites and dolomitic limestones of North America. Dolomites precipitated within relatively closed hydrologies tend to be calcian (shaded histogram region), while those formed under more open hydrologies (white-filled histogram region) tend toward more stoichiometric chemistries (after Sperber et al., 1984). (B) Evaporite (black) and nonevaporite (grey-shaded) associated dolomites showing evaporitic dolomites tend to be more stoichiometric (after Lumsden and Chimahusky, 1980).

mineral) tends toward ideal stoichiometry when formed in evaporite settings (Fig. 4B, shaded black), perhaps reflecting the higher Mg/Ca ratios of marine-derived hypersaline waters compared to many other dolomite-precipitating waters.

At the hand-specimen scale, dolomites tend to be composed of either spar or micrite. Historically, many workers have ignored the detailed petrography of dolostones believing that most primary textures were obliterated by the growth of dolomite spar. More recent work has shown this is not the case. As Carozzi (1993; p 134 ff.) concludes, among all but the coarsest dolostones, many when examined with diffused, plane-polarized light preserve depositional textures that reveal detailed microfacies. Even better results can be obtained using cathodoluminescence (Braithwaite and Heath, 1996), fluorescence microscopy (Dravis and Yurewicz, 1985), or the much cheaper white-card technique of Folk (1987).

Advancing levels of replacement, ranging from mimetic to obliterated (mosaic or sucrosic) texture can be present in a single formation and sometimes even in a single outcrop or thin section (Braithwaite, 1991). An early attempt at classifying dolomite diversity based on texture was made by Friedman (1965). Sibley and Gregg (1987) later modified this system on the basis of crystal boundary relationships and crystal size distribution (Table 1; Fig. 5).

Crystal boundaries are classified as either planar or nonplanar. Planar dolomite is characterized by planar compromise boundaries with many crystal-face junctions. Nonplanar dolomite is characterized by boundaries between crystals that are curved, lobate, serrated, or otherwise irregular, with few preserved crystal-face junctions. Planar dolomite develops when crystals undergo faceted growth and is characteristic of dolomite crystals formed early during diagenesis and, under certain conditions, at elevated temperatures. Nonplanar boundaries develop when crystals undergo nonfaceted growth. According to Gregg and Sibley (1984), mosaics with planar crystal boundaries (idiotopic) indicate growth temperatures below 50°C, while those with nonplanar boundaries (xenotopic) result from elevated temperatures greater than 50°C. Both planar and nonplanar dolomite can form as a cement, by replacement of limestone, or by neomorphic recrystallization of a precursor dolomite (Gregg and Sibley, 1984; Sibley and Gregg, 1987). Sibley and Gregg's simple classification is descriptive, but carries genetic implications because crystal size is controlled by both nucleation and growth kinetics, while crystal shape is controlled by growth kinetics.

Many lower temperature sparry planar dolomites are dominated by cloudy centered, clear-rimmed crystals. These cloudy centers may have developed in precursors that originally consisted of low-Mg calcite and may now contain inclusions of this type of calcite. Alternatively, the cloudy center can be dominated by voids created by Mg-calcite dissolution, or by fluid-filled micro-cavities. Chemical dif-

Table 1
Guide to observational steps used in classifying dolomite textures using classification of Sibley and Gregg (1987) as shown in Fig. 5

Steps for classifying dolomite textures	
Step 1: What is the dolomite crystal size?	Unimodal (crystals mostly of the same size) Polymodal (at least two size populations)
Step 2: What is the dominant dolomite crystal shape?	Planar (euhedral, suhedral) Nonplanar (anhedral)
Step 3: Describe and name $CaCO_3$ precursor Allochems? Matrix? Cement?	Are the various components unreplaced, replaced or moulds? If replaced, is it partial or complete replacement? Is the replacement a mimic or nonmimic of the precursor texture
Step 4. Describe any void filling dolomite	Limpid, rhombic, drusy, saddle/baroque?

ferences between the inner and outer parts of these rhombs are mainly variations in iron and manganese (Choquette and Steinen, 1980; Fairchild, 1983; Gawthorpe, 1987). Land et al. (1975) documented trace element differences between cloudy centers and clear rims. These could be interpreted as indicating the rims precipitated from solutions that were undersaturated with respect to low-Mg calcite, thus explaining the absence of inclusions (Sibley, 1980). Alternatively, the variations may reflect changes in

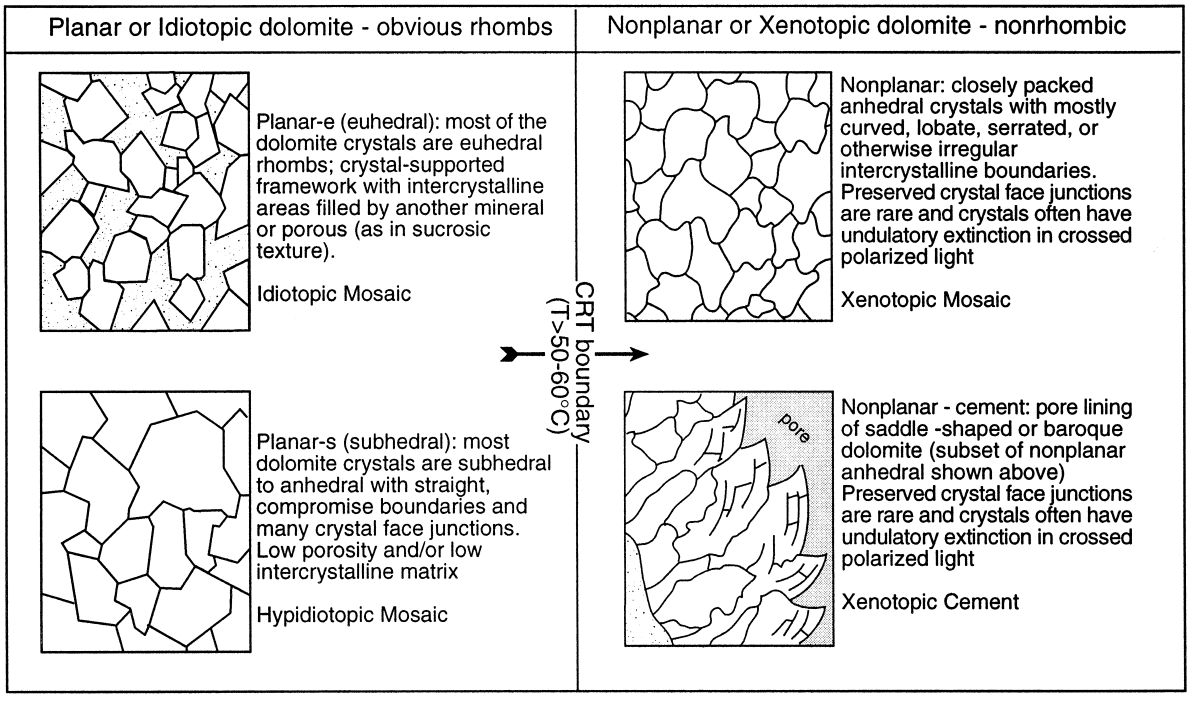

Fig. 5. Common dolomite textures emphasizing the effect of temperature on the style of dolomite development (after Gregg and Sibley, 1984; Sibley and Gregg, 1987). Used in combination with observation criteria listed in Table 1. See text for explanation.

crystal growth rate or in the dissolution/reprecipitation of the outer portions of precursor crystals.

Saddle dolomite, also called baroque dolomite, forms at the same elevated temperatures as nonplanar dolomite (Fig. 5; Radke and Mathis, 1980; Machel, 1987; Kretz, 1992). Crystals may be clear or turbid, with characteristic curved faces and cleavage traces. They typically show a sweeping extinction under crossed polars caused by a distorted crystal lattice structure. Under cathodoluminescence, crystals often display internal zonation due to varying iron and manganese content. Saddle dolomite, which may contain hydrocarbon and metal sulfide inclusions, is a useful geothermometer, indicating minimum burial temperatures of 60° to 150°C (equivalent to the oil window). It is often a byproduct of chemical compaction and thermochemical sulfate reduction, and it is typically related to the throughflow of high-temperature hypersaline basinal brines that may also be carrying base metals.

Mosaics of anhedral to subhedral dolomite crystals apparently represent the final product of dolomitization, and a pervasive coarse-grained overprint can destroy any original depositional fabrics. Typically, some of the crystals in these mosaics retain cloudy cores and clear rims. The generation of dolomite mosaics indicates a lengthy diagenetic history often involving fracture and rehealing of crystals, as well as overgrowths and replacements reflected in internal dissolution surfaces and other crystallographic/mineralogic discontinuities.

4. Dolomitization models

Our increasing understanding of the reactivity of different types of dolomite in the laboratory has led to an improvement in the way dolomites are interpreted at the reservoir or outcrop scale and to a merging of dolomitization models that were previously considered distinct but not well documented paradigms. Once the metastable nature of sedimentary dolomite was recognized in the mid to late 1980s, it became apparent that the mineral evolves ("ages") as it moves through earth-space and time. Changing conditions of burial depth, pore brine chemistry, temperature and pressure mean that dolomites may re-equilibrate many times during their burial history. The process only slows once matrix permeability is lost as strata enter the anchizone. Rather than being seen as a single event, the dolomitization process now encompasses successive responses to compositionally diverse and evolving pore fluids that produce a suite of replacive and cementing phases (Land, 1985; Warren, 1989, 1990; Gregg and Shelton, 1990; Gregg et al., 1992; Qing and Mountjoy, 1994a,b; Suchy et al., 1996; Reinhold, 1998). Thus, depositional or early diagenetic dolomites can evolve or re-equilibrate into new forms as conditions change.

Hydrological constraints are central to the evolution of natural dolomites. For crystals to precipitate or re-equilibrate there must be a solution throughput that is capable of supplying and maintaining sufficient volumes of magnesium to generate and sustain supersaturation. To dolomitize a typical limestone containing 6% $MgCO_3$ with 40% porosity requires that 807 pore volumes of seawater flow through the rock (Land, 1985). With seawater diluted 10 times with meteoric water (mixing zone model), something like 8100 pore volumes are needed, while with a halite-saturated, seawater-derived brine (brine reflux model), only 44 pore volumes are sufficient. If the brine has reached the bittern stage, only 10 to 12 pore volumes are required. In these idealized scenarios, no pore volume reduction has occurred during the throughflow. To reduce the porosity of our theoretical model to values common in ancient dolomites requires either chemical compaction or even greater volumes of solution to flow through the rock.

These simple volume calculations clearly show the need for any model to be based on realistic physical mechanism relevant to the hydrological setting. For example, it is difficult to move large volumes of meteoric waters through rocks that are accumulating in a hypersaline setting (Chap. 2 in Warren, 1999). Similarly, large volumes of basinal fluid cannot pass easily through deeply buried lime mudstones, unless some other earlier process has generated/retained porosity. The fact that much smaller pore volumes of hypersaline water are required to dolomitize a given volume of limestone, and the allied observation that most modern dolomite is associated with evaporitic settings, has led Friedman (1980) to state "dolomite is an evaporite mineral," while Sun (1994) suggests that most large-scale

dolomite has had an origin related to salinity-elevated seawaters. Let us see if this is so by looking at the current deposits and models that attempt to explain the various forms of dolomite.

4.1. Syndepositional dolomite

4.1.1. Sabkha-style dolomite

Dolomite is currently forming as thin (< 1–2 m thick) patchy stratiform beds in many evaporitic tidal flats (sabkhas) on the southern and western margins of the Arabian Gulf (Warren, 1991). The Arabian Gulf is probably the warmest sea in the world; surface temperatures in the open gulf range from 20°C in February to 34°C in August. Water temperatures on the open shelf in the vicinity of Abu Dhabi Island range from 23°C to 34°C, and those in the inner lagoons from 15° to 40°C with an annual average temperature of 29°C. The shallow, inner lagoon waters of Khor al Bazam have diurnal ranges of up to 10°C. Air temperatures on the sabkha can be as low as 5°C and as high as 50°C with average temperatures ranging from 23° to 33°C. Surface temperatures on the sabkha are even more variable, with values up to 60°C–80°C on the algal mats (Kinsman, 1965). Temperatures in shallow subsurface sediments range from 22°C to 40°C. In the summer, the sabkha can be extremely humid, especially at night when it is often above 95%, yet by midafternoon on the same day the humidity can fall to around 30% (Bush, 1973).

Small volumes of micritic dolomite are common in modern intertidal/supratidal sabkha sediments, but also occur in subtidal sediments of the Arabian Gulf (Illing et al., 1965; Illing and Taylor, 1993; Mackenzie, 1981; Wenk et al., 1993; Shinn, 1983; Chafetz and Rush, 1994). Dolomite is accumulating within the supratidal zone of the prograding sabkha, usually within aragonite muds that lie less than a meter beneath the sabkha surface. On sabkhas bordering the Qatar Peninsula, the dolomite is most abundant on the landward margins where it forms 1–5 μm euhedral crystals in aragonitic muds beneath the high intertidal zone (Fig. 6; Illing and Taylor, 1993).

TEM study has shown that much of the dolomite in the Abu Dhabi sabkha is actually a pore precipitate and not a replacement of precursor aragonite (Wenk et al., 1993). Only rarely does it directly replace an aragonite precursor at the scale of crystallites. Whether one considers this dolomicrite, a replacement of aragonite mud, which sometimes appears to be dissolving, or a primary dolomite precipitate depends on how one defines primary versus secondary dolomite (see Warren, 1989, Chap. 5 for discussion). There are actually two forms of dolomite in the Abu Dhabi sabkhas: (1) an ordered dolomite, often showing a modulated microstructure, and (2) a mostly disordered calcium magnesium carbonate with submicrometer-sized ordered domains (Wenk et al., 1993). Both the ordered and partially ordered dolomite form by direct precipitation from pore flu-

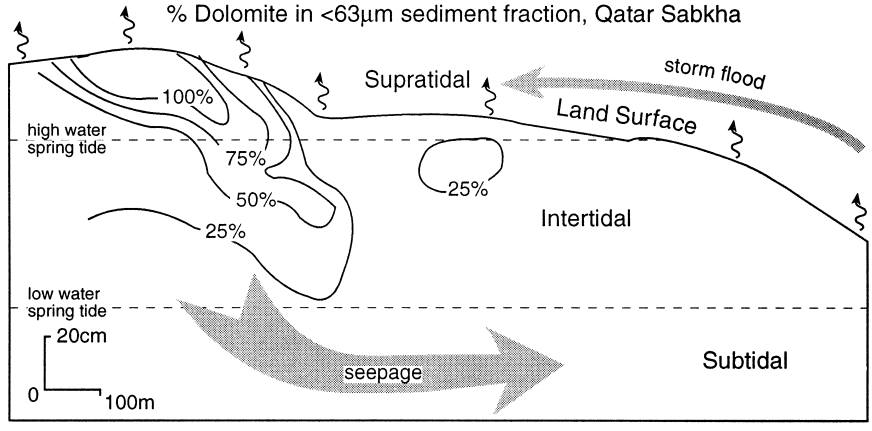

Fig. 6. Dolomite in the Arabian Gulf. Cross-section of peritidal sediments on a sabkha on the Qatar peninsula, Arabian Gulf. Contours are of percentage dolomite in the fine fraction of the sediment. Note the strong tie to the spring tide high water mark (after Bush, 1973).

ids. Both appear simultaneously during early diagenesis. With time, the dolomite seems to "age": there is an increased ordering in the crystal structure, an increase in crystal size, and continued isotopic equilibration with brines at the lower temperatures beneath the sabkha surface (Mackenzie, 1981).

Most dolomite in the Abu Dhabi sabkha is a cement, precipitating from hypersaline fluids into pores of varying sizes down to a few microns (Wenk et al., 1993). It forms in isotopic equilibrium with brines at temperatures between 34° and 49°C. Calcium–magnesium-carbonate perhaps serves as an intermediate in the formation of the dolomite, which then proceeds to a more ordered ("aged") form via micro-scale dissolution–reprecipitation. Diagenetic changes and isotopic re-equilibration occur in the coexisting $CaCO_3$ phases.

Currently, dolomite precipitates in areas of maximum flux of hypersaline brines beneath the supratidal surface (Fig. 6; Bush, 1973; Patterson and Kinsman, 1981, 1982). It occurs sporadically to depths of 2–3 m landward of the algal mat. The most intense precipitation typically occurs in buried (<1 m below the surface) algal mats and lagoonal muds (Fig. 6; Bush, 1973). Patterson and Kinsman (1982) argue that the zone of maximum precipitation occurs in sediments located just above the high spring watermark. This zone migrates seaward as the sabkha progrades into the lagoon.

Storms and high spring tides drive seawater from the lagoon onto the sabkha flat, while continental groundwaters and storm runoff move terrestrial waters into the landward side of the sabkha. As surface waters sink into the sediments and begin to seep seaward, some pore water escapes to the atmosphere via capillary evaporation. As it does so, the remaining pore water concentrates to the point where it deposits aragonite and anhydrite or gypsum. Precipitation of these minerals removes calcium from the pore solution and so raises the Mg/Ca ratio favoring dolomite precipitation or dolomitization (Fig. 7).

The relative proportions of continental, mixed or marine waters feeding the areas precipitating dolomite are still not well understood (Hardie, 1987). Mackenzie et al. (1980) found that the Mg/Ca molar ratios in areas of dolomite range from 2.5 to 7.5, lower than seaward areas where flood recharge is more frequent and aragonite and gypsum are being

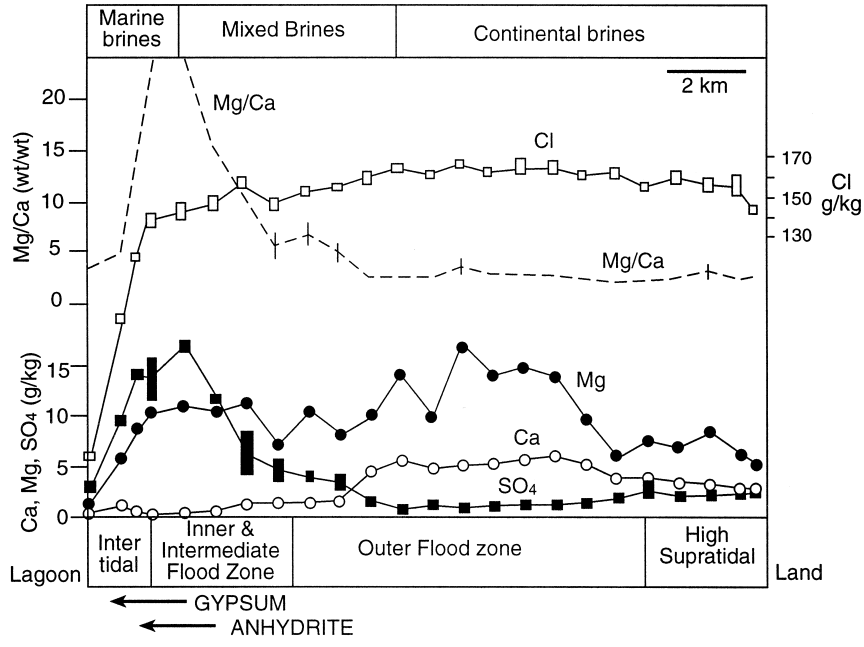

Fig. 7. Pore fluid chemistry across the Abu Dhabi sabkha showing variations in major ions and the Mg/Ca ratio (after Hardie, 1987 who replotted the data in Butler, 1969).

precipitated (Mg/Ca = 7 to 27). In contrast, Patterson and Kinsman (1982) found that in areas of dolomitization the Mg/Ca was > 6, pH = 6.3 to 6.9 and the sulfate content lower than seawater. These authors also concluded that dolomite was replacing an aragonite precursor, so supplying Ca to the pore solution that was subsequently removed by precipitation of more gypsum. Mackenzie et al. (1980) argued that replacement of aragonite occurs via a high-Mg calcite intermediate, while Hardie (1987) argued for direct microscale cementation in the pore waters, a view later confirmed by TEM work (Wenk et al., 1993). Views on the ultimate genesis of the sabkha dolomite are still diverse and the origins of groundwaters that precipitate the dolomite are not yet resolved.

Hsu and Schneider (1973) proposed a hydrological alternative to the model of surface flooding followed by seaward reflux of the dolomite precipitating brine. They called it evaporative pumping. It involved continuous subsurface seepage of lagoonal seawater into the sabkha to replace groundwater lost by evaporation at or near the surface. Under evaporative pumping, phreatic seawater flows landward beneath the sabkha flat in a direction opposite to seaward seepage in the surface flooding model. Field evidence for evaporative pumping is contradictory and many authors feel that it does not explain the distribution of dolomite in the sabkha (Morrow, 1982; Land, 1985). If landward seepage of phreatic seawater was the sole mechanism of supply for sabkha brines, then marine evaporites would quickly precipitate and plug capillary pores (hydroseal of Kendall, 1992). Without subsequent dissolution beneath surface flood waters, this would reduce the permeability of the sediments, cancel the head difference, and so choke off landward flow before sufficient magnesium had flushed through the region to form widespread dolomites landward of the evaporite plug.

Perhaps the mechanisms supplying seawater to the Abu Dhabi sabkha are not as simple as these models imply. Mackenzie et al. (1980) have shown that the sabkha hydrology may be characterized by three sequential stages; flood recharge, capillary evaporation and evaporative pumping. All three occur as the dolomitizing brine evolves and are repeated with each new flood event. In addition, the hydrology does not operate within a homogeneous unconfined aquifer; to the south of Abu Dhabi city, the sabkha is composed of three aquifers separated by cemented crusts which form aquitards.

In Al-Khiran lagoon in Kuwait, there is another modern sabkha dolomite, it also is interpreted as a diagenetic precipitate, but it is unlike the dolomite of the Trucial Coast. The Kuwaiti dolomite is found in the upper 10 cm of isolated lagoon sediments and is not associated with any gypsum or other evaporites (Gunatilaka and Mwango, 1987; Gunatilaka et al., 1987). Gunatilaka and Mwango (1987) proposed that bacterially induced sulfate reduction played a role in its formation. Nearby, in the sabkha behind the lagoon, Mg-rich dolomite forms in thin layers alternating with more commonplace Ca-rich dolomites. This Mg-rich variety occurs in parts of the sabkha that are today under the influence of continental groundwaters and rarely covered by seawater (Gunatilaka et al., 1987). In this region, the landward hydrology appears more akin to that of the continental Coorong system discussed below.

Not all the dolomite found in the peritidal margins of the Arabian Gulf is modern. Chafetz et al. (1999) document a 55-m-thick Pleistocene sabkha dolomite section with abundant evaporite layers. This was deposited as part of a series of vertically stacked sabkhas. Stable-isotope analyses of 385 samples defined four correlatable horizons, each with marked excursions to low $\delta^{13}C$ values; some shifts between vertically adjacent samples exceed 6‰. Values for $\delta^{18}O$ show a similar, but less pronounced, downward shift in the same stratigraphic horizons. Samples with low $\delta^{13}C$ and $\delta^{18}O$ values have greater admixtures of fine-grained siliciclastics, are light gray (implying reducing conditions), and have higher concentrations of Fe, Mn, and Zn than other parts of the deposit. Changes in $\delta^{13}C$ values may be due to diagenesis reflecting the descent of meteoric water beneath a soil or to bacterially mediated sulfate-reduction. Chafetz et al. (1999) favor sulfate reduction of laterally extensive microbial mats within the top of the sabkha sequences, very soon after the initial dolomitization.

Not all surficial dolomite in the Arabian Gulf was deposited by the hydrological processes characteristic of the current evaporitic setting. Shinn (1983) documents detrital seafloor dolomite deposited as offshore detrital sediment, along with quartz-silt and

various clay minerals. Pilkey (1966) recorded 10% detrital dolomite in fine-grained sediment from bottom sediments in the central axis of the Gulf. Anyone who has stood on an offshore rig during a dust storm has its origin blasted across their person and their equipment. Wind-carried silt-sized dolomite must be added to that found in the sabkha sediments. However, the contribution is probably minor. Whether or not detrital dolomite was also a catalyst for the nucleation of the initial calcian-rich diagenetic dolomites that formed the bulk of the modern sabkha dolomite, has yet to be addressed.

No matter what the ultimate origin of the sabkha dolomite, in terms of ancient counterparts, sabkha dolomites are syndepositional, thin (< 1–2 m thick), stratiform, micritic, mimetic and confined to restricted marine to supratidal facies, coprecipitating with nodular evaporites (Warren and Kendall, 1985; Warren, 1991). Sabkha dolomitization is tied to active evaporative hydrologies, but in the sabkha these are capillary scale mechanisms (> 1 m thick), which cannot alone explain the huge brine throughflow indicated by pervasive sparry dolomitization of marine limestones within ancient carbonate–evaporite platforms.

4.2. Coorong-style dolomite

The dolomite-forming schizohaline lakes of the Coorong region are situated in seepage-fed interdunal corridors on the prograding coastal plain of southeastern South Australia (Fig. 8). The Coorong

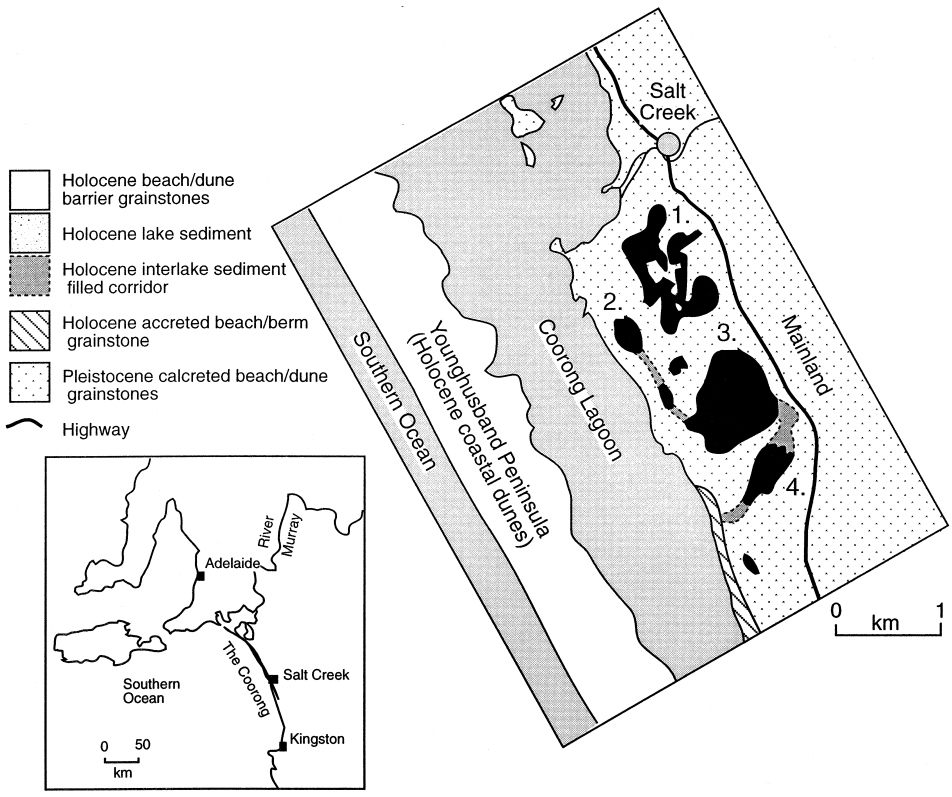

Fig. 8. Locality and map of the Coorong region. Geological plan of the Salt Creek regions shows how three of the four major lakes are joined by an interdurnal corridor and were connected to the Coorong lagoon earlier in the Holocene. Milne Lake, the best dolomite accumulator in the whole coastal plain, never had a surface connection with the Coorong Lagoon. Mineralogies: Lake 1 = Milne Lake (dolomite + magnesite), Lake 2 = Halite Lake (gypsum + aragonite overlain by hydromagnesite + aragonite in massive unit and currently covered by ephemeral halite crust), Lake 3 = Pellet Lake (dolomite + hydromagnesite + aragonite), Lake 4 = North Stromatolite Lake (hydromagnesite + aragonite; minor dolomite in basal unit and about lake edge) (after Warren, 1990).

Region was first documented as an area of modern dolomite precipitation by Mawson (1929), but was not studied in any detail until the work of Alderman and Skinner (1957), Skinner (1963), von der Borch (1965, 1976), von der Borch and Lock (1979), Rosen et al. (1988, 1989), and Warren (1988, 1990). The climate in the Coorong region is Mediterranean, with hot, dry summers (Dec.–Mar.) and cool wet winters (June–Sept.). Maximum rainfall is 800 mm in the far southeast of South Australia, 600 mm around Kingston, and 400 mm in the area about Salt Creek. In the last region, evaporation exceeds precipitation except for a few weeks in June and July. To the southeast, near Kingston, precipitation exceeds evaporation for 3–4 months each year (May–August). Air temperatures range annually from −1°C to 38°C with a mean of 13.5°C. Water temperatures vary between 10°C and 28°C with a pH of 8–10. Summer temperatures within subaerially exposed lake sediments are as high as 50°C, while winter temperatures are as low as 5°C. The Mg/Ca ratios of waters from different lakes varies from 1 to 20 (Von der Borch, 1965), sulfate concentrations in lakes in the coastal plain range from 6.1% to 8.2% (Skinner, 1963) and are close to the expected value for seawater sulfate (7.68%).

Von der Borch (1976) observed that Holocene dolomite occurs in areas of the coastal plain where rainfall is less than 700 mm, encompassing the area between Kingston and Salt Creek (Fig. 8). He suggested that south of the 700 mm isohyet, reduced evaporation rates and higher rainfall prevented the concentration of lake waters to salinities where dolomite could precipitate. Regional sampling of lakes across the area confirms his postulate and shows that the more magnesian-rich dolomites tend to occur in the more arid northwestern portion of the coastal plain, centered on lakes in the vicinity of Salt Creek (Warren, 1988, 1990).

Coring has shown that many of the lakes in the Salt Creek region contain two geochemically and isotopically distinct types of dolomite, typically in association with other precipitated carbonate minerals such as low Mg-calcite, high Mg-calcite, aragonite, magnesite and hydromagnesite (Table 2; Fig. 9B,C). Type A dolomite typically has a slightly heavier oxygen isotope signature than type B, and is 3%–6‰ heavier in carbon (Fig. 9B). Type A dolomite also has distinct unit cell dimensions (Fig. 9C). It tends to be magnesium-rich with up to 3 mol% excess $MgCO_3$ while type B is near stoichiometric or calcian-rich. Type A dolomite commonly occurs in association with magnesite and hydromagnesite, type B with Mg-calcite. Transmission electron microscopy (TEM) shows that type A dolomites have a heterogeneous microstructure due to closely spaced random defects, while type B dolomites exhibit a more homogeneous microstructure implying that excess calcium ions are evenly distributed throughout the lattice. TEM studies show that the

Table 2
Summary of properties of types A and B dolomite in Holocene lacustrine carbonates of the Coorong region (after Rosen et al., 1989; Warren, 1990)

Type A dolomite	Type B dolomite
Mg-rich	Ca-rich
Unit cell: contracted in a_0 direction, variable c_0 direction	Unit cell: ideal to expanded in both a_0 and c_0 directions
Isotopically heavy carbon	Isotopically light carbon
Relatively small variation in isotopic signature related to brine concentration	Relatively large variation in isotopic signature, brine is perhaps influenced by meteoric mixing
Heterogeneous microstructure under TEM	Variable microstructure
Forms in evaporative centres of larger, more arid lakes. Uncommon in dolomitic lakes in more humid regions of the coastal plain	Forms about the edges of lakes in arid regions, also found in basal units and interlake corridors near Salt Creek. Is more common than type A in dolomitic lakes in the more humid regions of the coastal plain

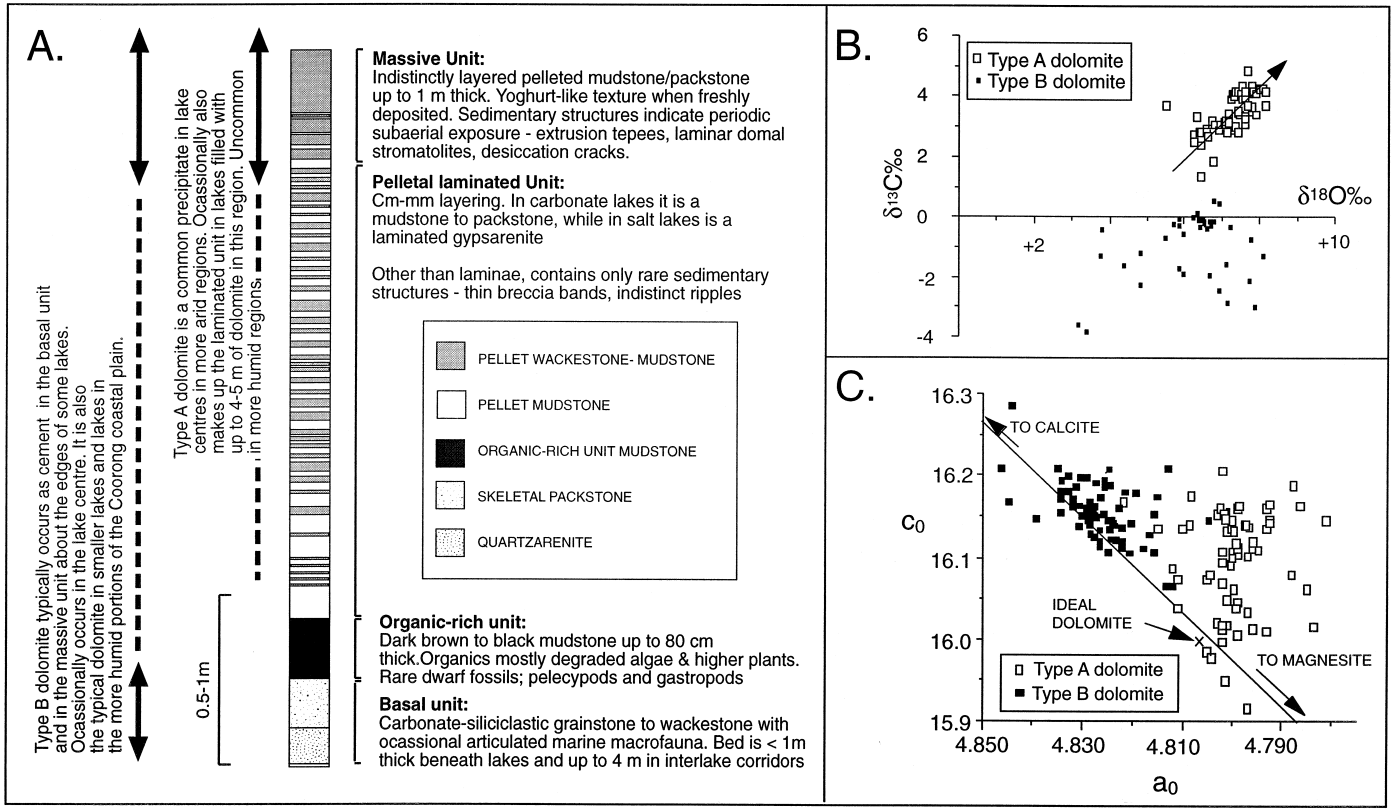

Fig. 9. Sedimentology of Coorong dolomites. (A) Typical vertical sequence in Holocene evaporitic lakes of the Coorong coastal plain. (B) Isotopic signatures of type A and type B dolomite. (C) Unit cell parameters of type A and type B dolomite (after Rosen et al., 1989; Warren, 1990).

two types of dolomite are distinct, and are not intermixed with other mineral phases; they are primary precipitates, and not replacements (Miser et al., 1987).

Regional sedimentological sequences in the Coorong lakes are independent of their mineral assemblages (Fig. 9A); some are filling with dolomite, others with low Mg-calcite still other with gypsum and aragonite. Whatever the mineral assemblage, the dominant textural feature in the lacustrine sediment columns is lamination passing up section into more massive units with evidence of seasonal subaerial exposure of the sedimentation surfaces. Coorong dolomites are penecontemporaneous carbonates, once thought to be free of associated preserved evaporites (von der Borch and Lock, 1979). Yet, the best dolomite-filled lake in the Coorong region, Milne Lake, lies less than a kilometer from Halite Lake a depression filled with laminated gypsum–aragonite and capped by a massive hydromagnesite/aragonite bed (Fig. 8; Warren, 1990). Milne Lake is fed by seaward flowing continental groundwaters while Halite Lake is fed by landward-flowing marine groundwaters during the gypsum-depositing drawdown stage. The close juxtaposition of these mineralogies means that ancient counterparts of the Coorong may also show a close association of evaporative dolomite with salts such as gypsum and halite.

A model of Coorong-style dolomites must include the following observations:

- There is a vertical sequence dominated by a laminated subaqueous unit, overlain by a massive unit capped by tepees, intraclast breccias and stromatolites.
- Dolomite is a primary precipitate. There are two distinct dolomites: (i) calcian dolomite associated with Mg-calcite occurs throughout the coastal plain (type B), (ii) dolomite associated with magnesite or more rarely with hydromagnesite (type A). Type A dolomites occur predominantly in the more arid northern areas of the Coorong complex near Salt Creek.
- Dolomite precipitates in lakes and ponds and accumulates above an extensive Pleistocene aquifer that supplies ions to the evaporating lake waters. In the Coorong region, the aquifer is a calcreted Quaternary coastal dune system.

Like those of the sabkhas, Coorong-style models of evaporative micritic dolomite precipitating in localized groundwater fed depressions cannot explain the bulk of ancient platform dolomites. These formed by replacement of thick beds spread across laterally extensive areas of platform carbonates (Warren, 1991). Ancient equivalents of the Coorong in a sea-marginal setting are most likely to be relatively thin, laminated subaqueous mudstone units showing patchy facies mosaics in plan view rather than elongate belts. They tend to develop atop regional paleoaquifers. Such dolomite typically occurs as a lacustrine capstone in regional paleotopographic lows. A Coorong-style model can only be used to explain local laminated micritic dolomites precipitated by evaporation within outflow zones of an extensive carbonate paleoaquifer.

Probably the best ancient counterparts to the Coorong Lakes are not in sea-marginal settings, but in continental lacustrine deposits. The carbonate mudflats of the Eocene Green River Formation, Utah, contain all the structures and textures present in the Coorong Lakes, as well as many of the same vertical transitions from laminated calcium carbonate sediments to massive dolomites. The Green River Formation was deposited in a large lake complex, part of a foreland basin that contained no marine waters. Green River carbonates consist of a series of stacked shoaling lacustrine cycles of laminated to massive dolomites and limestones (Wolfbauer and Surdam, 1974). Individual units contain stromatolites, ripples, flat pebble breccias, oolites, mudcracks and extrusion tepees.

This does not imply that Holocene continental lacustrine dolomite only forms in a Coorong-like setting. While this is certainly true of the more widespread examples of Holocene lacustrine dolomite, there are numerous others. A comprehensive and well-referenced review of these deposits is provided by Last (1990). However, like the Coorong, most are localized seepage outflow deposits and are not analogues for ancient platform dolomites.

4.3. Dolomite from normal seawater — a kinetic problem?

Land (1985) suggested that, if there is an efficient pump mechanism to move large volumes of seawater

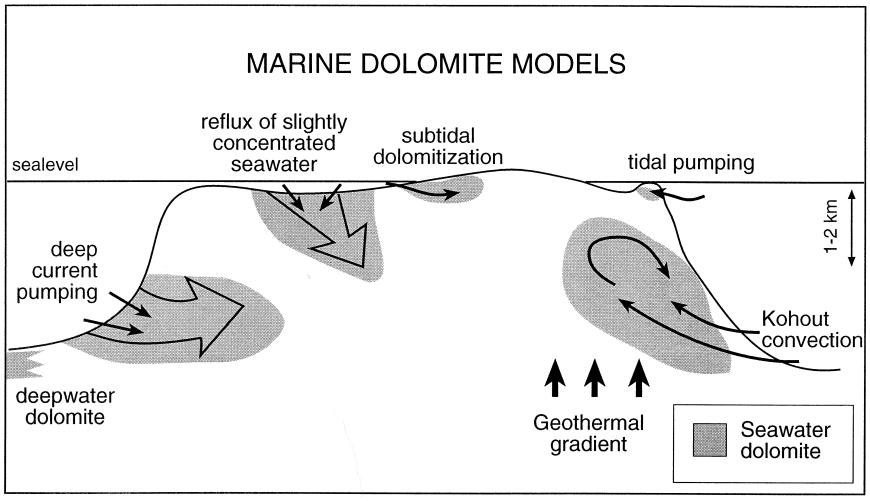

Fig. 10. Various models of marine dolomite formation in which the dolomitizing fluid is unmodified seawater (connate) that is pumped through porous limestones at depths ranging from at-surface to moderate burial ($\approx$ 2 km).

through carbonate sediments, then dolomite may precipitate as a marine cement directly from pores filled with completely unmodified seawater, all that is needed is sufficient time to grow primary crystals. In a later paper (Land, 1991), he repudiated the mixing zone model in its type area, the Hope Gate Formation of Jamaica, in favor of dolomitization by normal seawater. In most pre-1990s dolomitization models, the kinetic problems in precipitating dolomite directly from seawater (or its subsurface equivalent-connate[1] water) are overcome by evaporation, dilution or cooling. Some early models of seawater-derived dolomites invoked slight concentration of lagoonal seawater (an increase of perhaps 5%–10‰ above normal) to drive these slightly denser seawaters into the underlying platform sediments (Fig. 10). Since the early 1990s, many widespread ancient platform dolomites are increasingly being explained as the result of dolomitization by normal seawater or connate pore fluids (Vahrenkamp and Swart, 1994; Whitaker et al., 1994). In a similar fashion, Budd (1997) argues geometries and ages of most island dolomites relative to overlying limestones indicate that seawater, derived laterally, is the parent fluid. He concludes that many Cenozoic island dolomites, interpreted as mixing-zone or hypersaline reflux products, are probably misinterpretations based on unreasonable or extreme assumptions about D–Sr, $\delta^{18}O$ or the chemistry of hypothetical end-member dolomites.

Mazzullo et al. (1995) referred to dolomite precipitated from seawater as "subtidal dolomite." One of the first examples of Holocene subtidal dolomite forming from unmodified seawater came from Jamaica, where dolomite precipitates in modern shallow water deposits and in underlying Pliocene–Pleistocene rocks bathed in normal seawater (Mitchell et al., 1987; McCullough and Land, 1992). Subtidal dolomite may also have precipitated in cool-water shelf deposits in Australia (James et al., 1993). However, the Jamaican dolomites comprise $< 1\%$ of the samples examined, and are only found within a local section of limited thickness.

In contrast, an average of 5% subtidal dolomite (range 1%–30%), with an average crystal size of 10 μm (range 10–50 μm), is found in the Cangrejo shoals mudbank in Belize (Mazzullo et al., 1995). It occurs throughout the upper 4.3 m of subtidal deposits, which are about the same age (< 5600 years) as those in Jamaica. Interestingly, dolomite has not

[1] Connate water is used to describe a subsurface water that has the ionic proportions of seawater (latin root *connatus* = with-born). It has a specific geochemical implication and should not be used to describe subsurface or basinal waters that have ionic proportions indicating extensive water–rock interaction. Such waters may have once been connate but this can no longer be determined from their ionic proportions.

been found in or around the seasonally hypersaline peritidal flats adjacent to the dolomitic Canjero shoals, and so a hypersaline or a meteoric parent fluid for these subtidal dolomites is unlikely. Mean $\delta^{18}O$ (+2‰) compositions of these high-Sr dolomites (mean 1000 ppm), together with near-normal marine salinities and Mg/Ca ratios of pore fluids, suggest their precipitation from near-normal seawater. Tidal and wind-driven circulation of seawater (tidal pumping) through the sediments supplies most of the Mg for dolomitization. The process appears to be promoted by elevated porewater alkalinity reflecting bacterially mediated oxidation of organic matter and, locally, the early stages of methanogenesis (Mazzullo et al., 1995). A variation on the marine subtidal dolomitization theme is documented by Carballo et al. (1987) who describe supratidal crusts formed by tidal pumping of normal seawater through elevated areas at Sugarloaf Key, FL (Fig. 10). Similar seawater-derived humid-zone supratidal crust dolomites also occur on Ambergis Cay in Belize (Mazzullo et al., 1987; Gregg et al., 1992).

Lumsden (1988) suggested that precipitation of small volumes of micritic dolomite (≈ 6 μm) also takes place in cool marine pore waters within recent deep-water sediments. Such dolomite is interpreted as a direct precipitate from normal seawater and makes up, on average, 1% of deep-water marine carbonate worldwide. It occurs in all sampled ocean basins throughout post-Jurassic sediments and is typically nonstoichiometric (≈ 56% $CaCO_3$) and poorly ordered. This form of deep-water dolomite is distinct from that created by sulfate-reduction/methanogenesis within organic-rich marine hosts (see later). Unlike other modern dolomites, it does not show downhole increases in crystal size or improvements in its stoichiometry. That is, it does not appear to age by dissolution–reprecipitation. Mullins et al. (1988) reported the formation of similar early authigenic dolomite (10–20 μm) in the Neogene Florida–Bahamas Platform from marine pore waters where temperatures are as low as 1.8°C–9.8°C.

Saller (1984) noted that cores from Enewetak atoll contain dolomitized Eocene algal-rotaline foram grainstone at depths between 1250 and 1400 m below sea level. The dolomite postdates the brittle fracture of the grains and so is thought to have precipitated after more than 610 m of burial. Fractured grains first appear in the Enewetak core at this depth. This is too deep for the sediment to be experiencing active circulation by brine reflux or meteoric infiltration. The only fluid currently circulating in pores at that depth is seawater. The $\delta^{18}O$ values of the dolomite (+2.5‰) are relatively heavy and consistent with precipitation from normal seawater at lower temperatures (15°C–18°C). The temperature of marine waters at that depth is 10°C–20°C, much cooler than normal Pacific surface water (≈ 28°C). The $\delta^{13}C$ of the dolomite (+2.3‰) also suggests a marine source for the carbonate. The calcite saturation depth in the adjacent ocean is ≈ 1000 m. Saller (1984) noted that seawater is still supersaturated with respect to dolomite at this depth. He argued that the driving mechanism moving dolomite-saturated cold seawater into the pores of the island slope is oceanic tidal pumping. Deep wells of the island record tidal fluctuations even when cased to depths of more than 600 m and that temperature profiles in them mimic those of the open marine profile (Fig. 11). Both observations suggest

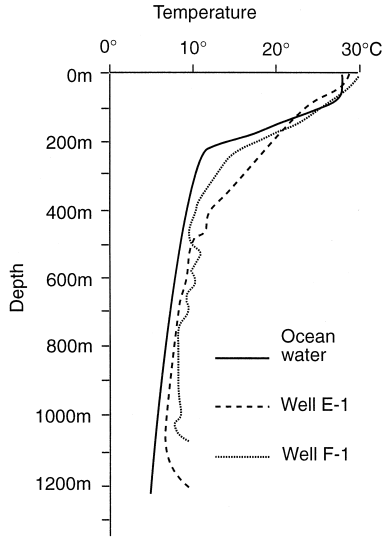

Fig. 11. Temperature profiles of wells E-1 and F-1 compared to an off-atoll ocean profile, Enewetak Atoll. Note the close parallelism of all profiles except near the base of the two wells where heating, related to nearby volcanic basement, caused the well profiles to depart from the deep water portion of the oceanic profile (after Saller, 1984).

that waters in the dolomitized intervals are in direct connection with deep ocean water.

An alternative view is that a thermal gradient has been set up within the atoll by the high geothermal gradient associated with the volcanic basement and this may also be pumping cool dense seawater into the atoll margin (Simms, 1984; Rougerie and Wauthy, 1988). Evidence for geothermal heating can be seen in increasing temperatures below 1000 m depth in wells E-1 and F-l close to the volcanic basement (Fig. 11). This heating may drive convective circulation of seawater via a set of processes called Kohout circulation. Kohout circulation occurs when cold dense deep ocean waters are drawn into a platform margin to replace heated (less dense and so buoyant) pore waters. This occurs at depths on slopes where, as in oceanic pumping, pore waters are undersaturated with respect to calcite but still saturated with respect to dolomite. Dolomites in such circulatory systems tend to precipitate within permeable aquifers fed from deep forereef and rise sediments. Sediments further into the atoll interior (buried lagoonal muds) are largely unaffected by this circulation. Kohout circulation is a long-term process that, although largely used to explain deep dolomite in oceanic atolls, probably has the potential to circulate large volumes of cool dolomite-saturated ocean water through continental platform-edge limestones (Simms, 1984).

Aharon et al. (1987) in a study at Nieu and other Pacific atolls confirm that many Tertiary-age island dolomites may have formed by geothermally driven seawater circulation (Table 3). They noted striking similarities between the dolomites from various atolls: (1) all the dolomites are of late Tertiary age with the exception of Enewetak (Eocene); (2) petrography shows that dolomitization is a late diagenetic event; (3) the dolomites contain an excess of Ca over Mg and their Sr compositions are remarkably similar ($\approx$ 150–200 ppm); (4) ^{18}O and ^{13}C values are consistently heavy, of the right order for a cold seawater parent, with little variation between atolls separated by large stretches of ocean. Earlier work on various atolls had called upon a reflux of slightly concentrated lagoonal seawater through the atoll interior to explain the heavy isotope signatures (Fig. 10; Sibley, 1980; Ohde and Kitano, 1981). But, as noted, these elevated isotope values are consistent with precipitation from cooler seawater and better explain the preferential formation of the dolomite in aquifers rather than in muds.

In summary, based on the occurrence of Neogene dolomites, it appears that unaltered cold seawater, seeping laterally into an island from the adjacent deep ocean is capable of precipitating dolomite. The main requirements are an effective pumping mechanism and sediments with suitable permeabilities to allow focused flushing of large volumes of seawater. However, such systems appear to be currently precipitating no more than small volumes of dolomite (Fig. 10).

4.4. Early burial dolomite

4.4.1. Brine reflux dolomite

Within ancient marine limestones, there are widespread areas of sparry dolomite with distributions that can be tied to the presence of overlying or adjacent platform and basinwide evaporites (Fig. 12; Warren, 1999). These evaporite-associated secondary dolomites typically form in regimes of brine reflux: such hydrological systems, like their associated platform and basinwide evaporites, have poor to nonexistent Holocene counterparts.

Brine-reflux was proposed as a dolomitizing mechanism by Adams and Rhodes (1960) to explain extensive lagoonal and reefal dolomites associated with platform evaporites of Guadalupian age in the Permian Basin of West Texas. Reflux dolomites form when, "hypersaline brines eventually become heavy enough to displace the connate waters and seep slowly downward through the slightly permeable carbonates at the lagoon floor" (Adams and Rhodes, 1960). It is thought that when $CaCO_3$ and gypsum precipitated in hypersaline areas on such platforms, the solution density was as high as 1.2 g/cm^3 and the Mg/Ca ratios of the remaining brines had increased along with salinity. As gypsum- and halite-saturated solutions seeped basinward through the platform limestones, they mixed with or displaced subsurface fluids that were originally marine-derived waters with densities around 1.03 g/cm^3. In this way, large volumes of Mg-rich brine passed through previously deposited shelf limestones and precipitated dolomite, both as a pore fill and as a replacement.

Table 3
Summary of stratigraphy and pertinent geochemistry of Pacific atoll dolomites (after Aharon et al., 1987)

Atoll (tectonic setting)	Dolomitized interval (m sub sl)	$\delta^{18}O$ (‰ PDB)	$\delta^{13}C$ (‰ PDB)	$^{87}Sr/^{86}Sr$	Biostrat. age	"Sr" age	Mg/Ca (molar)	Sr (ppm)	Sr/Ca ($\times 10^3$)
Enewetak (subsiding)	−1316 to −1318	3.4 ± 0.3	2.3 ± 0.1	0.70882 to 0.70918	Eocene	L. Miocene to Pleistocene	0.78	173	0.33
Funafuti (subsiding)	−194 to −340	4.9	3.1	–	L. Miocene to Pliocene	–	–	–	–
Kita-Daito-Jima (uplifting)	+5 to −103	5.3	3.2	–	L. Miocene to Pliocene	–	–	–	–
Lifou (uplifting)	+40 to −20 (?)	3.2 ± 0.3	2.2 ± 0.4	–	Miocene?	–	–	234	0.41
Midway (subsiding)	−125 to −147	3.6 ± 0.4	2.4 ± 0.3	–	L. Miocene to Pliocene	–	–	270	0.53
Minami-Daito-Jima (uplifting)	−125 to −147 −255 to −277	–	–	–	Pliocene to Pleistocene	–	0.79	202	0.38
Mururoa (subsiding)	surface to ?	3.5 ± 0.3	3.5 ± 0.3	–	E. to L. Miocene	–	–	170	0.33
Nauru (uplifting)	+65 to ?	2.2 ± 0.4	2.2 ± 0.4	0.70909 ± 4	Miocene?	Pliocene to Pleistocene	0.75	165	0.33
Niue (uplifting)	+35 to −200?	2.8 ± 0.5	2.0 ± 0.3	0.70914 ± 2	Miocene to L. Miocene	Pliocene to Pleistocene	0.75	217	0.40

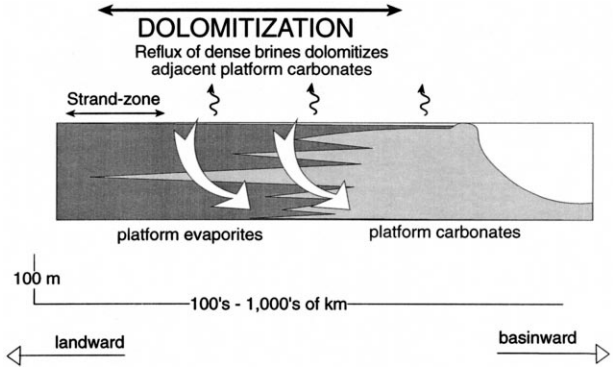

Fig. 12. Brine reflux dolomitizes platform carbonates associated with widespread platform evaporites (after Warren, 1991).

This model explained the dolomitization of the Permian reef complex where backreef, shelf and lagoonal carbonates are intensely dolomitized, while shelf edge carbonates, such as the Capitan reef, are not. It was thought that dolomitization took place via brine reflux through porous sub-saltern[2] sediments to depths of several hundred meters. The hydrological volume modeling of Kaufman (1994) and Shields and Brady (1995) mathematically confirmed the feasibility of the model (Fig. 13). In a study of the evaporitic carbonates of the Permian Salado Formation, Garber et al. (1990) also used a reflux model to explain magnesite in the same basin. They argued that when a brine has a Mg/Ca ratio of > 40, it will precipitate magnesite as a replacement rather than dolomite. Similar reflux processes, driven by the deposition of Zechstein evaporites, have precipitated magnesite cements in siliciclastic dune sands of Rotliegende reservoirs in the North Sea (Purvis, 1989).

By the mid 1960s, seepage reflux had gained a large number of proponents working in ancient evaporite-associated dolomites (Hsu and Siegenthaler, 1969). Deffeyes et al. (1965) reported modern Mg-rich brines in a marine spring-fed gypsum salina (Pekelmeer Lagoon) on Bonaire in the Netherlands Antilles in the Southern Caribbean. From the water chemistry, they predicted that concentrated lagoonal brines should be sinking and forming reflux dolomite in underlying sediments. They observed micritic dolomite in Holocene lagoon muds beneath gypsum crusts but, with only a soft sediment coring device, could not penetrate the cemented Pleistocene base. Outcropping on the opposite end of the island, well away from the present lagoon, they located a dolomite replacing what they interpreted as Pleistocene limestone and inferred that this had formed during an earlier episode of brine reflux.

Lucia (1968) subsequently drilled beneath the Pekelmeer Lagoon and found no widespread dolomites in the underlying Pleistocene carbonates. He also found that porewaters were of normal marine salinity in areas where brine was predicted by a seepage reflux model. A thin clayey ash layer of generally low permeability was found forming a hydroseal that separated sediments below with normal salinity from lagoonal sediments with elevated salinity. Thus, reflux was not occurring beneath the lagoon. Springs supplying seawater to the salina were in areas where the ash bed was broken or missing and formed the terminations of flow pathways in the underlying Pleistocene/Pliocene (Murray, 1969). For most of the year seawater seeped into the springs driven by evaporative drawdown. However, during a short period in the late summer, the springs were inactive and the hydrostatic pressure on the landward side was greater than that on the seaward side. Murray concluded that return flow or reflux could occur at such times but did not appear to do so with sufficient volumes of brine to form replacement dolomite.

[2] A saltern is an area of widespread subaqueous shoal water evaporite deposition (from [Warren, 1999, p. 69]).

A.

	Flow length (km)	Volume of slice (m^3)	Required Mg (kg)	Required volume (m^3)	
				brine 1	brine 2
1	1	1×10^5	3.5×10^6	5.19×10^6	2.59×10^6
2	10	1×10^6	3.5×10^7	5.19×10^7	2.59×10^7
3	100	1×10^7	3.5×10^8	5.19×10^8	2.59×10^8
4	1000	1×10^8	3.5×10^9	5.19×10^9	2.59×10^9

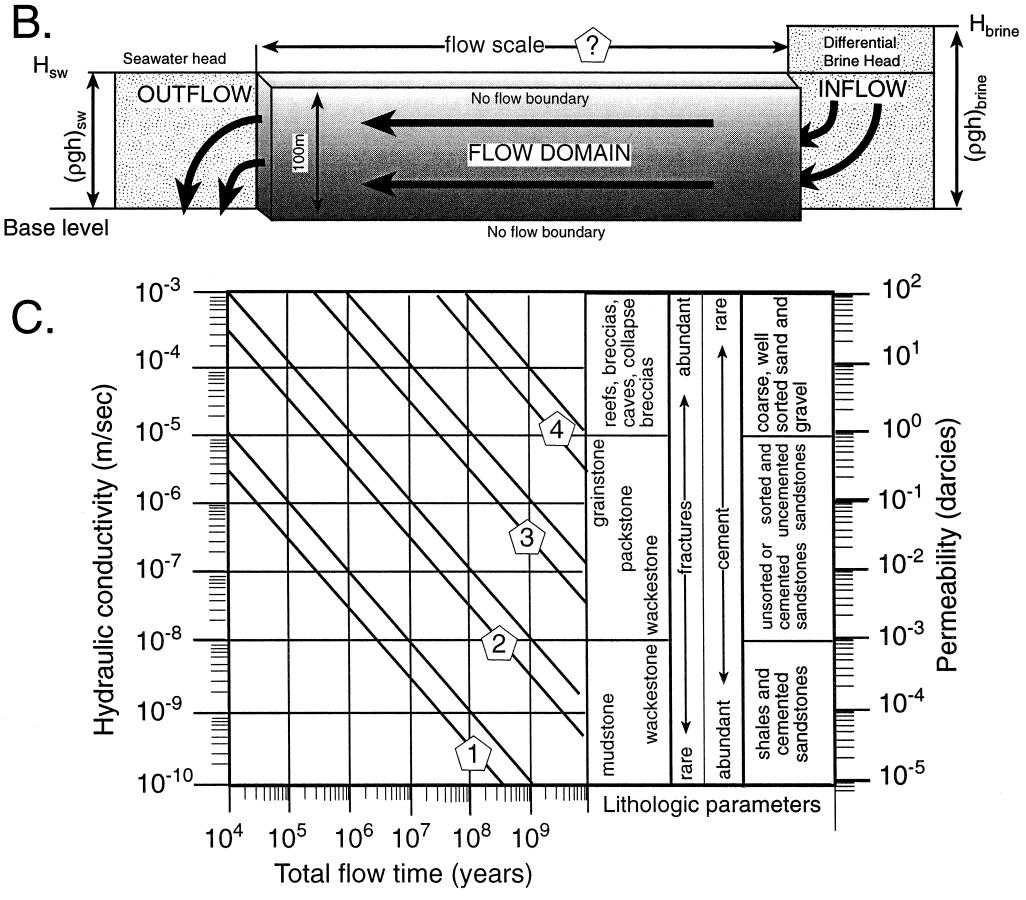

Fig. 13. Dimensional analysis of seepage reflux (after Shields and Brady, 1995). (A) Table of brine properties and amount of Mg required to convert calcite to a dolomite with 7% porosity. (B) Dimension of slice model used in their calculations. Slices are similar except that flow length varies from 1 to 1000 km. Base level is 100 m in all cases and head drops are 9.3 m for anhydrite saturated brine 1 and 17.1 m for halite saturated brine 2. (C) Dimensional analysis of Darcy's Law for a regional brine reflux system with 100 m base level. Diagram illustrates the time necessary for the minimum volume of dolomitizing brine to flow through a rectangular slice. All slices are 100 m thick and 1 m wide with varying flow lengths (1–4). It is assumed 350 kg/m^3 of Mg are required to dolomitize the block. The lower curve for each flow path represents brine at halite saturation with a Mg exchange efficiency of 47%. The upper curve represents brine at anhydrite saturation with a Mg exchange efficiency of 36%. Permeability conversions assume an average brine density of 1160 kg/m^3 and a viscosity of 8.904×10^{-3} $kg/(m/s)$ and a temperature of 40°C.

The claim that the Pekelmeer was forming extensive seepage reflux dolomites beneath an evaporite lagoon was further challenged when Sibley (1980) concluded that the solutions responsible for extensive dolomitization in Tertiary sediments on Bonaire (dolomites that were earlier used as evidence for reflux dolomite) were probably fresh to brackish meteoric waters mixed with seawater, and were not derived by reflux of the modern Pekelmeer hydrology. Later work by Fouke et al. (1996) on dolomite in the Seroe Domi (Miocene), a unit more than 20 m thick that extends 115 km across the Nederlands Antilles, has reinforced Sibley's conclusions. However, Lucia and Major (1994) continue to argue for a significant input of marine/hypersaline waters during Neogene dolomitization in the region.

There are, nevertheless, other islands in the tropics where localized brine reflux, associated with hypersaline conditions, is apparently forming Holocene dolomites. Müller and Teitz (1971) documented brine-reflux dolomite replacing an earlier carbonate cement in skeletal grainstones on the shoreline in Fuerteventura in the Canary Islands. Kocurko (1979) found brine-reflux dolomite a few meters above the high tide line, in the spray-zone pools of the shoreline of San Andres, Columbia. Aharon et al. (1977) described small volumes of reflux dolomite forming in Holocene sediments of "Solar Lake" a small coastal salina in the Gulf of Aqaba. Thin, localized brine-reflux dolomites can also be found about the present-day edges of Ras Mohammed on the Sinai Peninsula (see Warren, 1991 for a summary discussion of these deposits).

The hydrologies of modern brine-reflux dolomites never approach the scale of processes required to dolomitize shelf carbonates adjacent to ancient evaporites. This lack of parity is more than just a reflection of reaction kinetics; there is also a problem of parity of depositional setting. Many ancient evaporite deposits have no modern counterparts (Warren, 1999). In modern settings, where reflux dolomites have been noted beneath evaporite crusts, the areas of evaporite precipitation are small scale and localized. Their inherently small fluid potentials are caused by drawdown of no more than a meter or two through highly permeable sand/coral barriers no more than a few hundreds of meters to a kilometer or two wide. Modern coastal-margin evaporite systems, precipitate salts within platform hydrologies that in many areas have yet to reach equilibrium with the last sealevel rise. They lack extensive evaporites, sizeable brine volumes, and stable platform-wide groundwater/density heads capable of circulating large volumes of Mg-rich fluids into underlying limestones.

Hydrological modeling of ancient reflux systems by Shields and Brady (1995), using very conservative assumptions of brine head and drawdown, show that reflux can explain platform dolomites within geologically realistic time frames of burial (Fig. 13). Their flow model used flow lengths varying from 1 to 1000 km and the relative densities of seawater and brines of two end member compositions (Fig. 13A): brine 1 is anhydrite-saturated (density $\rho = 1120$ kg/m^3) and brine 2 is halite-saturated ($\rho = 1200$ kg/m^3). Brine 1 is approximately 9.3% denser than seawater ($\rho_{\text{seawater}} = 1024.5$ kg/m^3), and brine 2 is 17.1% denser. Using a 100 m tall and 1 m wide flow cell (Fig. 13B), brine 1 has approximately 9.3 m more hydraulic head than a comparable column of seawater while brine 2 has a differential hydraulic head of 17.1 m. Shields and Brady (1995) assume a pure calcite precursor and a final product that is 100% dolomite with 7% porosity; this requires 350 kg/m^3 of magnesium. The results (Fig. 13C) show that reflux flow could circulate the Mg necessary to completely dolomitize carbonate platforms with radii of a few tens of kilometers in a few million years. Shelves with shoreline-to-basin distances of the same order can be completely replaced in a similar period. Larger platforms require more time or that the evaporite recharge areas migrate with time. Carbonate platforms tens to several hundred kilometers across could be dolomitized by such hydrologies.

The relative abilities of rocks to transmit fluids will control where the bulk of the fluid flux occurs within platform limestones. Kaufmann's (1994) and Shields and Brady's (1995) models show that it is unrealistic to think of reflux dolomitization as a homogenous process uniformly overprinting all platform limestones. The inherent permeabilities of the various precursors clearly play an important role in dolomite intensity. The most permeable lithologies beneath the evaporite lagoon will focus the bulk of flow as the brine seeps seaward. Whatever unit is acting as the aquifer at the time of reflux will also be

the subject of the most intense dolomitization. High permeability units within flow paths of tens to hundreds of kilometers can channel the volume of necessary brine in time frames ≈ 1 Ma. Such high permeability units also have the potential to be dolomitized in regions well removed from the brine source (discussed in the porosity and permeability section later in this review).

The validity of reflux as a mechanism in ancient carbonates is reinforced by the depositional settings of ancient evaporites. Many authors have concluded that brine-reflux models can explain ancient thick (tens to hundreds of meters), laterally extensive (thousands to millions of square kilometers), "secondary" dolomites associated with evaporites or evaporite–dissolution breccias (Land, 1985; Machel and Mountjoy, 1986; Hardie, 1987; Warren, 1991).

The present may be the key to the past but it is simply not a good time to document depositional or diagenetic analogues for ancient platform and basinwide evaporites (Fig. 14; Warren, 1999). There are no modern counterparts to most types of ancient marine-platform and basinwide evaporites, hence, there are no modern counterparts to brine-reflux dolomites. Holocene evaporites are accumulating within an "icehouse" climatic phase. The current "icehouse" mode, typified by waxing and waning polar icesheets, has dominated the earth's climate for the last 12 Ma. "Icehouse" times, with their high frequency sealevel oscillations, are not conducive to the formation of thick platform evaporites. In contrast, "greenhouse" time, with their inherent lack of polar ice sheets, favor the formation of platform evaporites and, hence, widespread reflux dolomitization of platform carbonates. Basinwide evaporites and their associated dolomites form via tectonic controls on basin isolation that are independent of "icehouse versus greenhouse" sealevel scenarios.

An inherent problem with reflux hydrology, as inferred by Adams and Rhodes (1960), is that it requires reflux-associated evaporite deposition to occur in a lagoon with a surface connection to the open ocean. This was the prevailing understanding of a silled evaporite basin in the 1950s and was based on the models first postulated by Oschenius in the 1870s. We now know it requires near impossible internal

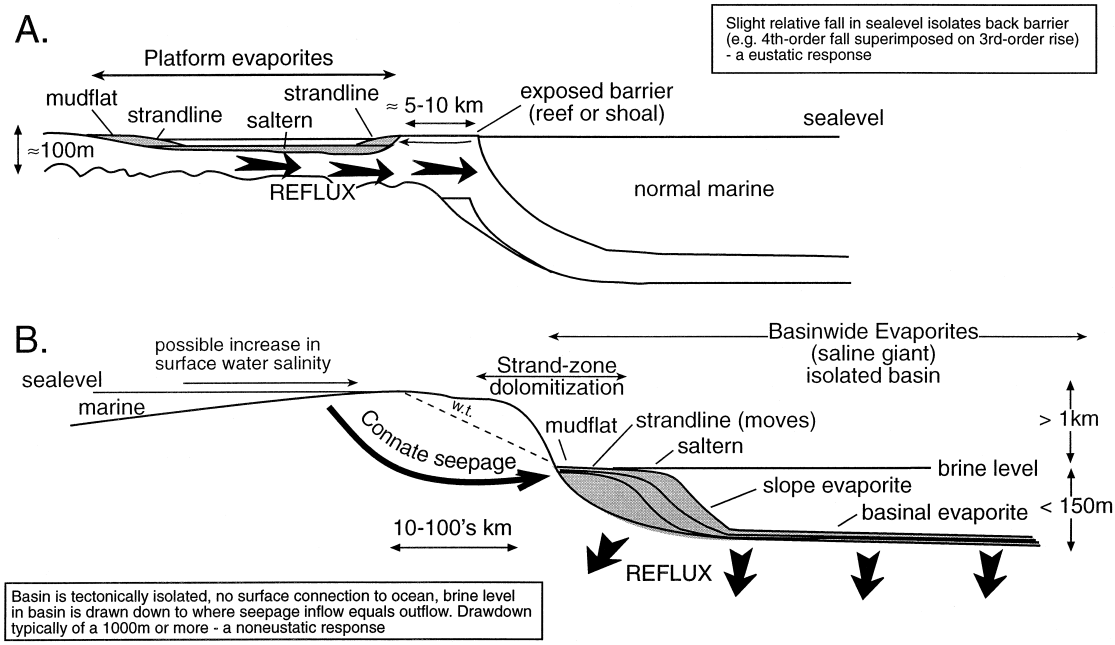

Fig. 14. Ancient evaporite settings that have no modern analogues (after Warren, 1999). (A) Platform evaporites, a combination of saltern and evaporitic mudflat sediment. (B) Basinwide evaporites, a combination of evaporitic mudflat, saltern, slope and basinal sediment (see text for explanation). Scales are schematic.

hydrologies involving sloping haloclines and brines of differing densities simultaneously depositing carbonate, anhydrite and halite within a single brine body connected at the surface to open marine waters. Such models are no longer considered physically viable for the deposition of widespread subaqueous evaporites (Lucia, 1972; Kendall, 1988, 1989; Warren, 1999). At times when widespread platform or basinwide evaporites were deposited, the accumulating evaporite area was not connected at the surface to the ocean. Much of the influx of seawater to the depression was via phreatic connate seepage through the margin of the brine lake or seaway.

Ancient marine-associated evaporites deposited either as platforms or as basinwide salts (Warren, 1999). Brines ranged from ephemeral to "deep" perennial, although most permanent brine bodies were less than a few tens of meters. Platform evaporites typically accumulated within carbonate platforms during minor falls in sea level following, or during, third order transgressions in times of "greenhouse" earth (Fig. 14A). These set up eustatically isolated platforms behind carbonate rims or shoals. In contrast, the larger volumes of basinwide evaporites accumulated in both "greenhouse" and "icehouse" climatic modes but required tectonic isolation of basins within a suitably arid climate. In this scenario, the center of the basin is the locus of thick subaqueous evaporite accumulation, while much of the former basin margin or platform is a subaerially exposed seepage system (Fig. 14). Under both platform and basinwide conditions, evaporative drawdown allows bedded salts to accumulate subaqueously in brine-filled depressions and seaways of varying depth (Kendall, 1992; Warren, 1999).

Within platforms, drawdown moved phreatic seawater into the rocks beneath the exposed rim, under head differences of no more than a few to tens of meters. At the same time, solar concentration in the isolated seaway created dense Mg-enriched that seeped downward as brines plumes or curtains into underlying limestones. Most published reflux models utilize a platform evaporite setting. Examples of brine reflux dolomites within carbonate platforms include: the Cambrian Ouldburra Formation in the Officer Basin, Australia (Kamali et al., 1995); the Devonian Birdbear (Nisku) Formation of Canada (Whittaker and Mountjoy, 1996); the Permian San Andres Formation, USA (Leary and Vogt, 1986; Ruppel and Cander, 1988; Elliott and Warren, 1989); the Permian Tansill and Yates formations of the Central Basin Platform, USA (Andreason, 1992; Garber et al., 1990); the Jurassic Smackover and Haynesville Formations of the Gulf of Mexico (Moore et al., 1988); the Lower Cretaceous Edwards Formation of Texas (Fisher and Rodda, 1969) and the Middle Palaeocene Beda Formation, of the Sirt Basin, Libya (Garea and Braithwaite, 1996).

The hydrology of such platform-evaporite associated systems responds to eustatic fluctuations that also control the geometries of the associated platform carbonates. It deposits interlayered platform carbonates and evaporites, where beds are of the order of tens of meters thick and salt beds are interlayered with restricted to normal marine platform carbonates (Fig. 14A). Reflux dolomitization in this setting can be easily recognized, even in core, as the intensity of dolomitization decreases the further down core or laterally one moves from the evaporite–carbonate contact (Fig. 15). If not completely re-equilibrated during later burial dolomitization, the oxygen isotope signatures of platform dolomites formed by reflux typically follow a lightening trend away from the evaporite unit; that is, the further one moves from the contact, the less was the sediment's isotopic signature influenced by the heavier reflux-derived brines. Although they may also be remobilized by later burial dolomitization, trace elements can give another clue to a reflux association. Sass and Bein (1988) found Neogene to Permian dolomites associated with gypsum/anhydrite tend to show 50%–57% $CaCO_3$ and the highest levels of sodium (up to 2700 ppm). Marine nonevaporitic dolomites (the counterparts of subtidal dolomites discussed earlier) have similar compositions, but sodium concentrations of only 150–350 ppm.

In contrast to well-documented platform evaporite associations, models of basinwide evaporites (saline giants) have only gained widespread acceptance in the geological community in the last decade. This reflects the acceptance that the Mediterranean formed such a drawdown salt giant in the Messinian some 5.5 Ma. Models of dolomitizing hydrologies in saline giants are more complicated than those of reflux dolomites within platforms, and are still under study. When basinwide evaporite systems were actively

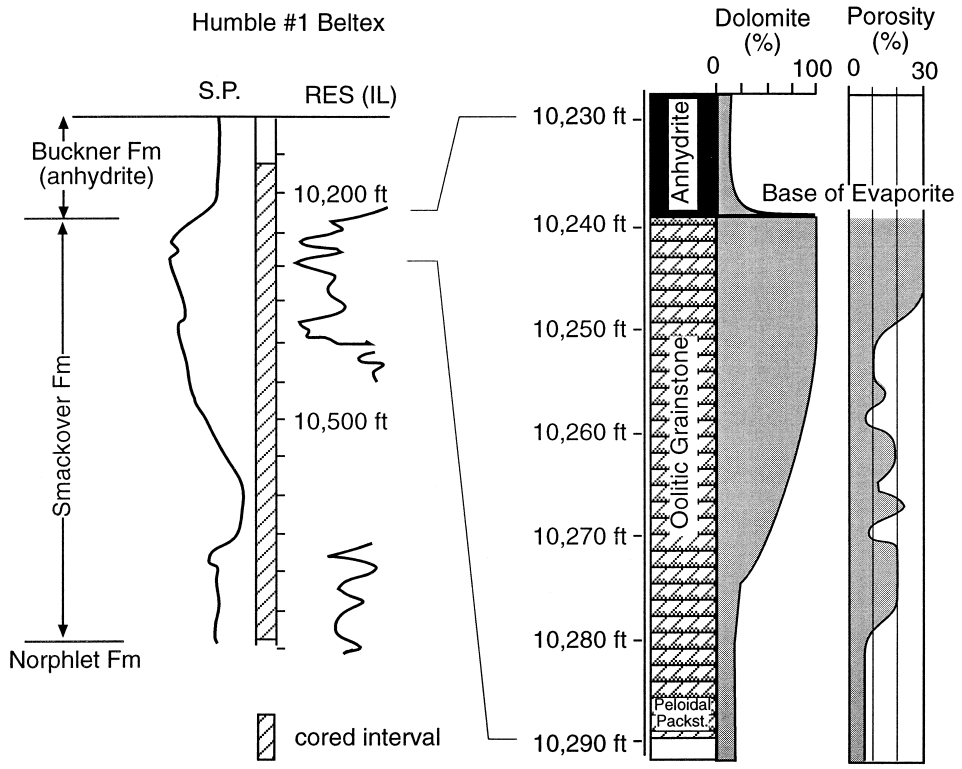

Fig. 15. Wireline signature and the interpreted core description of the Humble #1 Beltex Well, Bowie County, TX, show a close relationship between Buckner anhydrite and dolomitization in the underlying Smackover Formation. Note the changes in the proportion of dolomite and porosity in terms of proximity to evaporite contact (after Moore et al., 1988). Smaller scale porosity fluctuations within the dolomite indicate the effect of varying grain size, sorting and marine cementation in the limestone precursor.

accumulating salts, the salt beds were tens to hundreds of meters thick and deposited across brine-covered areas in the basin center that were hundreds to thousands of kilometers across (Fig. 14B). The system was driven by evaporative drawdown of the order of hundreds to thousands of meters. The strand zone about the edges of such perennial brine lakes and seaways moved rapidly over lateral distances of tens to hundreds of kilometers.[3] In contrast, the zones beneath more central regions that permanently covered by brine were continuously subject to reflux related to a permanent brine curtain (Warren, 1999).

The hydrological and diagenetic character of basinwide systems summarized in this section is based on published studies of the more accessible examples at outcrop in the Messinian evaporite/dolomite associations of the circum-Mediterranean (Sun and Esteban, 1995; Meyers et al., 1997), the Permian Zechsteinkalk dolomites of NW Europe (Clark, 1980; Smith, 1981) and the Devonian evaporites and dolomites of the Keg River-Pine Point Presqu'ile of Canada (Maiklem, 1971; Davies and Ludlam, 1973; Bebout and Maiklem, 1973; Skall, 1975; Kendall 1989) as well as my own work in these and other evaporite basins (see Warren, 1999; Chaps. 2 and 3 for a discussion of the hydrology and sedimentology of ancient evaporite basins).

Drawdown basins have the potential to flush huge volumes of waters through the basin edge as waters

[3] Flood and ebb cycles of the strandzone in basinwide evaporite settings are autocyclic and are driven by tectonism and climate change. The brine levels in saline giants are not related to marine tidal or sealevel influences. Hence, the use of the term peritidal or supratidal is inappropriate in describing the evaporites of these regions [(Warren, 1999; Chap. 3)].

in the basin center are lost by evaporation. These waters are continuously replaced via the seepage influx of varying proportions of: (a) phreatic seawater (connate water) seeping in through the basin edge; (b) subsurface waters whose lateral movement to the basin floor is driven by the kilometer-scale drawdown of the water level in the basin; and (c) by much smaller and episodic influxes of meteoric water (Figs. 14b and 16a). Potentiometric heads are not measured in meters but hundreds of meters. The position of seepage outflow zone is controlled by the edge of the perennial brine pool or seaway (Warren, 1999; Chap. 2).

As well as the primary dolomite that formed thin beds intercalated with the evaporites in such systems, there are two styles of more widespread diagenetic dolomite formed in carbonate aquifers that underlie and surround the drawdown basin. Their precipitation is driven by a hydrology inherent to the huge isolated depressions that accumulated basinwide evaporites. Style 1 are "strand-zone dolomites"[4] created by the mixed water hydrology that is inherent to regions subject to the rapid migration of the permanent edge of the perennial brine lake or seaway. Style 2 are classic reflux dolomites precipitated during the continual sinking of brine beneath the regions of a permanent brine curtain. Let us look at each in turn.

Maiklem (1971) and Kendall (1989) pointed out the potential for widespread dolomitization via seawater seepage and mixing zone interactions beneath subaerially exposed slopes about the drawndown basin margin of a saline giant (Fig. 16A). A groundwater-mixing zone develops where meteoric water floats atop denser seawater or saline brines. As the brine level in the basin responds to changes in tectonics and climate, this zone of mixed waters will move back and forth over the exposed basin edge. Fig. 16A is drawn assuming an unconfined aquifer separating the marine and seepage zones. The reality is much more likely to be a combination of confined and unconfined aquifers feeding predominantly seawater into the basin margin, as well as supplying connate crossflows beneath the descending brine plume of the basin center.

Outflow areas of resurging connate brine/meteoric waters develop characteristic sets of pisolitic/tepee cementstone lithologies termed strandline/seepage facies by Warren (1999). Kendall (1992) shows how this carbonate seepage facies can be used to define seawater and mixed-brine outflow points in the Devonian Keg River basin (Fig. 16B). Aprons of such spring-fed sediments are typically located about exposed former shelf slopes and bioherms. These permeable regions acted as aquifer outflow zones that were sometimes capable of breaching the active reflux curtain well out onto the basin floor (Fig. 16A,B; see Warren, 1999 for a more detailed discussion). Slightly down dip of this seepage facies, evaporitic mudflats are dominated by capillary anhydrite and halite fabrics, which pass into perennial surface brine bodies (the halite seaways of the Keg River Basin) on the lowermost sections of the basin floor.

In the past 5 years, more geologists have come to accept that the strand-zone edges of drawdown evaporite basins are subject to rapid climatic and water level oscillations. Thus, modified mixing-zone models have been increasingly used to explain dolomites precipitated from mixed waters in strand-zones typified by marginal dolomitized/pisolitic carbonates, which are interlayered with the edges of basinwide evaporite units (Gill et al., 1995; Magaritz and Peryt, 1994; Meyers et al., 1997; Peryt and Scholle, 1996). Suitable mixing zones hydrologies beneath the drawdown strand-zone form either between meteoric and hypersaline waters edge, or between displaced connate waters and fresher phreatic waters. The widespread formation of strand-zone dolomites in a basinwide setting is a reflection of the interaction between climate and substantial drawdown (up to kilometers). Such an oscillating mixing-zone system is not as well developed in platform evaporite settings where the adjacent carbonate shoal rim typically allows drawdown that is usually a few meters and always less than 20–30 m.

Some of the hydrological details of the mixed-water strand-zone margins of drawdown basins can

[4] This is a new term, designed to emphasize the difference in hydrological setting of this style of dolomite formed where the "to and fro" of the edge of a perennial brine body across a laterally extensive strand-zone drives before it a mixing zone capable of dolomitization. The brine passage that helps form this type of dolomite lies up-dip relative to the classical reflux model.

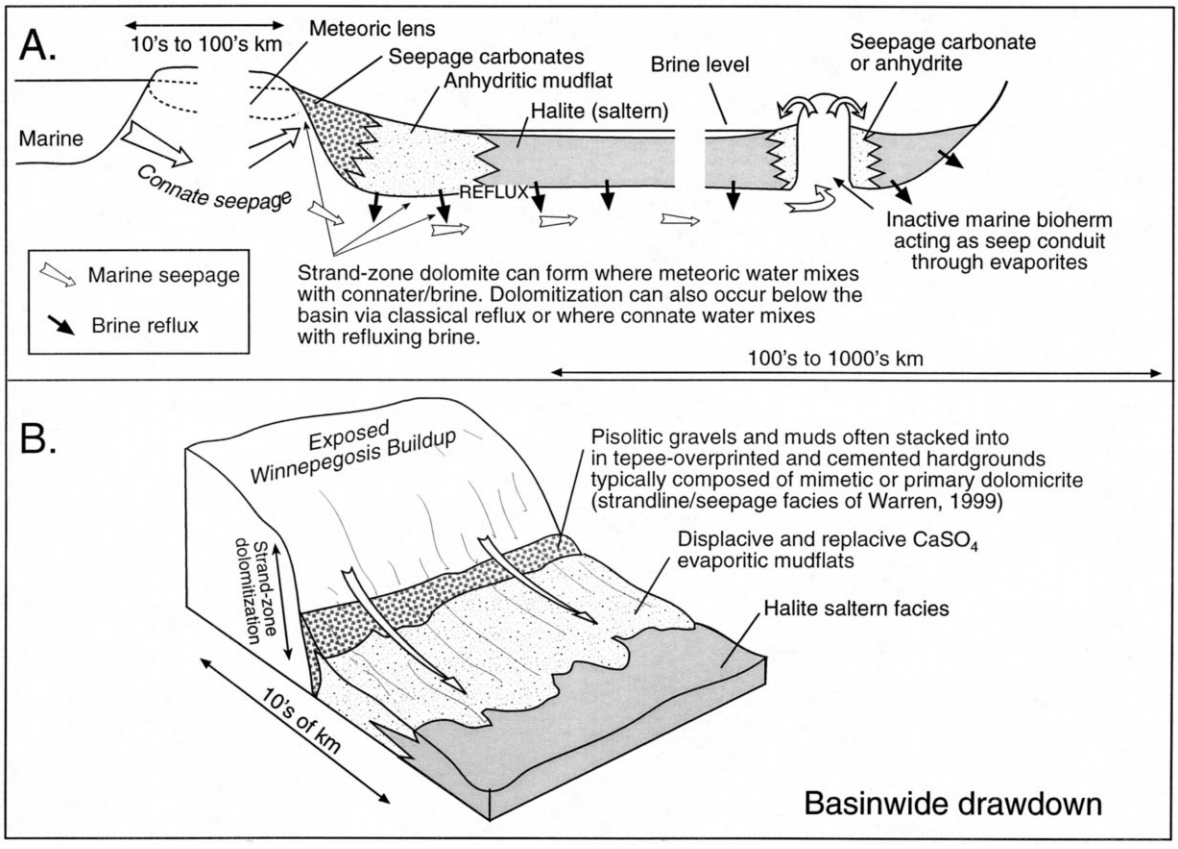

Fig. 16. Evaporative drawdown dolomitization. (A) Hydrology of basin showing seepage facies and halite in basin centre. Note the potential for the mixing of connate seepage and meteoric waters with refluxing brines beneath the strand-zone about the margin of the drawdown basin and the influence of the reflux curtain across much of the interior of the basin. (B) Close-up of facies pattern and potential for at surface strand-zone dolomitization associated with seepage outflow zones, vertical exaggeration ≈ 10:1 (after Maiklem, 1971; Kendall, 1989; Warren, 1999).

be inferred from dolomite distribution within the edges of the Neogene evaporitic sub-basins of the Mediterranean. There, in various basinwide settings, the lateral movement of mixed-water zones were driven by fluctuations in the basin's brine level, which drove before it phreatic lenses of less dense waters. Meyers et al. (1997) described pervasive dolomites that cut across Miocene sequence boundaries in the Nijar Platform and occur in the youngest Messinian reef/oolitic units. They do not cross the Miocene–Pliocene unconformity, although dolomite is present as clasts in overlying basal Pliocene grainstones. This constrains the timing of the strand-zone dolomitization as latest Miocene and pre-Pliocene in age, suggesting that widespread and pervasive dolomitization occurred within 600,000 years and possibly in less than 200,000 years. Such a short time frame underlines the effects of high levels of Mg throughput that typify concentrated seawater pore brines in the fluctuating strand-zone of a drawdown basin (Warren, 1999). The high flow rates and Mg concentrations of waters in such basins means the time required for pervasive dolomite formation is much shorter than in regions of meteoric/seawater mixing (see dorag discussion in Section 4.4.2).

The carbon and oxygen isotopes of the Nijar dolomites show marked positive covariation, with most values ranging from +5.4‰ to −1.2‰ $\delta^{18}O_{PDB}$ and +2.5 to −4.3‰ $\delta^{13}C_{PDB}$ (Meyers et al., 1997). The highest $\delta^{18}O$ values are heavier than

reasonable estimates of Messinian normal-salinity seawater dolomites, suggesting the involvement of evaporative brines in the dolomitization process. Calculations of covariations of O and C isotopes during water–rock interaction and fluid-fluid mixing argue against recrystallization of Nijar dolomites, an interpretation supported by their Ca richness (49–57 mol%). Mixing calculations show that four-fifths of Nijar data are consistent with dolomitization by mixtures of freshwater and a few tens of percent of marine-derived evaporite brine, while one-fifth are consistent with mixtures of freshwater and normal-salinity seawater. Modeling of the covariations of $^{87}Sr/^{86}Sr$ and Sr/Ca ratios that developed during mixing, further supports involvement of evaporite brine, and suggests that any freshwaters involved in the dolomitization had low Sr/Ca ratios but relatively high Sr and Ca concentrations. Na, Cl, and SO_4 concentrations (200–1700 ppm, 300–600 ppm, and 600–6500 ppm, respectively) also argue for brine involvement and for mixings of brine with freshwater and/or seawater.

Meyers et al. (1997) argues that most dolomitization occurred after Messinian reef formation, during multiple brine level changes associated with basin-wide evaporite precipitation. Carbonate deposition on the Nijar shelf occurred during higher sealevels mostly prior to widespread evaporite deposition, while evaporite deposition took place nearer the sub-basin center during times of lowered water level and basin isolation (drawdown episodes). Brines with up to $5x$- to $6x$-seawater concentration developed on the floor of the basin during drawdown. At their most concentrated these brine precipitated widespread subaqueous gypsum. Fluctuating brine base levels, associated with the onset of intrabasinal transgressive episodes, drove before them zones of freshened/meteoric water that when mixed with the rising evaporitic pore brines were capable of dolomitization.

The problem with dolomite distribution in the various Messinian sub-basins of the Mediterranean is that studies are concentrated in the exposed margins of relatively small circum-Mediterranean sub-basins in Spain, Italy, Cyprus and Sicily. The rocks beneath the thick basin-center evaporite fills of the various sub-basins, where classic reflux dolomites are more likely, are only poorly exposed. Where exposed, as in the "Calcare di Base" in Sicily, they have been extensively dolomitized by refluxing brines (Schreiber, 1988; Warren, 1989). Offshore, the substrates of much larger 1–2 km thick saline giants, which now lie beneath the deeper parts of the Mediterranean, have yet to be drilled, yet it is these more basin central regions where classic reflux dolomites should occur. These thick salt deposits formed on the Messinian floors of huge saltern lakes/seaways during the period of maximum drawdown when smaller marginward sub-basins were largely inactive (Butler et al., 1995). Hence, we must go to older basinwide evaporite basins where the substrates to the thick evaporites are exposed to confirm the presence of reflux dolomite.

More basin-central reflux dolomitization processes have overprinted the Zechstein carbonates of NW Europe where dolomitized algal-bryozoan reefs, oolites and intertidal to shallow subtidal skeletal grainstones and mudstones underlie widespread thick evaporites. The same dolomites are also interlayered with the platform portions of basinwide evaporites composed of anhydrite and halite deposited during the complete isolation and drawdown of the Zechstein basin. It was at such time of drawdown that reflux dolomites replaced the underlying Zechstein limestones (Smith, 1981; Clark, 1980). At the same time, the regression of facies associated with the drawdown of the brine base level caused the encroachment and displacement of formerly marine water by hypersaline and meteoric waters about the basin margins (e.g. dolomites of the Magnesian Limestone; Kaldi and Gidman, 1982).

Away from the strand-zone of any saline giant, the downward reflux of Mg-rich brine into underlying sediments will ultimately mix with underlying connate waters and other sub-evaporite waters (Fig. 16B). This continuously replenished hydrology of descending evaporitic creates a brine curtain with a subsurface chemistry capable of leaching calcite and precipitating dolomite (Bein and Land, 1983). Beneath a saline giant, this seawater/hypersaline brine mixing zone may extend under much of the evaporite (Fig. 16A). Its extent and potential to dolomitize is possibly far greater than that of zones of meteoric/seawater mixing in the strand-zones of the same basins and it operates in the same way as reflux dolomites form in platform settings.

Brine entering an evaporite basin may be connate (phreatic seawater) or continental water mixed with seawater or meteoric water (see next section). So far in our discussion of evaporite-associated dolomite, we have assumed seawater-like ionic proportions. The fundamental chemical requirement to form a dolomite from brine is an increase in Mg/Ca ratio at elevated salinities. In this context, it is important to note that not all continental waters will achieve elevated Mg/Ca ratios at elevated salinities. Rather, it happens only to those waters that have parents with $Ca < SO_4$. This is the same relationship as seawater-derived brines where sulfate is always present in much higher concentrations than Ca (Fig. 17A). In contrast, a sulfate-depleted parent water ($Ca > SO_4$) will have residual calcium, even after all the $CaSO_4$ is deposited (Fig. 17B). This concentrates along with brine components, including Mg, until sodium salts are deposited. In this situation, the Mg/Ca ratio increases only slowly, so creating a brine chemistry that is less likely to precipitate dolomite.

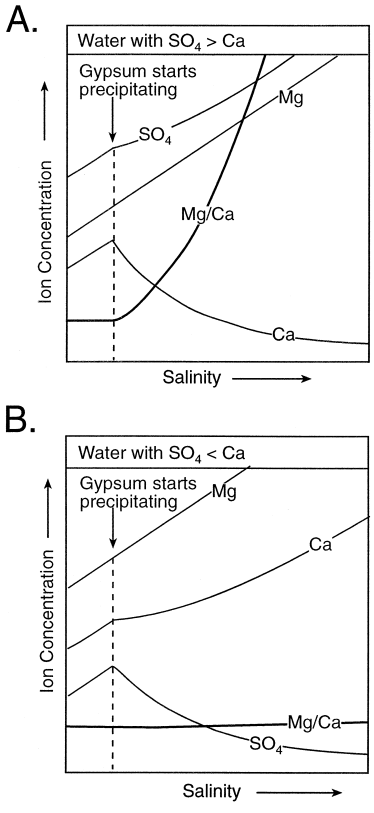

Fig. 17. Effect of ionic proportions in inflow water on Mg/Ca ratio in concentrating brine (after Hardie, 1987). (A) Concentration of seawater or continental water with $SO_4 > Ca$. (B) Continental water or brine with $SO_4 > Ca$.

4.4.2. Meteoric mixing zone dolomite

All the mixing zone model requires is the mixing of waters of two saturation states with respect to the minerals of interest (Fig. 18A,B). In the preceding section, we developed notions of dolomite formation around the margins of a drawdown basin by the mixing of phreatic seawater with hypersaline brines or meteoric waters. At the same time, more extensive reflux dolomites were forming in zones of mixing between phreatic seawater and refluxing brines below the central portions of a saline giant.

However, for more than three decades, a mixing zone model has been invoked to explain ancient subtidal shelf dolomites that were not associated with contemporaneous evaporites. The dolomitization event was typically a relatively early diagenetic episode (prior to mechanical grain compaction). In this nonevaporitic scenario, the mixing was envisioned as involving freshwater and seawater in a phreatic marine coastal zone. This is the "mixing zone" model used by Hanshow et al. (1971) to explain dolomite in the Tertiary limestone aquifers in Florida and by Land (1973) to explain dolomites in the Hope Gate Formation, Jamaica.

Badiozamani (1973) in a keynote paper used a meteoric-seawater mixing-zone model to explain extensive Middle Ordovician shelf dolomites that were again not associated with evaporites. He called this "dorag dolomitization"; *dorag* is Persian or Farsi for mixed blood. His model involved creating a dolomitizing solution by the subsurface mixing of seawater with meteoric water. Other examples of ancient meteoric-seawater mixing zone dolomites include the Palaeoproterozoic Malmani Dolomite of the Transvaal, South Africa (Eriksson and Warren, 1983), the Silurian reefs of Michigan (Sears and Lucia, 1980); the Devonian of Guangxi, south China (Xun and Fairchild, 1987); the lower Visean of Belgium (Muchez and Viaene, 1994); and the Jurassic reefs in the Jura of eastern France (Fookes, 1995).

Chemically, the mixing zone theory is straightforward and follows a very simple geochemical law.

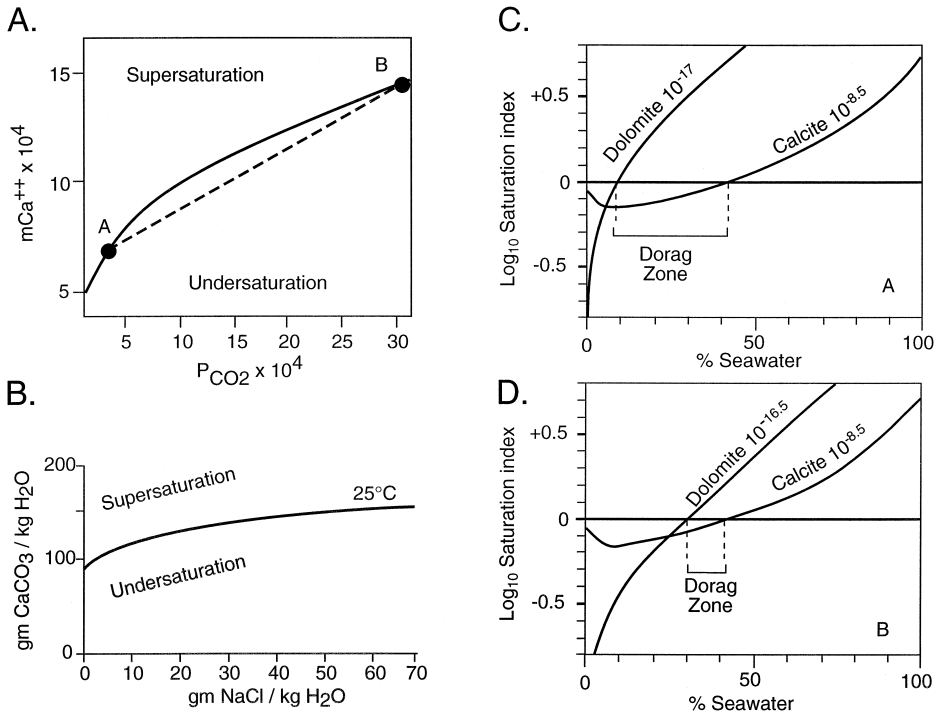

Fig. 18. Mixing-zone solubility curve chemistry. (A) Solubility of calcite as a function of partial pressure of CO_2. When solution A mixes with solution B the result (lies on dashed line AB) is undersaturated with respect to calcite (after Runnells, 1969). (B) Solubility of calcite with respect to salinity (after Runnells, 1969). (C) Solubility curves for dolomite and calcite in a seawater/freshwater mixture. Dolomitization is thought to occur in the zone where the mix is undersaturated with respect to calcite and supersaturated with respect to dolomite (this is the "dorag zone"). This curve is calculated using a $K_{sp} = 10^{-17}$, the value of ideal dolomite as used by Badiozamani (1973). (D) Solubility curve using dolomite $K_{sp} = 10^{-16.5}$, the value for typical disordered dolomite precipitates as estimated by Hardie (1987). Note the much narrower dorag zone (C and D after Hardie, 1987).

When two waters that are saturated with a particular phase are mixed, the resulting solution may be undersaturated with respect to that particular phase, while at the same time may remain saturated with respect to another mineral phase. The saturation state during mixing depends on the solubility curve of the mineral phase of interest (Runnells, 1969). The only requirement is that the solubility curve for that particular component is nonlinear. Consider the solubility curve of calcite as a function of the partial pressure of CO_2 (Fig. 18A) or as a function of salinity (Fig. 18B) When two waters are mixed (e.g. A and B in Fig. 18A) then the resultant solution is undersaturated with respect to calcite, which is thus liable to dissolution (the dashed line in Fig. 18A).

Fig. 18C shows theoretical saturation curves for both calcite and dolomite in varying mixtures of seawater and freshwater. It indicates that there is an interval of mixing (10%–35% seawater using the data of Badiozamani, 1973) where the solution is undersaturated with respect to calcite but supersaturated with respect to dolomite. This is the interval where mixing zone dolomitization is theoretically possible. The resultant texture should show evidence of calcite dissolution and dolomite precipitation. Hence, when CO_2-saturated meteoric groundwaters are diluted by seawater they will maintain the same Mg/Ca ratio but, because of lowered ionic strength, the lowered concentrations of sulfate, and the increased proportion of carbonate over bicarbonate in the solution, are more liable to precipitate dolomite (Fig. 19; Lippmann, 1973; Folk and Land, 1975). The magnesium ions that maintain the high Mg/Ca ratio of the diluted solution are derived mainly from the seawater, but some can also come from the carbonates dissolved in the mixing-zone. Many

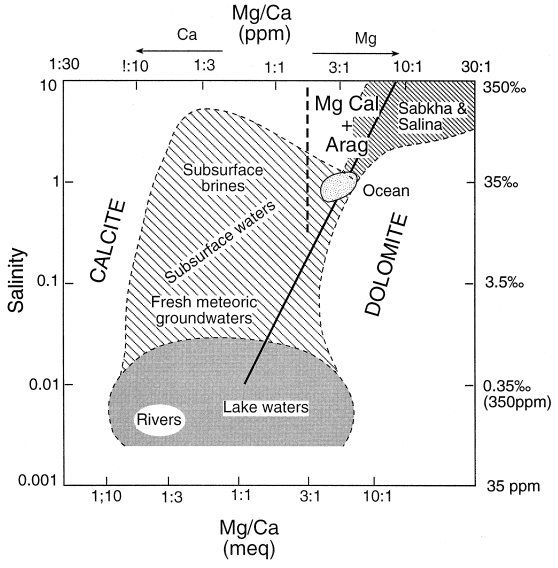

Fig. 19. Stability of major carbonate minerals in relation to Mg/Ca ratio and salinity of natural waters. Note how dilution in seawater or a brine by fresh groundwaters can move the solution into the dolomite stability field (after Folk and Land, 1975).

dolomite crystals from the Plio-Pleistocene mixing zones of the Caribbean region display distinctive cloudy centers surrounded by clear limpid rims. Sibley (1980) suggested this was a result of pore fluid evolution from a state of near saturation with calcite in the early stages of crystal growth to a state of undersaturation as growth continues in the mixing zone.

Recently, some workers have come to question the validity of a mixing zone between meteoric and seawater providing a viable mechanism for widespread platform dolomitization (Hardie, 1987; Machel and Mountjoy, 1986; Machel and Burton, 1994). Hardie (1987) showed that if the solubility products for the more soluble disordered dolomites that are the modern day precipitates ($K \approx 10^{-16.5}$) are used instead of the values that Badiozamani (1973) used, based on ancient stoichiometric dolomites ($K = 10^{-17}$), then the range of fluid composition suitable for mixing-zone dolomitization is greatly reduced (Fig. 18D).

The type example of Quaternary mixing zone dolomite is the Golden Grove dolomite in Barbados, as documented by Humphrey and Quinn (1989), has been shown by Machel and Burton (1994) not to be a meteoric-influenced precipitate. Their isotopic and chemical data show the dolomitizing fluid most likely was seawater of slightly variable temperature and/or slight degrees of evaporation, with enriched levels of bicarbonate from the local oxidation of methane. Even Land (1991), one of the leading proponents of mixing zone models in the early 1970s, has now come to the conclusion that the Neogene dolomites in the Hope Gate Formation of North Jamaica, which he once documented as type examples of a meteoric influence, are not mixing zone dolomites but are seawater derived.

There are very few examples of dolomite forming in an active mixing zone in recent sediments (Ward and Halley, 1985). One lies in the coastal plain of Israel, where Magaritz et al. (1980) reported dolomite cements composed of subhedral rhombs up to 50 μm across occurring in two distinct horizons in the Quaternary calcareous sands of the coastal aquifer. The shallower horizon is in the present mixing zone, the deeper is interpreted as an earlier mixing zone. However, the dolomites are found only as void-filling cements, and never appear to replace or develop pseudomorphs of a $CaCO_3$ phase as the ideal mixing zone model requires. Another possible example occurs in Eocene dolomites in central western Florida (Cander, 1994). Here, in a 20-m-thick interval, localized modern mixing zone dolomite overgrows precursor crystals of pervasive reflux dolomite. Interestingly, the mixing zone dolomite does not form in limestone equivalents of the same aquifer where calcite and not dolomite forms the substrate.

The formation of extensive shelf dolomites by diluted waters of a meteoric-seawater mixing zone probably requires a more stable hydrology in a shelf than has prevailed throughout the Quaternary. This has been a time of rapid, glacially induced sealevel change ("icehouse" earth). Few if any stable hydrological systems have yet formed along the coastlines of the world. The depositional systems, dynamics, and subsurface hydrologies of most present-day coasts are still adjusting to a sealevel rise of 120 to 140 m in the last 18,000 years. Such rapid changes in sealevel and the associated climatic changes have led to frequent and rapid changes in the position of shelf mixing zones over the last 1 to 2 million years. The mixing-zone model may have application in

ancient sequences, yet, like the examples of reflux dolomite in today's "icehouse" world, it cannot be fully tested within the short hydrological histories of present carbonate shelves.

Ye and Mazzullo (1993) suggested that meteoric dilution of seawater/evaporitic brines drove precipitation of the bulk of the platform dolostones in the Permian (Lower Leonardian) Wichita Formation in the Midland Basin, Texas. There are three dolostones in these regionally widespread platform dolomites: (1) nonporous dolostones comprising supratidal-intertidal facies (2) porous dolostones comprising subtidal–intertidal facies (3) porous subtidal dolostones. These consist of two types of dolomite, finely crystalline (5–40 μm) dolomite occurs in all three dolostones and has a mean $\delta^{18}O$ composition of +0.6‰ PDB, but is enriched in $\delta^{18}O$ by as much as 3.3‰ relative to estimated lower Leonardian sea water ($\delta^{18}O_{seawater} = -1.7‰$ to $-1.9‰$ during Leonardian; Ye and Mazzullo, 1993). This is best preserved in the supratidal–intertidal dolostones. More coarsely crystalline (> 40 μm, mean = 78 μm) dolomites are more common in the subtidal and subtidal–intertidal sediments. These have $\delta^{18}O$ compositions that are slightly lighter (mean = −0.25‰) than the finely crystalline dolomites, but are still enriched by a mean of 1.6‰ relative to Leonardian sea water (Fig. 20A). All these dolomites are near-stoichiometric, with $^{87}Sr/^{86}Sr$ within the range of values of lower Permian seawater. The coarse crystalline dolomites are more depleted in Sr, Mn, and Fe than the finely crystalline forms although all dolomites, regardless of crystal size, contain less than 125 ppm Sr and less than 100 ppm Mn (Fig. 20B,C).

The petrographic and geochemical data of Ye and Mazzullo (1993), in conjunction with their modeling of isotope data, suggest: (a) finely crystalline dolomites formed and evolved penecontemporane-

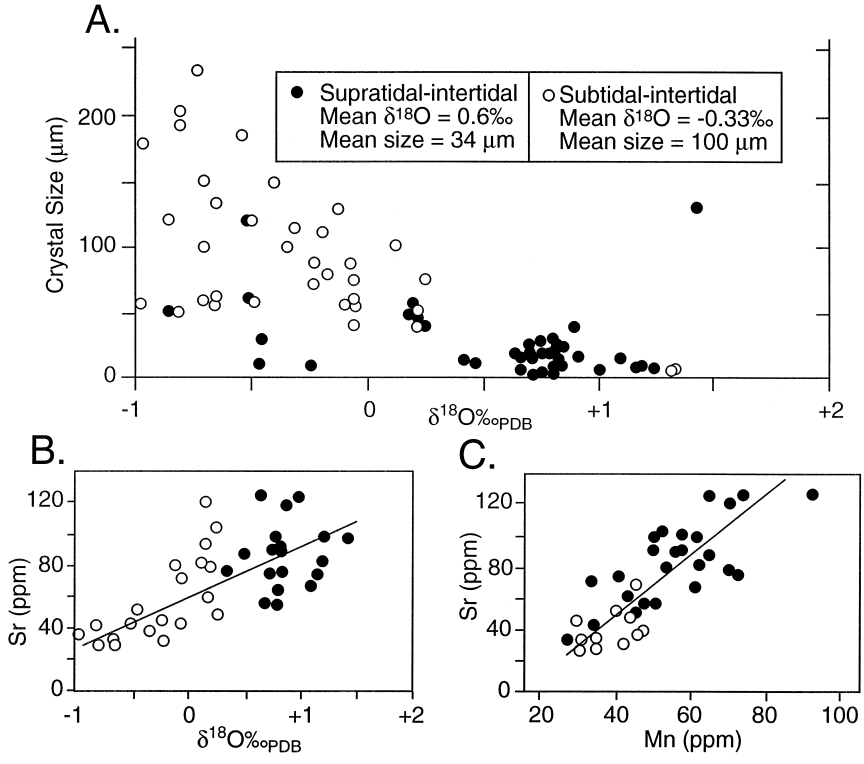

Fig. 20. Isotope and trace element signatures of Permian Wichita Formation, TX (after Ye and Mazzullo, 1993). (A) Oxygen isotope composition versus crystal size. (B) Oxygen isotope composition versus Sr concentration. (C) Sr versus Mn.

ously to 40 μm crystals in supratidal–intertidal settings. These were flushed by contemporaneous hypersaline fluids. Oxygen isotope values and trace element data suggest that these waters were not much more saline than seawater and had not attained the levels required to precipitate evaporite salts. (b) Enhanced fluid flow continued through more porous, subtidal and subtidal–intertidal dolostones syndepositionally or following very shallow burial. This resulted in further transformation of the micritic dolomite into mosaics of >40 μm crystals. Despite the slightly evaporitic setting, these later fluids were most likely of near-normal marine salinity and were probably derived by periodic meteoric dilution of hypersaline Leonardian marine pore waters. The oxygen and Sr isotope data, along with the lowered Mn composition, suggest these fluids were similar to those that precipitated the initial fine-grained dolomite. Most alteration occurred during relatively shallow burial (<1.5 km) by flushing by near normal marine waters with only minor meteoric mixing.

4.4.3. Organogenic / methanogenic dolomite in hemipelagic marine sediments

Precipitation from normal seawater today forms dolomites that are less than 1% of the total sediment volume (see section Dolomite from normal seawater). However, much higher proportions of dolomite (up to 10% of a 100-m-thick section) occur locally beneath organic-rich deep-marine sediments in the Gulf of California (Baker and Kastner, 1981; Morrow and Ricketts, 1988). Baker and Kastner (1981) demonstrated experimentally that the rate of dolomitization is increased when the level of sulfate is decreased. They concluded that high levels of sulfate, such as in normal seawater, inhibit dolomite formation. By contrast, the low sulfate levels, found in marine pore fluids that have undergone microbial reduction in organic-rich sediments, may create suitable environments for dolomite precipitation. Such reactions can be expressed chemically as:

$$2CH_2O\,(\text{organic material}) + SO_4^{2-} \rightarrow H_2S + 2HCO_3^-$$

However, Baker and Kastner's (1981) experiments were conducted at temperatures of 200°C and their extrapolation to the lower temperatures that occur beneath the deep sea floor may not be justified. Their conclusions are disputed by many dolomite workers who have argued that the presence of sulfate encourages dolomitization (Eugster and Hardie, 1978; Land 1985; Hardie, 1987).

The common association of gypsum/anhydrite with mimetic dolomite in ancient evaporite successions (e.g. Warren, 1991, 1999) argues against the inhibition of dolomite formation by high sulfate levels in ambient waters. Hardie (1987) suggested that the precipitation of dolomite in areas of sulfate removal may be more related to the local enrichment in HCO_3^- (alkalinity) rather than the dissolved sulfate acting as an inhibitor to precipitation. The other significant factor in the formation of organogenic dolomite is the ubiquitous presence of bacteria in the zone of sulfate reduction and the underlying zone of methanogenesis. The influence of bacteria in generating sulfate-depleted microenvironments, which are conducive to dolomite precipitation, is largely unknown, but such bacteria may act as important facilitators (see Section 4.5 Bacterial mediation).

In the Gulf of California dolomite is first encountered in an ooze 60 m below the seafloor in water more than 700 m deep (Fig. 21A; Kelts and Mackenzie, 1982). At still deeper levels, there are firm to lithified and impervious beds of micritic dolomite. Most appear to be cements within generally $CaCO_3$-poor muds where some pelagic microfossils have dissolved, while others are replaced. Invariably, the dolomitic mudstones retain the fine structure of the original deep-water sediment and dolomitic horizons typically make up no more than 3%–5% of the sediment column. The dolomites range from Ca-rich to near stoichiometric (42%–51% $MgCO_3$) with more stoichiometric forms occurring at greater depths and in the more lithified layers. Since the work of Kelts and Mackenzie (1982), many other authigenic dolomite layers and concretions have been documented in bacterially altered organic-rich deepwater sediments (Garrison and Graham, 1984; Baker and Burns, 1985; Compton and Siever, 1986; Compton, 1988; Suess et al., 1988; Middleburg et al., 1990).

Dolomite precipitating in the sulfate reduction zone shows negative (depleted) $\delta^{13}C$ signatures of $-20‰$, while that formed slightly deeper in the zone of methane oxidation have even more depleted (-ve) $\delta^{13}C$ values as low as $-70‰$ (Fig. 21B).

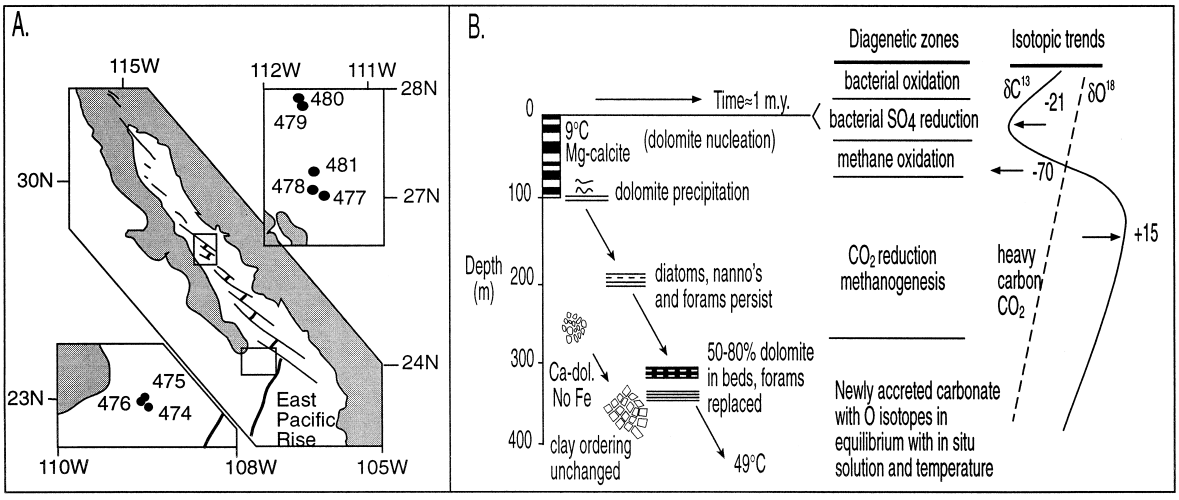

Fig. 21. Quaternary deep-sea dolomite, Gulf of California (after Kelts and Mackenzie, 1982): (A) Locality map of DSDP sites 474 to 481, rectangles indicate areas with documented diagenetic dolomite; (B) Summary model for depth of nucleation and the slow accretion of dolomite layers with burial, it is based on site 479. The vertical scale on the isotopic trends is schematic. It is not directly tied to the listed depth scale of the various dolomite occurrences as the extent of the zones varies according to sedimentation rate.

Dolomite forming deeper in the zone CO_2 reduction and methanogenesis shows somewhat more positive values but these values too trend toward isotopically lighter carbon at greater depths. When sedimentation rates are low, dolomites may form in or just below the zone of sulfate reduction and have negative $\delta^{13}C$ values (Malone et al., 1994). When sedimentation rates are high, dolomite will precipitate within the zone of methanogenesis and well below the zone of sulfate reduction and so have positive $\delta^{13}C$ values. This style of methanogenic dolomite has positive values up to 13.8‰ in the Gulf of California (av. 9.8‰; Kelts and Mackenzie, 1982). With further burial newly formed dolomite once again takes on $\delta^{13}C$ values that are increasingly negative.

Roehl and Weinbrandt (1985) propose that this increasingly negative trend continues beyond the 400 + -m depths penetrated by the DSDP wells in the Gulf of California. They argue that growing crystals acquire increasingly lighter carbon from newly generated petroleum. Hence, dolomites in reservoirs of the Miocene Monterey Formation have much more negative carbon values than those from the Plio-Pleistocene of the Gulf of California. Deepwater organic-rich dolomites comprise thin stratiform, pinch and swell beds with kilometer-scale lateral continuity and local intrabed swells up to 2 to 3 m thick within the Miocene Monterey Formation of the Santa Barbara Basin, California (Garrison and Graham, 1984). There they are sandwiched between dark organic-rich laminated diatomaceous opaline cherts. In total, the dolomitized horizons make up no more than 10% of the chert section.

These dolomites demonstrate continuing dolomite aging through recrystallization (Malone et al., 1994). They show decreasing $\delta^{18}O$ and $\delta^{13}C$ values, decreasing Sr and increasing Mg contents with increasing burial depths and temperatures from east to west in the basin. Maximum temperature probably increased from $< 45°C$ in the east to $> 80°C$ in the west. The $\delta^{18}O$ values vary from 5.3‰ in the east to -5.5‰ PDB in the west and are interpreted to reflect the greater extent and higher temperature of dolomite recrystallization in the west. The $\delta^{13}C$ values vary in parallel with $\delta^{18}O$ and decrease from 13.6‰ in the east to -8.7‰ PDB in the west. Sr concentrations also correlate positively with $\delta^{18}O$ values and decrease from a mean of 750 ppm in the east to a mean of 250 ppm in the west. Mol% $MgCO_3$ values inversely correlate with $\delta^{18}O$ values and increase from a minimum of 41.0‰ in the east to a maximum of 51.4‰ in the west. This region

shows undeniable evidence that dolomite isotopes and trace elements are reset during diagenesis.

Organogenic dolomite is also forming in organic-rich sediments beneath lagoonal waters up to 400 m deep in Kau Bay, Indonesia. It occurs as a 2-cm-thick layer some 3.5 m below the present sediment surface where sulfate levels are bacterially depleted and there is a marked increase in the alkalinity of the interstitial waters (Middleburg et al., 1990). Similar dolomite is found in an older 8-cm-thick layer some 7.45 m below the sedimentation surface and defines the interface between marine and freshwater sediment. The isotope signature of this dolomite indicates that carbon was derived from degrading organic matter (Fig. 27). It is interpreted as forming under highly alkalinity conditions initiated in the zone of anoxic methane oxidation below the zone of sulfate reduction. The reaction can be summarized as:

$$CH_4 + SO_4^{2-} \rightarrow HCO_3^- + HS^- + H_2O$$

Pore fluids in the vicinity of the upper layer show Ca depletion suggesting that the supply of calcium rather than of magnesium is the rate-limiting factor in this region.

Few would doubt that organogenic dolomite precipitation is a widespread early diagenetic mechanism of marine dolomite precipitation. But the amount of dolomite that can form by such a mechanism is small ($< 5\%$), and is limited by the rate of diffusive resupply of calcium or magnesium, always an ineffective pump beneath the deep seafloor (Land, 1985; Kelts and Mackenzie, 1982; Baker and Burns, 1985). Such Ca or Mg as is present is supplied by advection or diffusion from the overlying seawater or is derived from dewatering and diagenetic alteration of clays, biogenic silica, organic matter, interstitial water, and the solution of Mg calcite or calcite. Additional carbon is supplied by methane derived from below the zone of high alkalinity or the upward passage of thermocatalytic methane into shallow seeps on the seafloor.

4.5. Bacterial mediation

The recognition of the importance of bacterial metabolism in dolomite formation in organic-rich hemipelagic sediments has led to an appreciation of bacterial processes in facilitating precipitation in other settings. Dolomite does not easily precipitate in the laboratory at earth-surface temperatures, or in natural modern day settings. This barrier is related to kinetic factors (Land, 1985; Machel and Mountjoy, 1986; Sibley and Gregg, 1987). Recently, Vasconcelos et al. (1995) have suggested that direct mediation of bacteria can overcome this kinetic barrier and may play an active role in the formation of dolomite. This can occur wherever conditions are suitable for bacterial growth and so can range from the depositional surface to depths of 1–3 km.

Petrographic work is showing that particular dolomite crystal habits and textures are related to specific microbial physicochemical environments and processes. Gunatilaka (1989) correlated spheroidal dolomite occurrences with hydrocarbon seepages and suggested that bacteria feeding on hydrocarbons mediated the growth of the dolomite. Host sediments included Miocene–Pleistocene continental strata and extensively karstified, silicified and dedolomitized Eocene lithologies.

Dumbbell and spindle-shaped dolomite crystals have also been recorded from other microbially influenced settings and include groundwater dolocretes of Quaternary (Khalaf, 1990; El-Sayed et al., 1991) and Late Triassic age (Spotl and Wright, 1992) as well as cavities in vadose and phreatic environments of outcropping Miocene reefs (Monty et al., 1987). The presence of former "bacterial" microspheres in ancient rocks has also been inferred from SEM examination (e.g. Camoin and Maurin, 1988; Camoin et al. 1989; Folk, 1993, 1994; Nielsen et al., 1997). These "paleo" bacteria are generally preserved as spherical and/or deflated carbonate bodies. Spherical bacteria, filaments and organic tissues from other primitive organisms readily decay, leaving moldic microporosity (Chafetz and Folk, 1984). This could explain the abundance of micropores within spherulitic and dumbbell crystals in many ancient dolomites.

Many authors have suggested that bacteria can concentrate Ca and Mg on their cell surfaces and so create microenvironments where the ion activity product of calcite or dolomite exceeds saturation, so favoring carbonate precipitation around the bacterial body (e.g. Folk, 1993, 1994; Krumbein, 1979; Gebelein and Hoffman, 1973). Many noticed that

magnesium can be preferentially retained on an organic matter substrate and that these Mg-enriched sites may act as dolomite nucleation and crystallization centers. Sulfate-reducing bacteria are often cited as the taxa most involved in carbonate precipitation.

The discovery of bacterially mediated dolomite accumulations in Lagoa Vermelha, a shallow-water isolated hypersaline coastal salina east of Rio de Janeiro, Brazil, provides the best evidence to date of the participation of particular species of sulfate-reducing bacteria in dolomite precipitation (Vasconcelos and Mackenzie, 1997). There Ca-dolomite crystallizes under anoxic hypersaline conditions within a black sludge layer at the sediment surface (Fig. 22). Following precipitation, the dolomite undergoes an "aging" process, in which increased ordering of the crystal structure occurs. Both the initial precipitation and early diagenetic evolution are strongly mediated by microbial activity. In fact, sulfate-reducing bacteria cultured in the laboratory at low temperatures from Lagoa Vermelha samples produced a highly ordered dolomite (Vasconcelos and Mackenzie, 1997).

Vasconcelos et al. (1995) suggest that sulfate-reducing bacteria promote the essential conditions needed for dolomite precipitation. Sulfate ions form strong ion pairs with Mg^{2+} ions and are held together in space like a single particle. When sulfate-reducing bacteria, metabolize SO_4 ions, they also use the accompanying Mg^{2+} ions inside their cells. Magnesium is essential for many vital physiological functions in the cell, and makes up 0.5% of the cell's dry weight. During bacterial metabolism, excess Mg is released together with other byproducts of sulfate reduction, such as bicarbonate ions and hydrogen sulfide. Saturation with magnesium in microenvironments around the bacterial cell probably creates conditions favorable for preferential precipitation of dolomite, as was observed in lab-based bacterial culture experiments. Wright (1999) presents a similar set of arguments to explain dolomite precipitation in the Coorong lakes.

Using the Lagoa Vermelha system as their starting point, Vasconcelos and Mackenzie (1997) propose a new actualistic model for dolomite formation that they call the microbial dolomite model (Fig. 22). In this model, the anoxic turbid layer at the sediment surface creates a special environment where photosynthetically produced organic matter can be microbially recycled by sulfate-reducing bacteria on a submicron scale, with concomitant precipitation of high-Mg calcite and Ca-dolomite. In contrast to the sulfate-reduction model of Kastner (1984), this model requires a continuing supply of sulfate to precipitate

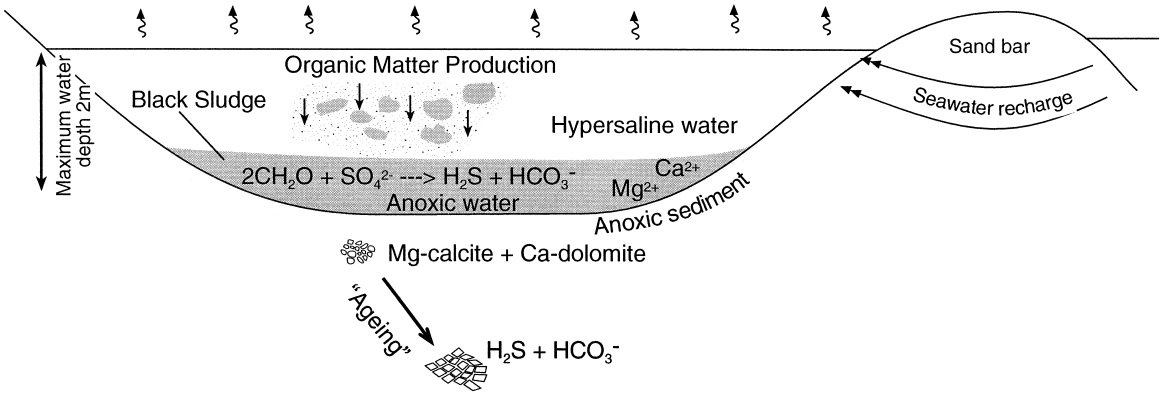

Fig. 22. Schematic of microbial dolomite formation in Lagoa Vermelha. Evaporation in the dry season lowers the lagoon water level and drawdown then allows seawater to enter via seepage through the dune barrier. Elevated productivity in the lagoon leads to anoxia at the sediment–water interface and the formation of a black organic-rich sludge on the lagoon floor. The highly saline waters have elevated sulphate levels that provide a sulphur source for bacterial sulphate reduction as well as elevated magnesium that is precipitated as Mg-calcite and calcian dolomite. Microbial activity in the sludge mediates the precipitation of these primary carbonates that then "age" with burial. Eventually, the microbial activity ceases, but the diagenetic precipitation of dolomite continues atop the microbially precipitated crystal substrate (after Vasconcelos and Mackenzie, 1997).

the dolomite (Fig. 22). The bacteria are required to overcome the kinetic problems of dolomite formation. They control the microenvironment and provide a surface on which the dolomite nanocrystals nucleate. The bacteria require sulfate ions for their metabolism, whereas dolomite precipitation requires excess Mg along with the increased alkalinity.

Once nucleation has occurred, the Ca-dolomite undergoes an "aging" process, as seen by concretions still growing some 14 cm below the Lagoa Vermelha sediment surface. Growth and aging are also seen in the trend towards more negative $\delta^{13}C$ values and increased ordering in the crystals with depth. Bacteria apparently remain important, as seen by the continued presence of nanobacteria on the surfaces of the "aging" crystals. With time, and deeper in the sedimentary section (70–90 cm), the crystals grow by a layer-by-layer mechanism that creates smooth euhedral forms. Apparently, once the dolomite is nucleated, the crystals can continue to grow by inorganic processes, but each new layers still appears to be composed of coalesced submicron-size bacterial balls (spheroids). The microbial dolomite model requires an ongoing supply of sulfate to maintain the microbial activity promoting dolomite precipitation. In contrast, it may be that the presence of sulfate in a sterile (bacteria-free) environment may act to inhibit dolomite precipitation as shown in the experiments of Baker and Kastner (1981) and Morrow and Ricketts (1988).

In eastern Belgium, bacterially induced spheroidal fabrics have been discovered within an ancient, karstified, and Pb–Zn mineralized, Lower Carboniferous dolomite (Nielsen et al., 1997). Arguments supporting a bacterial interpretation in this and similar ancient dolomites include:

- the textural similarities to documented bacteriogenic precipitates, such as dumbbell-shaped crystal aggregates;
- the presence of microspheres embedded in spheroidal dolomite crystals;
- the negative $\delta^{13}C$ of the dolomites;
- the omnipresence of framboidal pyrite embedded in the spheroidal dolomite crystals and their absence in the cement;
- the very negative $\delta^{34}S$ of later framboidal pyrites;
- the general geological setting in which bacterial processes are likely to have occurred.

The microspheres described by Nielsen et al. (1997) were mainly composed of pyrite or carbonate. Some carbonate microspheres were not dissolved during surface etching of the dolomite crystals, suggesting that a thin organic coating may still exist. Calcite spots observed within polished dolomites under SEM-backscatter mode might relate to calcite-filled micropores after bacteria but may also represent relics of a precursor limestone or exsolution of calcite during dolomite recrystallization

The presence of framboidal pyrite in association with spheroidal dolomites testifies to a period of bacterial sulfate reduction during early diagenesis (Raiswell, 1982; Berner and Westrich, 1985). If iron is present, the H_2S generated during sulfate reduction usually precipitates at or near the site as iron monosulfide or pyrite, although it may only form in minor amounts.

Dolomite can also form by sulfate reduction at oil–water or gas–water contacts in zones of oil/gas washing and bacterially induced hydrocarbon degradation. In the subsurface, oil–water or gas–water contacts define aerobic/anaerobic (redox) transition zones between reduced paraffinic crude oils or gases and oxygenated groundwaters. Locally anoxic conditions provided by the buildup of hydrocarbons at these interfaces mean that aerobic bacteria can provide nutrients to the anaerobes, while the through-flowing basinal waters supply the required Ca, Mg and SO_4. Such oil–water or gas–water contact dolomites can even form cements in otherwise carbonate free sandstones. Carbon isotope signatures in the dolomites tend to be very negative as the carbon in the dolomite is derived from methane and other ^{13}C-depleted hydrocarbons. Thick (2–3 m) dolomite spar cements occur at present-day and former gas–water contacts in some oil and gas fields hosted in quartz sands in offshore Brunei (pers. obs.). There the carbon isotope signatures of the dolomites are in the range $\delta^{13}C \approx -20‰$ to $-50‰$ (Fig. 27). This is in marked contrast to the isotopically heavy signatures in carbon of organogenic dolomites that formed in the much shallower zone of methanogenesis. Carbon-13 depleted siderite and ankerite are common coprecipitates with these subsurface-formed dolomites. The varying mineralogies reflect the varying availability of Fe, Mg and Ca in the pore fluids.

4.6. Burial dolomite

Burial dolomites are subsurface cements and replacements that form below the active phreatic zone (reflux and mixing zones) in permeable intervals flushed by warm to hot magnesium-enriched basinal and hydrothermal waters. Prior to the 1960s, burial processes were considered important to dolomite formation; they explained the paucity of modern dolomites and their increased abundance in Paleozoic and Precambrian rocks compared to those of the Mesozoic and the Paleozoic. The idea lost its appeal as more and more ancient dolomites were interpreted using Quaternary analogues. Today, most geologists recognize the kinetic limitations inherent in the strict application of Quaternary analog models, and the implications of dissolution–reprecipitation processes. The notion of burial dolomitization is again gaining in popularity. Unlike earlier models, however, recent concepts of burial dolomitization typically suggest that it is part of a continuing series of dolomitization overprints. Many dolomitization events begin early in the depositional/diagenetic cycle and are overprinted or cannibalized during burial (Gao et al., 1992, 1995; Amthor et al., 1993; Wojcik et al., 1994; Montañez, 1994; Ayalon and Longstaffe, 1995).

Dolomitization under burial conditions probably suffers least from the kinetic inhibition associated with lower temperature syntheses of dolomite precipitates. At its simplest, it requires a throughflow of warm to hot, magnesium-rich basinal fluids. By a depth of a few kilometers temperatures are in excess of 60°C–70°C. Dolomite that is precipitating/recrystallizing in such an environment exceeds the critical roughening temperature and so resets its textural-chemical parameters (Gregg and Sibley, 1984). Fig. 23 is a plot of waters in such a system, it shows that most basinal waters are capable of becoming dolomitizing fluids at temperatures above 60°C–70°C (Hardie, 1987).

Rather than being limited by lower temperatures, a burial dolomite model must explain how substantial volumes of magnesium are supplied and how fluids are pumped through deeply buried low-permeability strata at viable rates. Magnesium can come from a number of sources: from the chemical reworking of nearby and perhaps earlier dolomites, from structural Mg^{2+} expelled during the montmorillonite-to-illite transformation, and from the deep subsurface dissolution of bittern salts such as carnallite — $K_2MgCl_3 \cdot 6H2O$, polyhalite — $K_2MgCa_2(SO_4)_4 \cdot 2H_2O$, and kieserite — $MgSO_4 \cdot H_2O$).

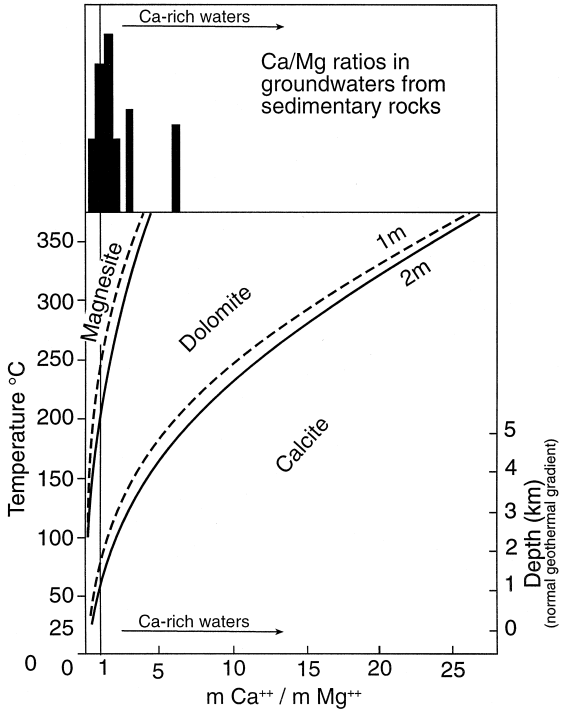

Fig. 23. Subsurface waters. Lower diagram is a plot of the expected stability field of dolomite as a function of temperature and Ca/Mg ratio in 1 M and 2 M chloride brines. The upper diagram is a histogram of the Ca/Mg ratios of natural groundwaters in contact with a variety of sedimentary rocks. The diagram clearly shows that most natural waters are capable of becoming dolomitizing fluids at temperatures above 60°C–70°C (after Hardie, 1987).

Historically, clay mineral transformations in shales were the most commonly cited source of magnesium (Kahle, 1965) whereby the illitization of smectite released magnesium into basinal brines to dolomitize adjacent platform carbonates. In a similar fashion, Boles and Franks (1979) argued that the illitization of clay minerals in interbedded shales at depths of more than 2500 m was a likely source of the iron and magnesium precipitated in ferroan dolomite cements in Tertiary sands of the Gulf of Mexico. But the amount of dolomite formed by the escape of basinal waters in the Gulf Coast is small in relation

to the volume of fluid flow and only small amounts of dolomite cement has formed (Milliken et al., 1981; Land, 1984). In fact, dolomite is much less common than calcite as an authigenic cement in the sandstones of the Texas Gulf coast. Where magnesian-rich cements are locally abundant, they are ankeritic rather than dolomitic (Boles, 1978). Diagenetic formation of chlorite in a sedimentary basin commonly consumes magnesium, not supplies it, so that in the compacting shales of the Gulf of Mexico, the formation of chlorite and illite from smectite provides an efficient internal sink for magnesium, little is released into escaping basinal brines (Land, 1985). No massive release of magnesium by compacting shales has yet been observed in any compacting sedimentary basin.

There are also flow rate problems inherent in moving large volumes of Mg-entraining subsurface waters through a deeply buried shelf limestone. Dolomitization must take place at depths where compaction has reduced matrix porosity to less than 5% to 10% and permeabilities to < 0.1 md. These limitations imply that little new dolomite can be generated from compactional flow of modified-marine pore fluids. At best, burial fluids can introduce relatively small volumes of new magnesium into the carbonate platform of a subsiding and compacting shale basin (Morrow, 1982; Land, 1985). Burial dolomitization within such a setting is either a focused flow of hot brine along permeable beds and faults at the basin edge, or it is largely the result of cannibalization and re-equilibration of earlier dolomites. The potential for moving larger volumes of Mg-rich basinal fluids through a platform margin is greater in a basin undergoing collision compression, especially if the basin also contains thick dissolving salt sequences. Hydrologic mechanisms that drive and focus fluids creating regional burial dolomites are still not fully understood, our 3D models are largely qualitative rather than quantitative (Garven et al., 1999).

Hydro-tectonic processes driving burial dolomitization have been divided by Heydari (1997) into three hydrologic realms: (1) passive margin burial diagenesis, (2) collision margin burial diagenesis, and (3) post-orogenic burial diagenesis. Passive margin burial diagenesis is characterized by extensional tectonics, growth faulting, relatively slow and steady subsidence and, in some basins, by salt tectonics (Fig. 24A). The Gulf of Mexico and Atlantic-margin basins during the Mesozoic are typical examples of this realm. The shallowest part of this realm, down to ≈ 1 km depth, is typified by active phreatic circulation (mixing zone and brine reflux) that was discussed earlier. Below this (> 1 km depth) is a zone of compactional flow which entrains both horizontal flow regimes (average rates of 6 cm/year) and vertical flow regimes (average rates of 0.15 cm/year). Deeper still, or in zones of thermal anomalies around salt structures and mud diapirs, there is the thermohaline flow regime. Salt beds and

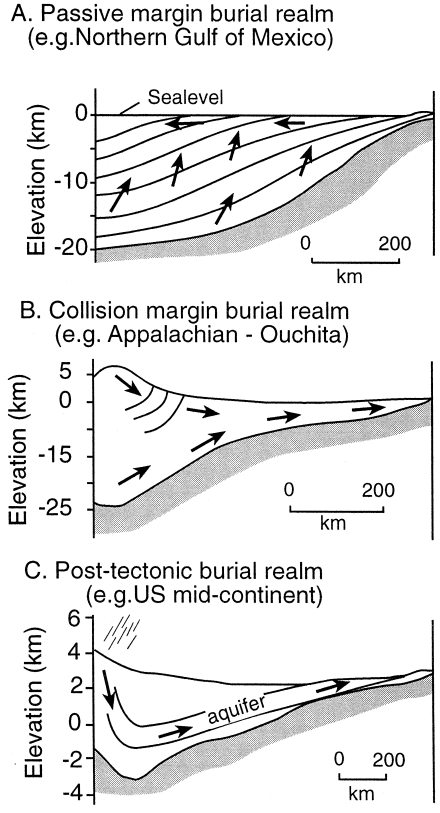

Fig. 24. Hydrologic flow patterns for burial dolomitization (after Heydari, 1997). (A) Passive margin circulation with burial water flow driven by sediment compaction and catabaric/thermohaline flow. (B) Collision margin circulation where thrust sheet emplacement drives burial water from sediments caught up in the orogenic belt into the craton interior. (C) Post-tectonic circulation where deep burial flow in the basin sediments is driven by gravity head supplied by adjacent weathering mountain belt. Note the varying vertical and horizontal scales.

allochthons act as foci for the escaping basinal fluids (Warren, 1999). Away from local thermal anomalies, temperatures within this realm increase steadily with depth according to regional geothermal gradients, which range from 15°C–30°C/km. Sediments shallower than 3 km are typically hydrostatically pressured, while deeper strata are geopressured. A transition to overpressuring can occur at much shallower depths where salt, not shale, is the aquitard ($\approx$ 1 km; Warren, 1999). Burial dolomites formed in passive margin platforms are often intimately associated with the movement of compactional fluids along the extensional faults or active growth faults (McManus and Wallace, 1992).

Collision margin burial diagenesis is characterized by compressional tectonics, thrust faulting, extensive fracturing of carbonate strata and episodic fluid flow in response to tectonic loading (Fig. 24B; Heydari, 1997). Hot (100°C to $>$ 250°C), saline and highly pressured fluids are moved laterally out of the collision zone, typically toward the craton or continental interior through porous and permeable horizons and vertically through faults and fractures (Oliver, 1986). Such systems are typified by burial and hydrothermal dolomites formed in the Appalachian–Ouachita collision belt (Montañez, 1994), the Devonian–Carboniferous and Tertiary orogenies of Alberta (Qing and Mountjoy, 1994a), the Variscan orogeny of Sardinia (Boni et al., 2000) and the Hercynian orogeny of southeastern Ireland (Hitzman et al., 1998). All these compression driven hydrologies are capable of forming widespread burial dolomites and Pb–Zn deposits both within the orogenic belts and the continental interior (see Dolomite as ore hosts section).

Post-orogenic burial diagenesis is characterized by a lack of tectonic activity, dominance of topographically driven flow, and high fluid flow rates ranging from 100 to 3000 cm/year (Fig. 24C; Heydari, 1997). This hydrology begins once the main phase of tectonic collision ends and is driven by the elevation gradient created during the preceding orogenic phase. The composition of the deeply circulating basinal and meteoric waters is controlled by water–rock interaction with the aquifers through which they flow. This hydrologic style is thought to exemplify late stage dolomites of the US mid-continent. In terms of dolomitization, this style of hydrology is more variable and so less understood than that of collision or passive margins, and some authors have claimed it tends to dedolomitize rather than dolomitize the craton carbonates (Back et al., 1983; Morrow, 1998; Ramsey and Onasch, 1999).

Qing and Mountjoy (1994a,b,c) found that late-stage, coarsely crystalline replacement dolomite and associated saddle dolomite cements, along with late-stage dissolution vugs and caverns, constitute a widespread collision margin burial diagenetic facies in the Middle Devonian Presqu'ile barrier. The hydrologic realm extends southwestward from Pine Point to the subsurface of the Foothills in northeastern British Columbia. The resulting burial dolomites create hydrocarbon reservoirs in otherwise tight limestones in the subsurface of the Northwest Territories and northeastern British Columbia, as well as acting as ore hosts to MVT Pb–Zn deposits at Pine Point. They (a) replace blocky sparry calcite cement, (b) occur continuously across the sub-Watt Mountain unconformity, (c) postdate stylolites and earlier replacement dolomites, and (d) overlap sulfide mineralization. Along the Presqu'ile barrier, the $\delta^{18}O$ values of both replacement and saddle dolomites increase eastward and updip (i.e. away from the region of most intense orogenesis). Values range from -16‰ PDB in the deeper areas of northeastern British Columbia to -7‰ PDB at Pine Point. Corresponding homogenization temperatures of saddle dolomite fluid inclusions decrease from 178°C to 92°C. The $^{87}Sr/^{86}Sr$ ratios of coarsely crystalline and saddle dolomites also decrease eastward along the Presqu'ile barrier from about 0.7106 in northeastern British Columbia to 0.7081 at Pine Point. All of these geochemical trends imply basin-scale migration of hot, dolomitizing fluids updip along the Presqu'ile barrier. These large-scale fluid movements are interpreted to be related to tectonic compression and sedimentary loading of the Western Canada Basin. Such compression occurred at least twice in the Phanerozoic history of the basin: first during early burial between the Late Devonian and Early Carboniferous and then during deep burial between the Late Jurassic and early Tertiary (Qing and Mountjoy, 1994a,b,c).

Montañez (1994) concluded that the late diagenetic burial dolomites of the Lower Ordovician, Upper Knox Group in the southern Appalachian basin

were also associated with tectonic compression, widespread secondary porosity development, hydrocarbon migration, and local MVT mineralization. This regionally extensive (approximately 70,000 km^2) unit is made up of replacement dolomites and zoned dolomite cements. Replacement dolomite comprises 15% to 50% of all the Knox matrix dolomites. The $\delta^{18}O$ ($-11.9‰$ to $-5.3‰$), $\delta^{13}C$ ($-3.8‰$ to $+0.9‰$), and $^{87}Sr/^{86}Sr$ (0.70895 to 0.70918) values of replacement dolomites overlap with those of earlier cements and Lower Ordovician marine calcites. This overlap is interpreted as indicating rock buffering of initial dolomitizing fluids, as well as extensive neomorphism of replacement dolomites by late diagenetic fluids. The later dolomites have porosities of 1%–16% and permeabilities of 0–1030 md, values significantly greater than those of either earlier replacements or their host limestones (1%–6% and 0.0–0.04 md).

Montañez (1994) was able to regionally correlate five generations of dolomite cements that recorded regionally extensive diagenetic events. The $\delta^{18}O$ (-12.4 to $-3.0‰$) and $^{87}Sr/^{86}Sr$ (0.70885 to 0.71000) values, along with Sr (18 to 147 ppm), Mn (63 to 1069 ppm), and Fe (109 to 8452 ppm) contents of zoned dolomites, in conjunction with fluid inclusion data, indicate that late dolomites precipitated from hot (80°C to >165°C), saline (13 to 22 wt.% NaCl equivalent) basinal brines that had undergone extensive fluid–rock interaction with clastics. Precipitation temperatures estimated from fluid inclusion geothermometry and systematic trends in $\delta^{18}O$ values record a regionally developed, prograde-to-retrograde thermal history. Montañez (1994) interprets these dolomites as recording the spatial and temporal evolution of large-scale fluid flow systems that had developed in response to differing burial and tectonic stages of the southern Appalachian basin. The occurrence of zoned dolomite cements in tectonic fractures and breccias, and their close association with noncarbonate diagenetic minerals of Pennsylvanian to Early Permian ages, suggest that most Knox Group dolomites record deep subsurface (2 to >5 km) fluid migration in response to late Paleozoic Alleghenian tectonism (330 to 265 Ma). They served as long-lived conduits that focused and channeled fluids. The occurrence of bitumen in secondary porosity indicates that these dolomites were the most viable reservoirs during hydrocarbon migration in the late Paleozoic.

Morrow (1998) argues that both "tectonic compression" and "topographic recharge" models for subsurface fluid flow may have been overapplied when explaining regional burial dolomite bodies. He argues tectonic compression requires an unreasonable degree of fluid focusing to achieve precipitation temperatures equal to observed fluid inclusion temperatures, which are typically much hotter than those of their surrounding carbonate hosts. This argument is based on a limited sampling set, some burial dolomites are hotter, some are the same and others are cooler than their surrounds. The variability in types of focused burial dolomite will be discussed in a later section dealing with dolomite as an ore host. He goes on to argue that topographic recharge has the limitation of flushing solutes out of the system, rendering it incapable of further dolomitization. In addition, he feels both topographic recharge and tectonic compaction are unlikely flow mechanisms to explain the origin of extensive open space dolomite cement because of their limited supply of solute. He argues that thermal convection (a variation on the Kohout circulation discussed earlier) is a more viable hydrologic drive as it can support long-lived flow systems in the subsurface, which are also capable of recycling solutions many times through the deeply buried rock mass. This enhances the opportunity for ongoing cementation and cannibalization. Because thermal convection can occur in confined aquifers beneath the seabed, seawater-derived (connate) solutions enhancing the dolomitization potential may be continually added to the convection system. The documentation of crustal scale thermal convection systems within subaerially exposed orogenic belts, and the outcrop evidence of both upward and downward extending bodies of burial dolomite add credence to the hypothesis that thermally driven convective flow occurred within ancient platform carbonates, and may have induced regional burial dolomitization (Morrow, 1998).

Whatever process drives the circulation, burial dolomites are typically characterized by coarsely crystalline nonplanar and sparry crystals, often of saddle dolomite within residual pores. Saddle dolomite is turbid, coarsely crystalline and typically has a curved crystal lattice showing sweeping extinc-

tion in cross-polarized light (Radke and Mathis, 1980). Burial dolomites tend have negative $\delta^{18}O$ values indicating precipitation from fluids at somewhat higher temperatures than those of earlier platform dolomites. Trace elements such as Sr and Na are low as the limestone precursor has long since converted to low Mg–Calcite and successive episodes of dolomitization have reduced the levels of these elements even further. Some burial dolomites may have slightly elevated levels of Fe and other metals indicating a throughflux of metalliferous catabaric pore waters. Growing crystals may also entrain mature hydrocarbons in their fluid inclusions for the same reason. The modification of earlier formed dolomites by basinal fluids can generate crystals with low $\delta^{18}O$ values, modified $^{87}Sr/^{86}Sr$ ratios, and more saline higher temperature inclusions (Banner et al., 1988).

As primary dolomitization of a limestone by basinal fluids generates similar characteristics to those of a replacive burial dolomite (Machel and Burton, 1991), there is often controversy when two groups of workers study the same dolomite body. For example, Lee and Friedman (1987, 1988) concluded that most of the Ordovician Ellenberger dolomite in Texas and New Mexico was the result of burial dolomitization. In contrast, Kupecz and Land (1994) concluded that it formed during early diagenesis and was modified during burial by discharge of basinal fluids along dolomite aquifers.

4.7. Hydrothermal dolomite

Not all late stage or burial dolomites are pervasive or widespread replacements of shelf dolomites. Some are much more focused in their geometry and form within higher temperature haloes about what were relatively permeable conduits, such as faults, thrust planes, or zones beneath impermeable, often evaporitic, seals. Deeply circulating basinal waters only become hydrothermal,[5] locally mineralizing and capable of dolomite precipitation/replacement, when they are transmitted upward into cooler, shallower parts of the basin (Hardie, 1991). They reflect a focused outflow of hydrothermal waters that sometimes also fed base metal mineralizing systems (Braithwaite and Rizzi, 1997; Warren and Kempton, 1997). They are, in effect, more focused variants of the burial dolomitization mechanisms discussed in the preceding section and can form in all three burial realms. They are discussed as a separate grouping because they are more obvious examples of focused hydrologic outflow and cooling typically along faults and fractures. They indicate the effect of fluid flows with high Rayleigh numbers, their inclusion and isotopic values typically indicate precipitation from fluids that were much warmer than those effecting immediately adjacent carbonates.

As basinal waters become heated during hydrothermal circulation their buoyancy increases and they rise upwards and outwards along bedding, faults or other permeability paths (Freeze and Cherry, 1979). The shape of these flow paths is governed by the Rayleigh number (the ratio of buoyant to viscous forces). For relatively cool systems, fluids will rise and geometry will be determined by the ratio of vertical to horizontal permeability. For high Raleigh numbers, buoyant forces are stronger, and the rising fluid forms a concentrated, dominantly vertical, plume. Within this plume, temperatures, flow rates, and chemical potential may be expected to decrease from the center towards the margins. Maximum temperatures and the temperature differentials needed to drive such a circulatory system may be quite low (20°C–25°C; Aharon et al., 1987).

One of the best-documented occurrences of such a late-diagenetic fault-focused dolomite is hosted in the Ordovician Trenton-Black River limestones of Michigan and southwestern Ontario (Fig. 25A; Taylor and Sibley, 1986; Hurley and Budros, 1990; Middleton et al., 1993). There the dolomite defines zones of faulting and fracturing in the surrounding limestones. It is of two types, a widespread “cap” dolomite and a more localized “trend” dolomite associated with fault planes. The latter forms highly localized and linear hydrocarbon plays such as the Scipio-Albion field (Fig. 25B).

The cap dolomite replaces the upper few meters of the Trenton Group, while the later “trend”

[5] Hydrothermal water is a subsurface water whose temperature is high enough to make it geologically or hydrologically significant, whether or not it is hotter than the rock containing it. It does not have to be generated by magmatic processes (see AGI Glossary of Geology).

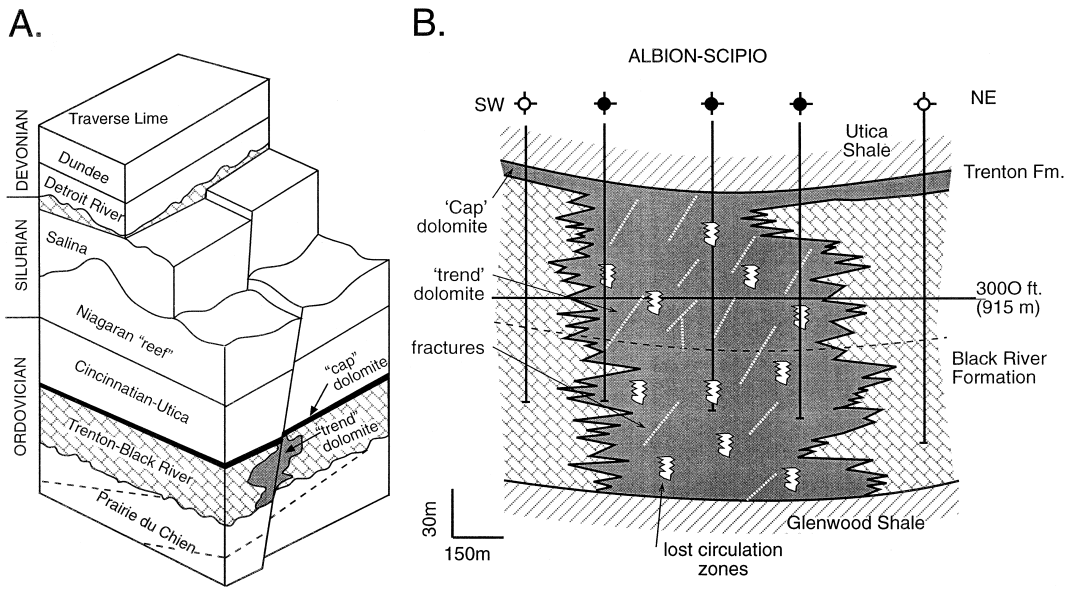

Fig. 25. Fault-focused late dolomitization in the Scipio-Albion trend, Michigan (after Hurley and Budros, 1990). (A) Structural stratigraphic interpretation of the Albion-Scipio trend. The fault/fracture set controlling dolomitization is pre-Devonian. The dashed lines indicate bedding planes beneath the unconformity at the base of the Trenton-Black River. (B) Structural cross-section of the Albion-Scipio field. Note that the field is located in a synclinal trend (not usual for a hydrocarbon trap) and there is a rapid lateral transition from a regional nonreservoir limestone into a permeable reservoir dolomite. Lost circulation and fractures zones are common in this dolomite.

dolomite is developed in the vicinity of fractures (Middleton et al., 1993). Late stage calcite and anhydrite cement, as well as minor sulfides, fluorite and barite, postdate dolomitization. The cap dolomite is petrographically and geochemically distinct from fracture-related dolomite. Where fracture-related dolomite occurs in the upper few meters of the Trenton Group; however, the cap dolomite is no longer obvious, suggesting that it was overprinted.

Fluid inclusions in fracture-related saddle dolomite cements in the "trend" dolomite are saline (24 to 41 wt.% NaCl eq.) and homogenization temperatures range between 100°C and 220°C (Middleton et al., 1993). These temperatures are considerably higher than those likely to have been generated during peak burial of the adjacent limestones ($\approx$ 70°C). Late-stage calcite cements have fluid inclusion homogenization temperatures ranging from 70°C to 170°C and were precipitated by less saline brines (16 to 28 wt.% NaCl eq.).

Middleton et al. (1993) interpret the cap dolomite as a result of compactional dewatering of the overlying shales of the Blue Mountain/Utica Formation. Subsequently, the fracture-related 'trend' dolomite appears to have resulted from fluid flow along reactivated fractures. Various possible Mg and fluid sources for dolomitization exist: (1) compactional dewatering of basinal shales and evaporites and focusing of fluids updip towards the basin margins and (2) flushing of Silurian or younger brines down into the Ordovician sequence. The cause of the elevated temperatures associated with the dolomitization is still not known.

4.8. Applying the models

To decipher the depositional and diagenetic history of a dolomite requires the investigator to call upon as many chemical and physical techniques as he or she can economically justify. The four most common groups of tools in use are: (a) stable isotopes, (b) trace elements, (c) fluid inclusions, and (d) geometry/petrography of a deposit. The first three are best conducted on fresh core or cuttings, while a

study of geometry/petrography requires a combination of seismic analysis, detailed sedimentological logging of core or outcrop and/or a suite of detailed wireline logs, cuttings and sidewall cores from representative wells. (The reader interested in more information on chemical techniques is referred to: Roedder, 1984; Aulstead et al., 1988; Tucker and Wright, 1990; Banner, 1995.) Despite more than three decades of intense study, unequivocal genetic interpretations tracing the complete depositional and burial evolution of a dolomite are still problematic (Land, 1980 vs. Veizer, 1983).

At the core of this problem is the notion of, how does an ancient dolomite form? What is the point of studying the trace element and isotopic signatures of a mineral we know has undergone multiple episodes of dissolution and reprecipitation (Land, 1980)? The trace element and isotopic character will be reset each time the dolomite re-equilibrates with a new water. Neither trace element nor isotopic studies will determine unequivocally the ultimate origin of an ancient dolomite. Fluid inclusions tend to preserve the chemistry of the resetting fluid and are most useful in determining the character of the burial environment. What approaches (a) through (c) can indicate are factors like: the evolution of fluid chemistry with time, fluid sources and pathways, and the degree of fluid–rock interaction. The geometry of a dolomite body is a far better indicator of its origin than its geochemistry.

An evolutionary history of dolomitization can be outlined only when all these methodologies are combined under the umbrella of detailed petrographic study, which allows a tie of the various geochemical values to appropriate crystal stratigraphy (e.g. Drivet and Mountjoy, 1997; Yoo et al., 2000).

4.8.1. Trace elements

The trace elements usually used to constrain dolomite evolution are Sr, Na, Fe and Na. Their concentrations in ancient dolomites are determined by: (1) the concentrations of the element in the parent fluids, (2) the level of water–rock interaction (how open was the system?) and (3) what is the effective distribution coefficient between the dolomite and its parent water.

Ambiguity in interpreting trace element values in dolomites revolve around a number of factors, the most important of which are: (a) our inability to synthesize dolomite in the laboratory and so measure partition coefficients under controlled conditions at room temperatures, and (b) difficulties in quantifying the volumes of various diagenetic fluids and their chemical overprints, which alter crystal chemistry from the time of initial dolomite precipitation. The lumping problems inherent to older analytical techniques using whole rock sampling are no longer a problem with the rise of microsampling (microprobe and micropipette) techniques.

Difficulties in synthesizing dolomite have led to a poor knowledge of distribution coefficients of elements in the mineral, and so large degrees of variation must be accepted (Banner, 1995). For example, because seawater has such a high ionic strength in comparison to meteoric water, mixtures with more than 5% seawater will have Sr/Ca molar ratios similar to that of seawater. Dolomites precipitated from a meteoric/seawater mixture with more than 20% seawater may have a typical marine Sr content (whatever that is, as we still have a poor understanding of effective distribution coefficients). A commonly used value is $\approx$ 550 ppm (Tucker and Wright, 1990). Ancient dolomites with Sr values higher than this are thought to be associated with hypersaline waters.

In relatively closed burial systems, where the level of water–rock interaction is low, the mineralogy of the precursor carbonate is also important in controlling the trace element signature. This further complicates interpretations based on trace elements. Marine aragonite, with its high Sr content of 8000 to 10,000 ppm will form dolomites with Sr contents of 500–600 ppm (e.g. Table 3). Marine high- and low-Mg calcites (Sr $\approx$ 1000–2000 ppm) should form dolomites with Sr $\approx$ 200–300 ppm, but a diagenetic low-Mg calcite precursor, with its much lower Sr content will form Sr-depleted dolomites. Generally, fine-grained early dolomites have higher Sr contents than later diagenetic coarsely crystalline dolomites.

Sodium levels are relatively high in marine dolomites. Modern marine dolomites in the Caribbean, the Arabian Gulf, and Texas entrain 1000–3000 ppm Na (Land and Hoops, 1973). Mixing-zone (?) dolomites have Na levels of several hundred ppm while Pacific atoll (seawater flushed) dolomites have 500–800 ppm of Na (Rodgers et al.,

1982). Most ancient dolomites have only a few hundred ppm Na. As with Sr values, the levels of Na in a dolomite can be used to distinguish dolomite types and perhaps give an indication of possible parent waters but all values are relative, not absolute, indicators.

Fe and Mn tend to increase during successively later episodes of diagenetic recrystallization (Tucker and Wright, 1990). There are two reasons for this: (1) iron and manganese are typically present only at very low levels in seawater but can be present in significant amounts in diagenetic pore fluids and, (2) the distribution coefficients for both elements are greater than unity so that Fe and Mn are preferentially taken into the dolomite lattice during diagenesis. Apart from cation concentration, the redox potential of the pore fluids also controls the levels of these trace elements in the dolomite lattice. The presence of both elements is favored by reducing conditions in the burial fluids. Thus, early nearsurface dolomites tend to have low Fe and Mn levels owing to oxidizing conditions, while later burial dolomites may have much higher levels due to the reducing conditions that typify most deeper basinal waters (also higher levels of Fe and Mn in solution). This variation in trace element content is also used to explain why later burial calcites and dolomites are nonluminescent phases under cathodoluminescence (e.g. Dix, 1993).

4.8.2. Stable isotopes

As in trace element studies, the use of stable isotopes in defining the conditions of dolomite formation is only as good as the detailed petrography that must accompany such analysis. Many isotopic fields overlap and, due to continuing recrystallization, isotope proportions are overprinted and reset by later diagenetic episodes, especially in open fluid/rock systems. An important problem to overcome when interpreting the isotopic composition of the various types of ancient dolomite is to define the relationship between $\delta^{18}O_{water}$ and $\delta^{18}O_{dolomite}$. Fig. 26A shows a plot of temperature against $\delta^{18}O_{dolomite}$ as determined by various workers, giving a variation in temperature of around 15°C for any given isotopic composition or a variation of 4‰ for any given temperature. Once again, an inability to synthesize dolomite in the laboratory leads to problems in the interpretation of isotope values in natural dolomites (see Tucker and Wright, 1990 for discussion). Also shown in Fig. 26A is the much better constrained

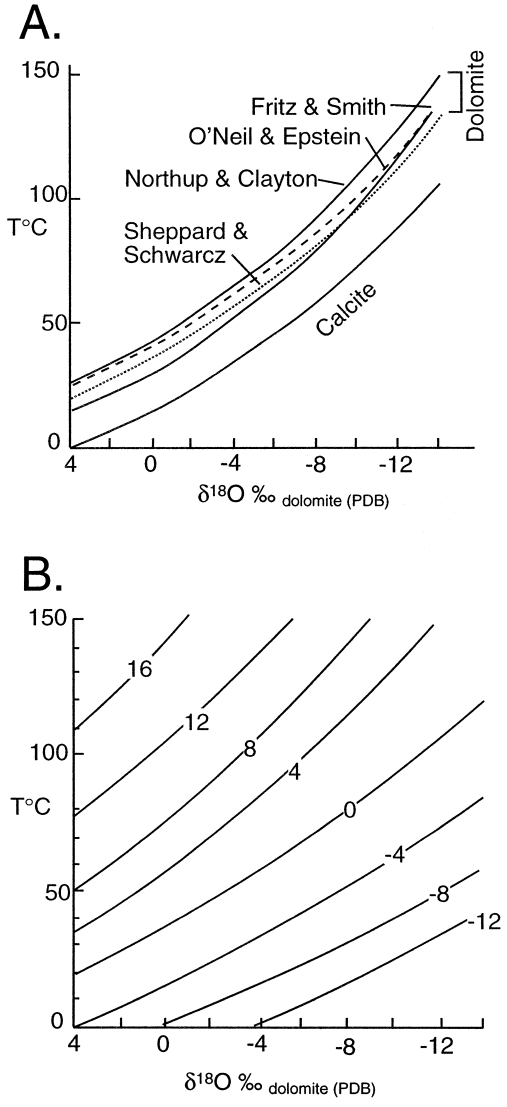

Fig. 26. Oxygen isotopes in dolomites. (A) Dolomite-water fractionation equations as a function of temperature plotted for a $\delta^{18}O$ of 0‰ SMOW from a number of published sources listed in Land (1985). The calcite-water equation is also shown (after Tucker and Wright, 1990). (B) $\delta^{18}O_{dolomite}$ versus temperature for various $\delta^{18}O_{water}$ values derived from the fractionation equation; $10^3 \ln\delta_{dolomite\ water} = 3.2\times10^6 T^2 - 3.3$ (after Land, 1985).

calcite–water fractionation curve ($10^3 \ln \alpha_{\text{calcite water}} = 2.78 \times 10^6 T^2 - 2.89$). Fig. 26B shows the temperature against $\delta^{18}O_{\text{water}}$ based on a fractionation;

$$10^3 \ln \alpha_{\text{dolomite water}} = 3.2 \times 10^6 T^2 - 3.3$$

(as calculated from Fig. 26A; Land, 1985).

The evolution of oxygen isotopes in a dolomite undergoing burial/alteration reflects the successive temperatures of precipitation and the isotopic compositions of the dolomitizing fluids (Fig. 26B). Fluid composition can be influenced both by temperature and the composition of the $CaCO_3$ precursor. Because most pore fluids contain abundant oxygen, the isotopic compositions of precursor minerals are only preserved in relatively closed systems characterized by low water–rock interactions. In most cases in the diagenetic realm dolomitization takes place in a hydrologically open system and is accompanied by throughflushing pore waters. Hence, the isotopic compositions of many subsurface dolomites reflect evolving pore fluid compositions and temperatures.

In contrast, the $\delta^{13}C$ value of a dolomite strongly reflects the value of the precursor carbonate, or, less often the influence of abundant hydrocarbons or organic matter. Typical pore fluids are initially low in carbon so that the $\delta^{13}C$ value of the dolomite reflects that of its precursor. In addition, there is little isotopic fractionation of $^{13}C/^{12}C$ due to temperature. Hence, the $\delta^{13}C$ signature gives valuable information on the source of carbon in the carbonate. Values between 0‰ and 4‰ are typically marine. When diagenesis of organic matter is involved (as in organogenic dolomites) then extreme carbon signatures are possible. Very negative or depleted carbon values indicate that the carbon is derived from organic, rather than inorganic, sources via bacterially mediated sulfate reduction or methane oxidation. Typical $\delta^{13}C$ values lie in the range -22‰ to -30‰. Very positive carbon values, up to $+15$‰, also indicate an organic carbon source and result from organic fermentation and methanogenesis.

A cross plot of carbon and oxygen values is far more effective in distinguishing different styles of dolomite than a simple uni-axial determination (Fig. 27). Even so, the various fields show a strong degree of overlap. This underlines the importance of using stable isotope values, along with trace elements and inclusion studies, as tools in combination with detailed petrography. It also emphasizes the importance of microsampling rather than whole-rock analysis.

4.8.3. Fluid inclusions

Fluid inclusion studies of dolomite basically track the movement and thermal history of the of aqueous and petroleum/mineralising fluids that were present as the crystal precipitated. Fluids are trapped whenever the normal crystal growth is interrupted. This occurs when stresses or foreign objects dislocate the plane of growth. Subsequent disruption, after the crystal has stopped growing, can also cause cracking, and any surrounding fluids will then enter the cracks. In either case, the crystal grows around the fluid, sealing in the exact conditions of fluid entrapment, i.e. the fluid composition and pressure–temperature conditions at the time of entrapment. Sizes of fluid inclusions range from less than 1 μm to several centimeters. When a dolomite cools after precipitation, the fluid in the inclusion can shrink more than the surrounding mineral, and so create a vapour bubble. Heating the inclusion to the temperature at which the bubble is reabsorbed and daughter crystals dissolve gives an estimate of the minimum temperature at the moment of dolomite formation. Such studies should only be conducted on inclusion groups in crystals that show no evidence of inclusion stretching or leakage.

A heating-cooling stage is used to bring the sample through a range of temperatures. Liquid nitrogen is typically pumped through the microscope stage, allowing a minimum temperature between -180°C and -190°C. A variable voltage source connected to a thermal coil is the heat source, and a thermocouple is used to monitor temperature to 0.1°C. As the sample is brought through temperature ranges, groups of fluid inclusions in the dolomite are observed for phase changes. The type of phase change is dependent on the fluid system and conditions of entrapment. Water and NaCl systems trapped at typical pressures for dolomite precipitation will show melting of ice below 0°C and a homogenization of the liquid and vapour phases to the liquid phase typically above 70°C. There are many other inclusion fluid systems that are possible in dolomite crystals, including hydrocarbons. A H_2O–CO_2 system may show the formation and disappearance of clathrate (a cage

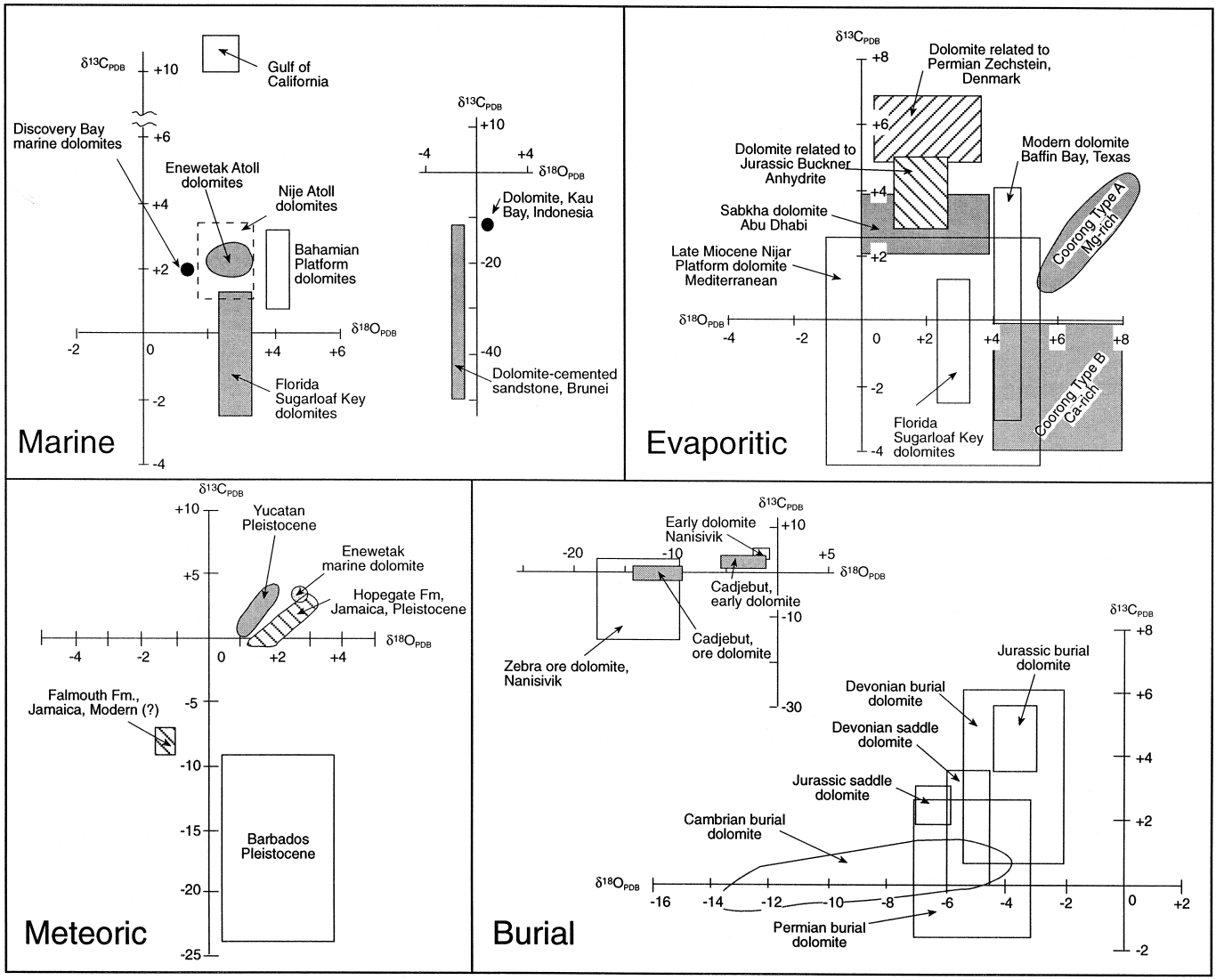

Fig. 27. Carbon–oxygen isotopic compositions of modern and ancient dolomites subdivided according to dominant pore water fluids where the dolomites are forming (compiled from various sources listed in text).

Table 4
Characteristics of dolomitization models (see text for discussion)

Syndepositional			Shallow burial (early diagenetic,
Lacustrine (Coorong-style)	Normal marine	Arid Peritidal (Sabkha-style)	Brine reflux dolomite
Laminar to massive lacustrine basin centre precipitates Playa margin mudflats and dolocretes Fine-grained (<10 μm), stratiform micritic dolomites (mudstones). Typically, stratiform with sharp upper and lower contacts in beds usually 1 m, but up to 5 m, thick. Often show good preservation of primary lacustrine sedimentary features indicative of shoaling depositional setting (laminites overlain by tepees, intraclast breccias, rhizoconcretions, mudcracks, domal stromatolites and dolocretes. Geochemistry reflects evaporitic pore fluids if sequence is buried as a relatively closed system (positive $\delta^{18}O$, elevated Sr and Na). Otherwise, dissolution reprecipitation can reset stable isotopes and trace element values	Subtidal to supratidal dolomites Fine-grained (<10 μm), stratiform syngenetic dolomite (mudstones) and cement horizons. Crystal size may increase during later burial. Beds are typically stratiform and thin with sharp upper and lower contact. Ancient units often are part of a stacked peritidal platform succession. Dolomite tends to precipitate in a micritic host. Unless recrystallized by later burial re-equilibration, the unit preserves fine grain size and typical sedimentary structures that indicate a peritidal mode of deposition. Geochemistry reflects marine pore fluids if the sequence is buried and remains as a relatively closed system. Otherwise, ongoing burial dissolution/reprecipitation can reset stable isotopes and trace element values.	Fine-grained (<10 μm), stratiform micritic dolomites (mudstones). Typically stratiform with sharp upper erosioal contact and more diffuse lower contact. Dolomite forms bed >1–2 m thick near the contact of the supratidal and intertidal facies. It is part of a shoaling peritidal sequence by algal laminites as predominant intertidal facies, open-restricted marine subtidal facies and the supratidal facies characterized by nodulat and displacive evaporites capped by an erosion surface. Sabkha dolomites can be either marine or continental. If the sequence is buried as part of a relatively closed system, its geochemistry reflects evaporitic pore fluids (positive $\delta^{18}O$, elevated Sr and Na). Otherwise, ongoing burial dissolution/reprecipitation can reset stable isotopes and trace element values.	Medium-grained (10–100 μm) stratabound replacement dolomite typically developed in regional palaeo-topographic depressions as units that may be tens to hundreds of metres thick and extend over large areas. The top of the dolomite lies beneath a widespread, mostly subaqueous evaporite horizon or a dissolution breccia associated with a former evaporite horizon. Intensity of dolomitization decreases downward or away from the former evaporite layer of source of the refluxing brine. Commonly reflux dolomites are associated with platform and basinwide evaporite beds (evaporitic salterns and mudflats). If not reset by later burial overprint, $\delta^{18}O$ values tend to decrease away from the evaporite dolomite contact. Trace elements such as Na and Sr also tend to decrease away from the source of the refluxing brine
Bacterial mediation can occur and may drive precipitation of initial crystallites that then age via Ostwald ripening (bacterial mediation			

of CO_2 around H_2O) and separate melting of CO_2 and H_2O. The post-entrapment deformation of inclusion walls, the necking-down of single inclusions into multiple inclusions, or leakage of contents prior to observation, can all lead to changes in the homogenization temperatures.

Because of the extremely small size of fluid inclusions in most sedimentary dolomite, determining the ionic composition of the trapped fluids is often difficult and until recently was typically a two-phase process. Once the total amount of dissolved solids is determined by observing the freezing/melting points of the inclusions, the sample is then crushed and rinsed with water. This water is recovered and analyzed by using a sensitive analytical technique to determine the ratios of the elements contributed by the trapped fluid. These ratios are used to calculate the composition of the fluid. Com-

active phreatic)			Deep burial (later diagenetic)
Mixing zone dolomite		Hemipelagic organogenic	Regional and focused hydrothermal
Marine-meteoric (humid) Medium-grained (10–100 μm) stratabound replacement dolomite typically developed in platform carbonate units as units that are tens to hundreds of metres thick and extend over large areas. The top of the dolomite lies beneath a regional karstic unconformity and formed beneath paleo-shorelines. Tend to be best developed about the edge of the sedimentary basin. Dolomite distribution is not tied to evaporites but to petrographic features that indicate meteoric diagenesis: moldic porosity, early precompaction isopachous calcite spar cement, vadose cements. Unless reset by later burial overprint, the isotopic values parallel the meteoric calcite line but are slightly offset to more positive values due to dolomitization. Diluted trace element values for Sr and Na relative to brines formed from seawater or hypersaline brines	Hypersaline-marine-meteoric (oscillating arid-humid and beneath strand-zone) Medium-grained (10–100 μm) stratabound replacement dolomite typically developed as replacements in marine carbonates about the margins of saline giants during times of evaporative drawdown. It forms beneath strand-zones as units that are tens to hundreds of metres thick and extend over large areas. Lies below and unconformity that marks the main basinwide drawdown episode. Connate outflow zones are typically associated with pisolitic/tepee strandline facies and an apron of mudflat anhydrite. Tend to be best developed about the edge of the sedimentary basin, but may even form in areas located well into the evaporite facies of the drawdown basin where connate seawater is seeping back to the surface through a reflux curtain. If not reset by later burial overprint, $\delta^{18}O$ values tend to be more positive than the meteoric mixing zone dolomites. Trace elements such as Na and Sr also tend to be elevated.	Dolomite tend to be micritic to microsparry with beds up to a metre or two thick and hosted in laminated organic-rich deep water muds (precursor was typically a limestone bed within a siliceous/chert host). Characteristic association with deep water host and forms beds that make up not more than 10% of the total sediment interval. Carbon isotope values depend on sedimentation rate. When sedimentation rates are high dolomite tends to precipitate in the zone of methanogenesis so that carbon values tend to be positive (10‰). When sedimentation rates are low, dolomite forms in or just below the zone of sulphate reduction and carbon values tend to be negative. Isotope values tend to be reset by increasing temperatures and the presence of hydrocarbons	Dolomite tend to be sparry and nonplanar with saddle morphologies indicating its formation at temperatures > 50°C. Tends to show geometries controlled by geometry of conduits in deep subsurface; faults and or residual aquifer porosity. Forms in passive margin, collision margin and post-orogenic burial diagenetic settings. Bodies may show evidence of bathyphreatic karstification or may follow earlier formed permeability trends. Vugs may contain base metals and/or degraded hydrocarbon films. Oxygen isotopes values tend to be depleted, indicating precipitation at elevated temperatures. Carbon isotopes may indicate a possible association with hydrocarbons sourced from thermochemical sulphate reduction. Na and Sr tend to be low while Fe and Mn may be elevated due to reducing conditions that typify the deep subsurface

indicated by characteristic textures: spheroidal dolomite, dumb-bell and spindle outlines in cores of dolomite crystals)

positions in dolomites range from aqueous solutions with salt content similar to meteoric water to hypersaline brines. The problem with this method, like the older techniques of whole-rock analyses for stable isotopes, is that it tends to give results that average multiple generations of inclusion fluids. In the last decade, micro-sampling techniques have become increasingly important. These techniques allow the direct sampling of inclusions, typically based on detailed petrographic analysis, and so allow the development of an inclusion history in a single coarse-grained crystal.

Inclusion studies in the last decade, in combination with isotope and trace element studies and detailed petrographic control on sample position, have illustrated the complex, multistage history of most ancient dolomites (e.g. Lopez-Gomez et al., 1993; Mriheel and Anketell, 1995; Nicolaides, 1995;

Zenger, 1996; Mountjoy et al., 2000; Yoo et al., 2000).

4.8.4. Geometry and petrographic character

As Hardie (1987), Warren (1989), Wilson et al. (1990), Braithwaite (1991) and others have noted, the most important practical guides in determining the origin of a dolomite are the geometry of the dolomite body and its lithological/petrographic associations (Fig. 28; Table 4). The position of a dolomite within a sedimentary basin is a direct indication of its position within the basin hydrology. Unlike limestones or siliciclastics, its position does not necessarily reflect biology or wave/current energy. However, one must always keep in mind that once formed, a dolomite body can evolve and alter and so may modify its geometry throughout its burial history. With this in mind, let us look at some of the more important geometric and petrographic characteristics of the various styles of dolomite formation. Relevant literature examples were discussed in detail in appropriate sections earlier in this review.

Sabkha- and Coorong-style dolomites are characterized by their fine-grained crystal sizes (<10 to 20 μm), their stratiform occurrence, and the characteristic sedimentary features associated with sabkhas or Coorong-style settings (Table 4). Sulfate-reduction, methanogenic and deepwater dolomites are also fine grained (typically mimetic in ancient counterparts) and show a characteristic sedimentary association of lagoonal or deepwater sediments, perhaps with associated chert deposition/diagenesis. The finer-grained crystals of these three settings reflect relatively rapid nucleation as dolomite precipitates as multiple bacterially mediated crystallites or replaces aragonitic micrites within meters of the sediment–water interface.

Reflux dolomites can be tied to overlying or adjacent evaporites or their dissolution breccias. Early dolomites located proximal to brine sources tend to be fine grained and mimetic, while those located distally tend to be replacive and more coarsely crystalline (see discussion in Dolomite porosity and permeability section). The proportion of dolomite in a reflux system generally increases towards the source of the Mg-rich evaporite solutions (Fig. 15). Oxygen isotopes are progressively enriched in the same direction together with levels of Sr and Na. Reflux dolomites tend more rapidly to stoichiometry than other early burial dolomites. The most important feature is their strong tie to evaporites or evaporite indicators and the fact that their geometries are generally stratiform and follow the distribution of the evaporites whose depositional system created them.

Less common are dolomite beds tied to the emplacement of salt allochthons and/or the dissolution of deeply burial salt units. Dolomites formed in this way are similar to burial or hydrothermal dolomites and may form coarse sparry ferroan haloes about salt and fault welds that acted as escape conduits for hot metal-rich brines (Warren, 1999).

Mixing zone dolomites occur near the edges of the former lenses of meteoric water. They are depleted in Sr and Na and generally more depleted with respect to oxygen and carbon isotopes than either marine or evaporitic dolomites. There may also be a positive correlation of $\delta^{18}O$ with $\delta^{13}C$ resulting from the mixing of waters with differing compositions. The formation of mixing zones associated with marine seepage or the reopening of basin-wide evaporite basin to marine waters is more complicated than that of the flow paths associated with marine platforms that still dominate the literature (see Warren, 1999 for a discussion of the hydrology of drawdown basins).

When a dolomite formed by the mixing of seawater and meteoric water, the most reliable tool for predicting occurrence is to map either intrabasin paleohighs or shoreline/strandline trends. Hence, widespread mixing-zone dolomites that formed in unconfined aquifers commonly occur below regional unconformities recognizable as sequence boundaries in seismic sections.

Confined aquifer systems are not so easily characterized. Meteoric groundwater circulation is most active in humid environments. A suitable hydrology for the formation of a seawater/meteoric mixing zone dolomite in an open marine basin is best developed during regional regression. This creates prograding hydrological fronts that displace near-surface marine waters. Dolomites formed by mixing of seawater with hypersaline water in central parts of drawdown basins have trends similar to reflux dolomites and it can be very difficult to separate the two. Toward the edges of the drawdown basins mixing zone dolomites follow the subaerial unconformities that define the drawdown stages of the

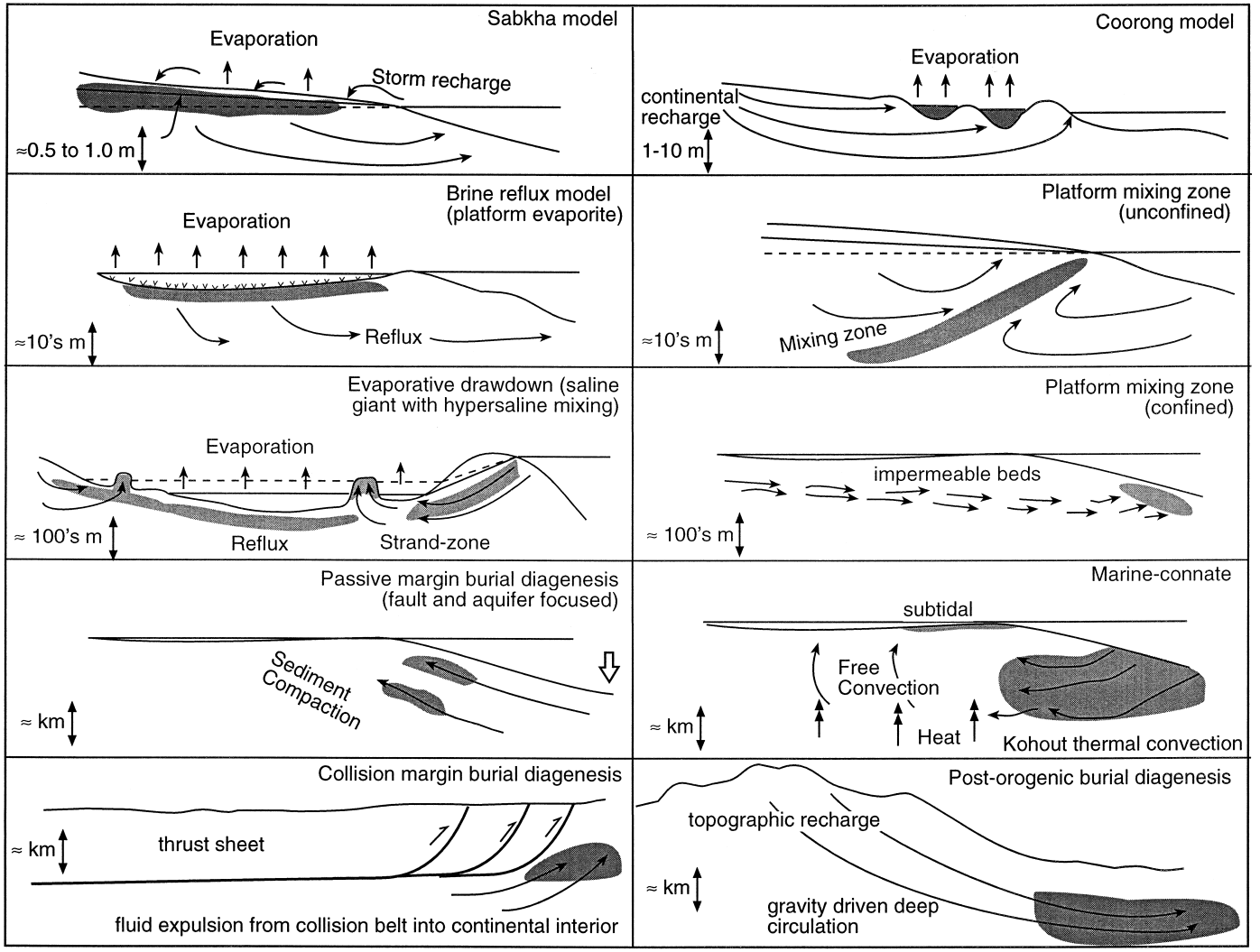

Fig. 28. Dolomitization models (see text for discussion). Note that the position and geometry of the dolomite is a result of its hydrological setting.

basin's evolution. Basinwide evaporite systems do not fit the current marine paradigms of sequence stratigraphy, while platform evaporites do (see Warren, 1999; Chap. 3). Rapid sealevel or paleowaterlevel changes during and soon after dolomite precipitation can greatly complicate either trend.

Evaporitic reflux and strand-zone dolomites away from the brine source are coarser than penecontemporaneous dolomites; crystals are often in excess of 20 μm. Coarser crystals probably reflect more stable pore fluid chemistries. Ancient coarse-grained dolomites are often termed "sucrosic" and are usually composed of euhedral rhombs with crystals between 20 and 120 μm. Marine/meteoric mixing zone dolomites show negative oxygen isotope signatures, while evaporite-associated mixing zone and reflux dolomites show more positive values.

Burial dolomites show negative oxygen isotope signatures, reflecting their elevated temperatures of formation. They form at temperatures that exceed the CRT and crystals have nonplanar faces. They are often associated with saddle dolomites. They can be either regional dolomitizing circulatory systems where whole aquifers are effected (Hitzman et al., 1998), or more focused upwelling systems where faults and fractures tend to limit the dolomitization process (Braithwaite and Rizzi, 1997; Warren and Kempton, 1997). The two dolomitization styles, regional burial and more localized hydrothermal upwelling, are typically part of the same deeply circulating aquifer system.

5. Dolomite porosity and permeability

Interpreting dolomites as fluid conduits, or fluid reservoirs, requires fundamental understanding of the complex interrelationships between petrophysical properties (porosity, permeability, and capillary pressure) and crystal textures in various styles of dolomite (e.g. Wardlaw and Taylor, 1976; Wardlaw and Cassan, 1978; Wardlaw et al., 1988; Ghosh and Friedman, 1989; Kopaska-Merkel and Friedman, 1989; Choquette et al., 1992; Woody et al., 1996; Durocher and Alaasm, 1997).

Early models of porosity development in dolomite used the notions of volume reduction to explain sucrosic textures with high intercrystal porosity (Fig. 29); Murray, 1960; Weyl, 1960). This model assumes dolomitization occurs within a relatively closed system, with a local source for Mg and CO_3^{2-} ions. In such a system, the replacement of limestone (calcite or aragonite) by dolomite reduces mineral volume (and so increases porosity) as dolomite has a smaller molar volume than either calcite or aragonite. The observation that increasing proportions of dolomite lead to an improvement in porosity was the basis for this model. A second factor recognized in these early models was the ability of the growing rhombs to create a rigid cemented framework. As calcite between the growing rhombs dissolves and collapses it leaves behind a rock framework that is made up of a porous grid of dolomite rhombs in crystal-to-crystal contact (the porosity crossover at 50% dolomite in Fig. 29.

Later work showed that if there is an external source of carbonate and magnesium ions then dolomitization of limestone typically results in a volume increase and a loss of total porosity (Lucia and Major, 1994). Dolomitization does not necessarily improve porosity or permeability. Assumptions of permeability, using carbonate classifications based on depositional textures, can result in oversimplified notions of porosity/permeability distribution within dolomitic reservoirs. Early formed dolomite porosity evolves with burial so that later diagenetic alteration (recrystallization and cementation) in the deeper parts of a basin can dramatically change the character of the porosity and permeability of dolomite formed earlier in the diagenetic history (e.g. Gregg et al., 1993).

Wardlaw (1976) divided the total pore system, or total porosity, of a dolomite into two different regions: the relatively large pores, representing the larger volume of porosity; and the pore throats, which comprise a relatively smaller volume. Permeability in many dolomites is not directly related to total porosity or crystal size, but is dependent on the connectivity of the pores via the pore throats. Connectivity concepts must include both the number of pore throats and their size. That is, two dolomites can have the same porosity but widely different permeabilities due to different pore throat properties. Those with intercrystalline porosity developed between large crystals generally have higher permeabil-

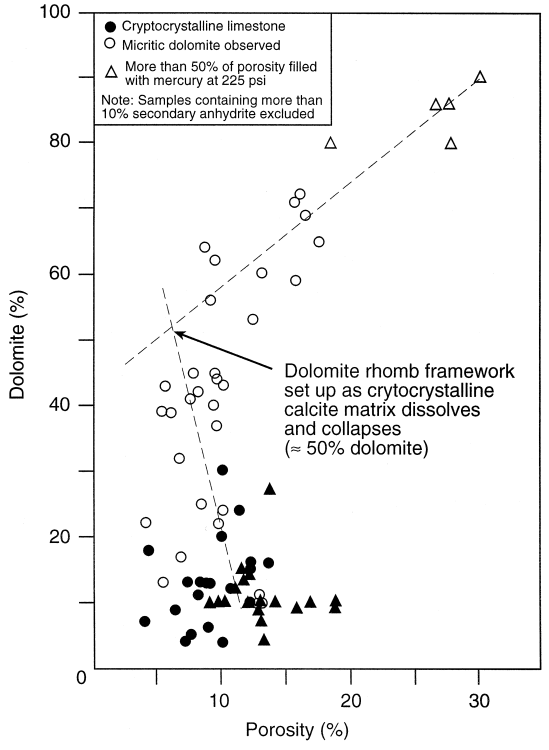

Fig. 29. Relationship of porosity to percentage of dolomite in the Midale Beds, Charles Formation, Midale Field, Saskatchewan (Murray, 1960).

ities than those with porosity developed between rhombs of microspar or micrite.

Using studies of resin pore casts, Wardlaw (1976) described carbonate pore systems as polyhedral or tetrahedral pores connected by sheet-like pore throats formed at compromise boundaries (Fig. 30). As crystal size increases, pore geometries change (Wardlaw, 1976) and ultimately pore throat networks are disrupted, leading to a reduction in permeability. Lucia (1983) calls this pore occlusion overdolomitization. As crystals grow, pores may be reduced from polyhedral to tetrahedral forms and ultimately to interboundary sheet pores (Fig. 30; Wardlaw, 1976).

Using the observations of Wardlaw, Lucia (1983) noted that the geometry of interparticle pore space in any carbonate is related to the size and shape of the particles, and to the amount and distribution of cement, postdepositional compaction, pore-filling mineralization, and crystal leaching. In a later paper, Lucia (1995) concluded that all carbonate pore space should be divided either into interparticle (intergrain/ intercrystalline) or vuggy pores (Table 5). In nonvuggy carbonates (including some dolomites), the permeability and capillary properties can be described in terms of particle/crystal size, sorting, and interparticle porosity. They respond to fluid flow in the same way as siliciclastic sands. With vuggy dolomites, the degree of vug isolation is of paramount importance in controlling the rate of fluid flow through the rock.

Lucia's (1995) classification catalogues porosity and lithology as it currently exists in the reservoir rock and is not based on depositional texture or fabric. For this reason, when Lucia applies Dunham's (1962) classification to a carbonate reservoir, he talks about grain-dominated or mud-dominated lithologies in terms of current fabric or crystal sizes. These may or may not be a direct indication of the grain/mud fabrics of the primary sediment. Lucia's (1995) porosity classification is a refinement of the widely used genetic porosity classification of Choquette and Pray (1970). The advantage of Lucia's

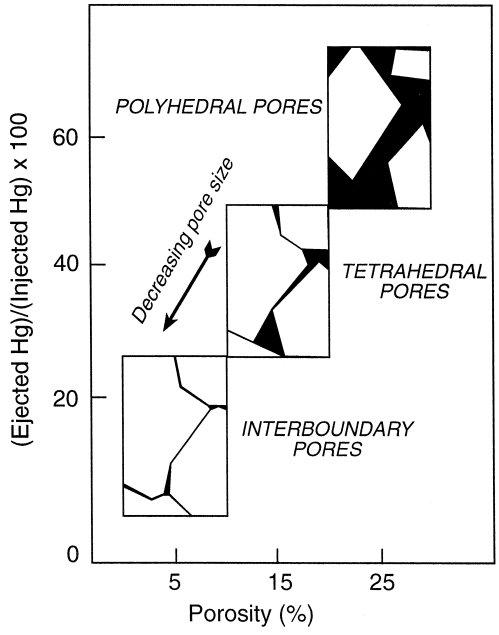

Fig. 30. Shape and evolution of dolomite pores. Note how ongoing growth finally occludes the porosity as the pores undergo a transition from polyhedral to tetrahedral to interboundary pores. Rocks dominated by this last stage where growth and compaction has occluded almost all effective porosity are sometimes called overdolomitized (after Wardlaw, 1976).

Table 5
Terminology of pore types comparing Lucia (1983) with Choquette and Pray (1970)

Porosity type	Abbreviations	
	Lucia (1983)	Choquette and Pray (1970)
Interparticle	IP	BP
Intergrain	IG	–
Intercrystal	IX	BC
Vug	VUG	VUG
Separate Vug (vug to matrix to vug)	SV	–
Moldic	MO	MO
Intraparticle	WP	WP
Intragrain	WG	–
Intracrystal	WX	–
Intrafossil	WF	–
Intragrain microporosity	μG	–
Shelter	SH	SH
Touching Vug (vug to vug)	TV	–
Fracture	FR	FR
Solution-enlarged fracture	SF	CH (channel)
Cavernous	CV	CV
Breccia	BR	BR
Fenestral	FE	FE

approach is that it does not try to interpret the depositional texture and grain-size. It looks only at the rocks current character and so allows a direct comparison of porosity with the likely permeability and petrophysical properties in a lithology. This is more useful when constructing a model of fluid flow. He suggests that when describing particle size and sorting in dolostones, dolomite crystal size terms should be added to a modified Dunham terminology (fine crystal size: < 20 μm; medium crystal size: 20–100 μm; and coarse crystal size: > 100 μm). This gives a partial measure of the potential size of intercrystalline pore throats.

Lucia (1999) argues that Holocene carbonates show little change in pore volume with increasing proportions of dolomite (Fig. 31A). He also found that Plio-Pleistocene dolomites are typically less porous than their limestone counterparts. For example, dolomitized Plio-Pleistocene limestones from Bonaire have an average porosity of 25%, while average porosity is only 11% for their dolomite equivalents, possibly reflecting overdolomitization. If dolomitization had occurred in a closed system, then the dolomites should have porosities ≈ 35%. In contrast to this relationship, Lucia (1999) found that

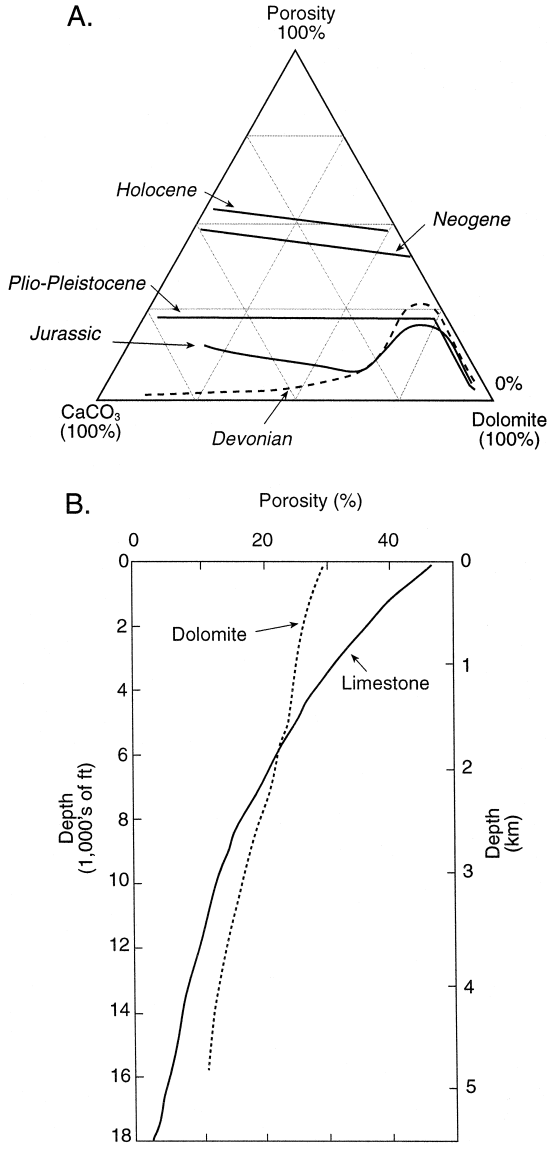

Fig. 31. Dolomite porosity. (A) Relationships between composition, porosity and time (after Lucia, 1999). Dolomite is less porous than limestone counterparts in younger carbonates and more porous in older carbonates. (B) Relationship of porosity to depths in limestones and dolomites in South Florida (after Halley and Schmoker, 1983). Dolomite crossover, below which dolomite becomes more porous than limestone, occurs at 1800 m (6000 ft).

Paleozoic dolomites are usually more porous than their associated limestones. Halley and Schmoker (1983) demonstrated a possible reason for this: they showed that dolomite porosity does not decrease as rapidly as that of limestones during burial. At shallower depths, the limestones have higher porosities, while at greater depths their porosities are less than that of the dolomites (Fig. 31B). In South Florida, the crossover depth is around 1800 m (Schmoker et al., 1985; Amthor et al., 1994). Lucia (1999) also concluded that, for samples at the same depth, dolomitized muds are much more likely to generate and retain porosity than their undolomitized grainstone equivalents.

Woody et al. (1996) used a somewhat different approach, based on Sibley and Gregg's (1987) classification but once again concentrating on the rocks current texture and not on their depositional texture. They showed that as porosity increases in a dolomite reservoir, permeability increases at a greater rate in planar-e dolomite than in planar-s dolomite (Fig. 32). Also, the porosity to permeability relationship in both categories of planar dolomite is more obvious than that in nonplanar dolomite. The relative loss of intercrystalline porosity volume and pore throat size, that is inherent in a transition from polyhedral to interboundary pores, encompasses the transition from planar-e to planar-s textures (Fig. 30). Woody et al. went on to conclude that, as planar or nonplanar textures are variously imparted to dolomite as the result of different burial histories, the diagenetic history of a dolomite exerts a major effect on its petrophysical properties.

To help explain this, and other similar porosity/permeability observations, Lucia (1999) separates ancient dolomites into two end members: (a)

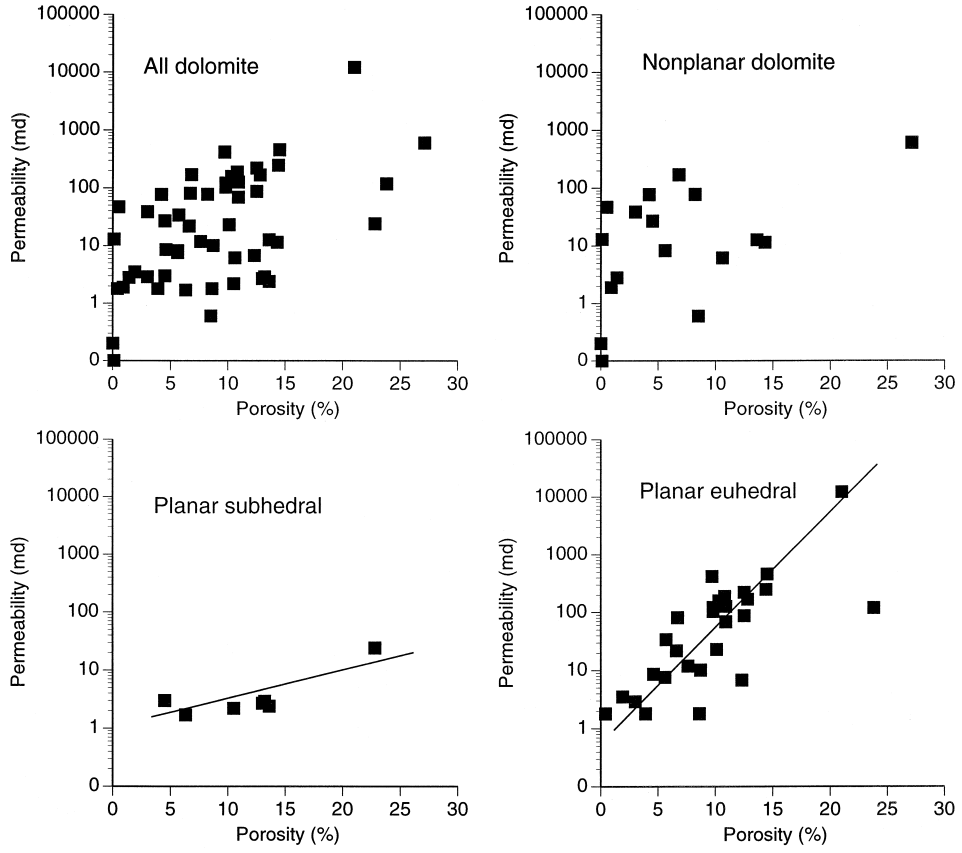

Fig. 32. Plots of porosity versus permeability for nonplanar, planar-s and planar-e dolomites (replotted from data in Table 1 in Woody et al., 1996).

dolomites where the precursor was mud-dominated and (b) dolomites where the precursor was a grainstone. He goes on to argue that there is an increase in pore size during dolomitization of mud-dominated limestone precursors (Fig. 31A). No such change seems to occur during the dolomitization of grain-dominated limestone precursors. He argues grainstone precursors are usually composed of grains with diameters that are much larger than the dolomite crystal size. Hence, the growth of dolomite rhombs does not have a significant effect on pore-size character. Grain-dominated packstones also have large grains that are in grain-to-grain contact and so during dolomitization behave much in the same way as a grainstone. In contrast, replacement of any interparticle mud by 100-μm-diameter dolomite crystals tends to enhance the intergrain flow character in such a rock. When mud-dominated limestones are dolomitized, there is often an enhancement of the flow capacity of the total rock. Newly formed dolomite crystals in the dissolving mud matrix show a range in crystal sizes from particles with diameters equivalent to the muds they are replacing, up to sparry crystals which may be several hundred microns across. When a coarse dolomite spar replaces mud, any porosity residing between the euhedral rhombs will have better flow properties than its finer-grained mud counterpart.

The concept of vuggy pore space must be added to that of intercrystalline pore throat size to complete the description of pore space in a dolomite (Table 5; Lucia, 1995, 1999). Vuggy pores are divided into two groups depending on how they are interconnected: (1) separate vugs, (2) touching vugs. Separate vugs are defined as interconnected only through interparticle (intercrystalline) pore space, while touching vugs themselves form an interconnected pore system often with much higher permeabilities. We are now ready to consider how the various styles of porosity and models of dolomitization can control the quality of dolomitic oil and gas reservoirs.

6. Dolomite as a hydrocarbon reservoir

Dolomite reservoirs account for approximately 80% of recoverable oil and gas in carbonate rocks of

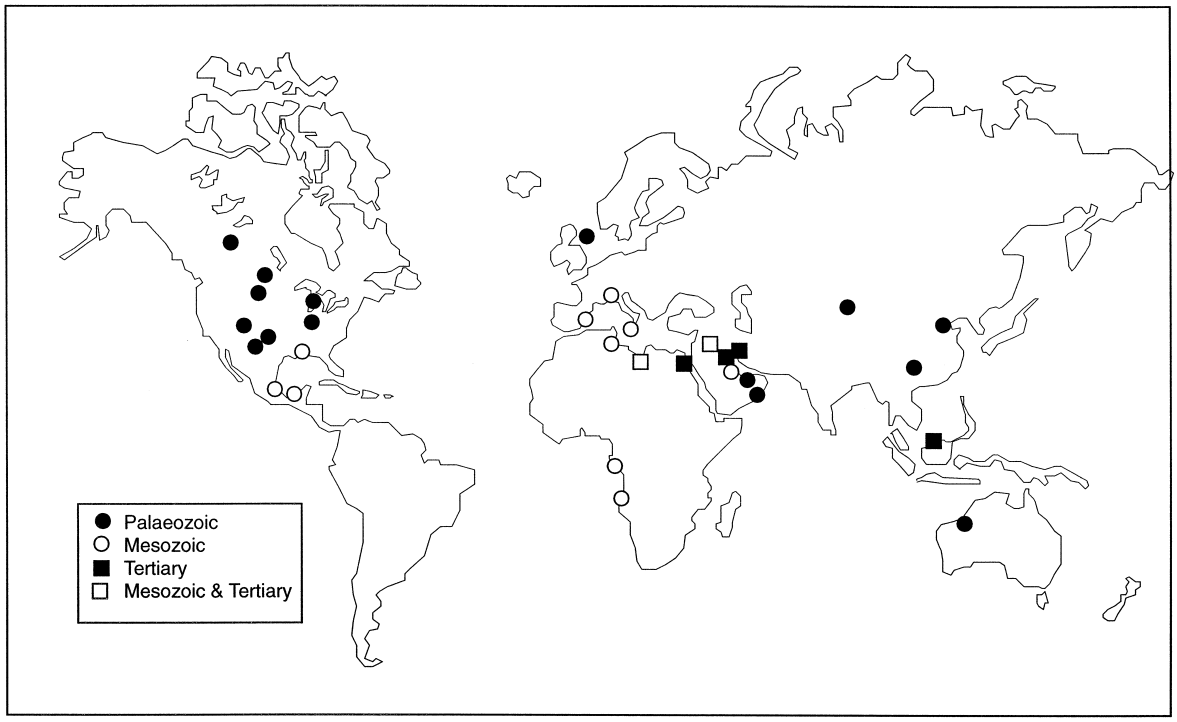

Fig. 33. Major dolomite reservoirs subdivided by age and geography (after Sun, 1995).

Table 6
Peritidal (syndepositional-mimetic) reservoirs (after Sun, 1995)

Basin/province	Formation	Geologic age	Postdolomitization modification	Porosity (%)	Perm. (md)	Reference
Bohai Gulf	Wumishan	Late Precambrian	Karstification and fracturing	5	0.1–10.0	Zhai and Zha, 1982; Horn, 1990
Tarim	Qigebulake	Late Precambrian	Karstification and burial corrosion	2.0–5.0	NA	Yie and Liu, 1991
Tarim	Qiulitage	Late Cambrian–Early Ordovician	Karstification and burial corrosion	3.0–6.0	NA	Yie, 1991; Hu, 1992
Anadarko	Arbuckle	Late Cambrian–Early Ordovician	Karstification	NA	NA	Gao and Land, 1991
Permian	Ellenburger	Early Ordovician	Karstification	3.5	10.0–50.0	Loucks and Anderson, 1985; Kerans, 1988
Canning	Nita	Middle Ordovician	Karstification and fracturing	2.0–18.0	35–3310	Karajas and Kernick, 1984; Bentley, 1984
Williston	Interlake	Silurian	Karstification	15	5	Roehl, 1985
Po	Dolomia	Late Triassic	Fracturing	3	50	Mattavelli and Margarucci, 1990
Po	Zandobbio	Early Jurassic	Fracturing	3	50	Mattavelli and Margarucci, 1990
N Arabian Platform	Kurrachine	Late Triassic	Fracturing	3.5–6.3	40	unpublished data
N Arabian Platform	Butmah	Early Jurassic	Fracturing	NA	NA	unpublished data

Table 7
Subtidal dolomite reservoirs associated with evaporitic tidal flat/lagoonal settings on carbonate platforms–reflux dolomites (after Sun, 1995)

Basin/province	Formation/group	Geologic age	Postdolomitization modification	Porosity (%)	Perm. (md)	Reference
Williston	Red River	Late Ordovician	NA	11.0–17.8	5.0–11.0	Clement, 1985; Ruzla and Friedman, 1985; Fischer et al., 1990; Longman et al., 1992
N Michigan	Niagara	Silurian	NA	NA	NA	Sears and Lucia, 1980
Permian	Thirty-one	Early-Middle Devonian	NA	6.8–12.6	6.2–11.7	Saller et al., 1991
Williston	Duperow	Late Devonian	NA	NA	NA	Ehrets and Kissling, 1985
Williston	Birdbear	Late Devonian	NA	NA	NA	Ehrets and Kissling, 1985
SE Alberta	Warbamun	Late Devonian	NA	6	NA	Metherell and Workman, 1969
Williston	Mission Canyon	Early Carboniferous	NA	14–16	25–30	Lindsay and Kendall, 1985; DeMis, 1992
Fossil	Mission Canyon	Early Carboniferous	NA	6.0–8.0	0.7–1.5	Sieverding and Royse (1990)
Williston	Charles	Early Carboniferous	NA	14	1.0–10.0	Longman and Schnidtman, 1985
Paradox	Leadville	Early Carboniferous	Karstification	5.5	22	Miller, 1985
Anadarko	Warsaw	Early Carboniferous	Karstification	15	35	Ebanks, 1991; Johnson and Budd, 1994
Sichuan	NA	Early Carboniferous	Karstification	6.0–12.0	1.1–18.5	Yang, 1986
Paradox	Hermosa	Late Carboniferous	NA	10	15	Peterson, 1992
Permian	San Andres	Late Permian	local karstification (e.g., Yates field)	10.0–12.0	2.2–11	Cowan and Harris, 1986; Chuber and Pusey, 1985; Craig, 1988
Permian	Grayburg	Late Permian	NA	9	2.5	Harris and Walker, 1990
Arabian Platform	Khuff	Late Permian	Fracturing	8.0–25.0	2–120	Alsharhan, 1993; Bos, 1989
N Gulf of Mexico	Smackover	Late Jurassic	NA	16–25	63–245	Feazel, 1985; Petta and Rapp, 1990
SE Mexico	NA	Late Jurassic	Fracturing	3.0–6.0	NA	Peterson, 1983; Santiago and Baro, 1992
E Arabia	Arab-C	Late Jurassic	NA	12.0–25.0	12–100	Wilson, 1985
E Arabia	Arab-D	Late Jurassic	NA	15–26	50–500	Powers, 1962; Wilson, 1985; QGPC, 1991
SE Mexico	NA	Early–Middle Cretaceous	Fracturing	3.0–9.0	NA	Peterson, 1983; Santiago and Baro, 1992
Central Mexico	NA	Middle Cretaceous	Karstification	NA	NA	Wilson, 1975
N Gulf of Mexico	Edwards	Middle Cretaceous	NA	14–21	2–200	Cook, 1979; Fisher and Rodda, 1969
N Iraq	Qamchuqa	Middle Cretaceous	Karstification and fracturing	10.0–30.0	50–250	Unpublished data source
Congo	Sendji	Middle Cretaceous	NA	20–30	700–1000	Baudouy and LeGorjus, 1991; Teisserene and Villemin, 1989
Cuanza (Angola)	Binga	Middle Cretaceous	Fracturing	15	50	Brognon and Verrier, 1966
Gabes-Tripolitana	Zebbag	Middle Cretaceous	NA	10.0–25.0	100–1000	Unpublished data source
Sirte	Lidam	Middle Cretaceous	NA	12	NA	Unpublished data source
Sirte	Sabil	Paleocene	NA	10.0–15.0	NA	Unpublished data source
Sirte	Gir	Eocene	NA	15	NA	Unpublished data source
Arabian Platform	Umm er Rudhuma	Eocene	NA	20–30	NA	Danielli, 1988
Mesopotamian	Asmari	Oligocene–Early Miocene	Fracturing	9.0–14.0	10	Hull and Warman, 1979; McQuillan, 1985
Mesopotamian	Euphrates-Jeribe	Early Miocene	Late corrosion	20–30	10–100	Sun and Esteban, 1994

Table 8
Dolomite reservoirs associated with basinwide evaporites (after Sun, 1995)

Basin/province	Formation	Geologic age	Postdolomitization modification	Porosity (%)	Perm. (md)	Reference
South Oman	Huqf	Late Precambrian–Early Cambrian	NA	6.0–12.0	1.0–100.0	Mattes and Conway, 1990
SE Michigan	Niagara	Silurian	NA	10	7.9	Gill, 1985; Jodry, 1969
Alberta	Keg River	Middle Devonian	Late corrosion	10.1	184	Schmidt et al., 1985
Zechstein	Zechstein	Late Permian	Karstification and late corrosion	5.0–20.0	10–100	Clark, 1980
Gulf of Suez	Rudeis	Middle Miocene	Late corrosion	17–22	50	Sun and Esteban, 1994
Gulf of Suez	Belayim	Middle Miocene	Late corrosion	15–16	32	Sun and Esteban, 1994

North America (Zenger et al., 1980). Significant proportions of the hydrocarbons in the former Soviet Union, northwestern and southern Europe, north and west Africa, the Middle East, and the Far Fast (Fig. 33; Sun, 1995) are also found in dolomite reservoirs. Once formed, dolomites preserve porosity and permeability much better during burial than limestones (Fig. 31B), which is in part a reflection of their greater ability to resist pressure dissolution (e.g. Amthor et al., 1994).

Nevertheless, although they generally provide better reservoirs than limestones at depth, not all dolomites are good reservoirs. Depending upon their original depositional fabric and nature and the volume of fluids passing through carbonate sediments, dolomitization can destroy, maintain, or enhance porosity. During the course of exploration or production, geologists need to predict not only where dolomite forms within a stratigraphic or structural framework, but more importantly where it contains and maintains the porosity of reservoir quality (Sun, 1995; Lucia 1999).

In a worldwide study of dolomite reservoirs, Sun (1995) found that the majority of hydrocarbon-producing reservoirs occur in four situations: (1) peritidal-dominated carbonate, (2) subtidal carbonate associated with evaporitic tidal flat/lagoon, (3) subtidal carbonate associated with basinwide evaporites, and

Table 9
Dolomite reservoirs in nonevaporitic carbonate settings (after Sun, 1995)

Basin/province	Formation	Geologic age	Postdolomitization modification	Porosity (%)	Perm. (md)	Reference
Michigan	Trenton and Black River	Middle Ordovician	NA	4	10	Hurley and Budros, 1990
Anadarko	Clarita	Silurian	NA	8	93	Morgan, 1985
Anadarko	Henryhouse	Silurian	NA	7	0.1–30	Morgan, 1985
Alberta	Sulphur Point	Middle Devonian	NA	NA	NA	Qing and Mountjoy, 1994a
Alberta	Slave Point	Late Devonian	NA	NA	NA	Phipps, 1989
Alberta	Swan Hills	Late Devonian	NA	NA	NA	Kaufman et al., 1991
Alberta	Leduc	Late Devonian	NA	7	25	Mountjoy and Amthor, 1994
Alberta	Nisku	Late Devonian	NA	9	340	Machel and Anderson, 1989; Watts et al., 1994
N Alberta	Wabamun	Late Devonian	NA	NA	NA	Mountjoy and Halim-Dihardja, 1991
Canning	Nullara	Late Devonian	NA	NA	NA	McManus and Wallace, 1992; Wallace, 1990
Illinois	St. Genevieve	Early Carboniferous	NA	27	12	Choquette and Steinen, 1980, 1985
Ragusa	Siracusa	Early Jurassic	NA	12.0–16.0	NA	Schramm and Livraga, 1986
Gulf of Valencia	NA	Late Jurassic	NA	7.0–12.0	1.0–2000	Watson, 1982; Esteban, 1988
Central Luconia	NA	Middle–Late Miocene	NA	15–30	10–500	Epting, 1980

(4) nonevaporitic carbonate sequences associated with topographic high/unconformity: platform-margin buildup or fault/fracture (Tables 6–9).

Peritidal dolomite reservoirs are often evaporitic and typically have low matrix porosity and permeability adjacent to any platform evaporite due to overdolomitization of the relatively fine-grained sediment host. The porosity occlusion associated with overdolomitization reflects the extended times for tidal-flat development under relatively stable "greenhouse" platform conditions. This allowed repeated pore-water flooding of magnesium and calcium bearing marine fluids during storm-driven replenishment or seepage into the saltern and evaporitic mudflats. Such fine-grained dolomites, intercalated with platform evaporites, form few economic reservoirs unless they are modified by karst or fractured (Table 6).

Peritidal dolomites are often associated down dip with dolomite reservoirs formed by brine reflux from the mudflats into marine subtidal platform carbonates (Fig. 34). Porosity in such subtidal dolomites typically occurs in multiple zones within stacked shallowing-upward cycles (Table 7; Sun, 1995; Warren, 1999). The base of each zone is formed by porous, partially to completely dolomitized subtidal carbonate that terminates upward in relatively tight mudflat carbonates and evaporites. Reservoir quality in the subtidal dolomite is related to depositional and diagenetic fabric. The best reservoirs are in high-energy, grain-dominated sediments (oolitic/pisolitic) or low-energy lagoonal dolomudstone/wackestone with a coarsely crystalline overprint. Finely crystalline, mud-dominated mimetic dolomites nearer the brine source are commonly poor reservoirs. In most cases, primary intergranular porosity in grain-dominated rocks is preserved due to the relatively arid climate and limited recharge of fresh water, minimizing meteoric leaching and calcite cementation. The extensive impermeable mudflat dolomites and anhydrites, which cap upward-shoaling cycles effectively, seal off the underlying carbonates from any later influx of freshwater or sulfate-bearing fluids.

Porous dolomites are generated via brine reflux as dense saline brines, generated by evaporative concentration in salterns and mudflats, percolate downward and basinward through the sediments (Adams and Rhodes, 1960; Elliott and Warren, 1989; Saller and Henderson, 1998). As they first pass out from their source, these refluxing brines are highly supersaturated with respect to dolomite and so precipitate large quantities in the proximal parts of the refluxing system. This pervasive precipitation lowers the

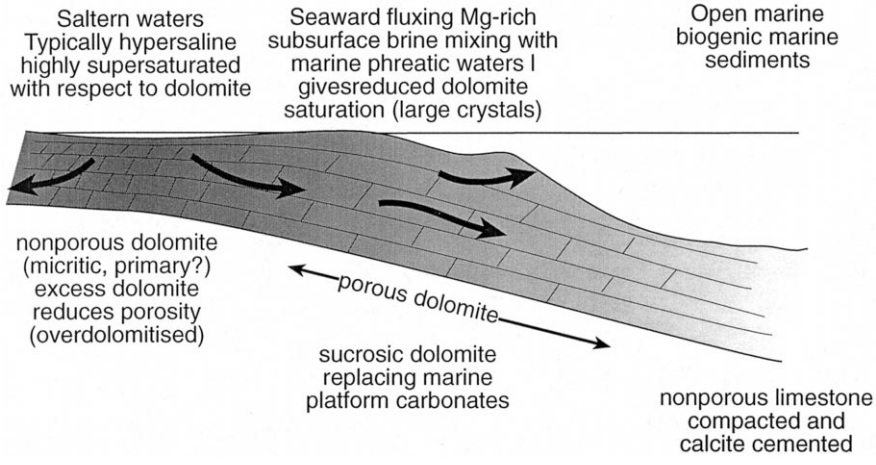

Fig. 34. Model of mudflat and subtidal reflux dolomite reservoirs in a platform evaporite setting exemplified by the various reservoirs of the Central Basin Platform in the Permian Basin of west Texas (in part after Saller and Henderson, 1998). Primary/mimetic dolomite that formed in and around brine pool/seaway is overdolomitized and so does not retain economic levels of porosity unless enhanced by later exposure or fracturing. Reflux/secondary dolomite formed as the dense brines sank through platform sediment pile and replaced permeable carbonates. This form of secondary dolomite tends to retain its permeability in more distal areas.

dolomite saturation in pore waters flushing the more distal portions of the reflux system. Lower saturation results in fewer nuclei and larger crystals. Hence, porosity and permeability are greater in the more distal parts of the system (Fig. 34). As reflux brines continued to circulate, they precipitate more dolomite, further decreasing porosity, especially in proximal platform-interior sediments. Burial and reflux salts also form pervasive cements in the more proximal areas (see Warren, 1999; Chap. 4 for a discussion of burial stage evaporites).

Lucia (1999; p. 147) pointed out that this downward cyclic transition from a relatively impervious peritidal dolomite cap (with intercalated evaporite seals) into dolomitized subtidal carbonate reservoirs corresponds to an downward increase in dolomite crystal size. He relates this to a downward decrease in dolomite saturation as the refluxing brines sink deeper and further from the evaporite source. Such mudflat and reflux dolomites are not forming today under climatic conditions characterized by major continental glaciation and high frequency high amplitude sealevel fluctuation (icehouse climatic mode). Formation of dolomite reservoirs associated with platform evaporites is more likely during times characterized by lower frequency, lower amplitude sealevel changes (greenhouse mode).

Dolomite reservoirs associated with basinwide evaporites are often preserved beneath the seal of the overlying salts. Such thick massive evaporites trap and preserve some of the oldest oil fields in the world (Table 8). Sun (1995) found that porosity distribution in subtidal dolomite reservoirs associated with basinal evaporites typically shows no direct relationship to stratigraphic position or depositional trends. This reflects a strong diagenetic overprint of primary porosity and patchy cementation of early generated secondary porosity by anhydrite/halite. It also indicates the problems of porosity prediction in a hydrological system characterized by large autocyclic fluctuations in hydrologic base level ($\approx$ 1 km) over thousands of years and the lack of differentiation of strand-zone versus basin-center reflux dolomites. Both dolomite styles typify basinwide evaporite settings (Warren, 1999).

During early dolomitization and limestone leaching, significant porosity was developed in sediments containing metastable skeletal components. However, in such sediments the hypersaline flushing commonly leached calcium ions, which then reacted with sulfate-rich brines to form anhydrite cements. In some regions, both depositional and diagenetic hypersaline leaching porosity was almost occluded by this cement. In these cases, karst formation, fracturing, or later corrosion were required to restore porosities and permeabilities beneath the evaporite seal. Unlike the dolomites associated with platform evaporites, this group of reservoirs cuts across both icehouse and greenhouse periods because basinwide evaporites require tectonic settings that are independent of sealevel character (Warren, 1999).

Most dolomite reservoirs in nonevaporitic carbonates are associated with topographic highs or unconformities, platform-margin buildups, or fault and fracture systems (Table 9; Sun, 1995). Formation of these dolomites is related either to reflux of slightly evaporated seawater, long-term flushing by connate water, mixing of seawater with fresher water or resurging burial-derived dolomitizing fluids. In the former (e.g., Early Carboniferous Saint Genevieve dolomite in the Illinois basin, USA, and middle-upper Miocene dolomite in the central Luconian platform, offshore Borneo), pore space is mainly of micro-intercrystalline type with subordinate moldic pores. Permeability resulted directly from early dolomitization of lime-muds that were preserved in subsequent burial diagenesis. Porosity occlusion, due to overdolomitization, is generally not a problem for reservoir development because of the limited duration of dolomitization.

Owing to the relatively low Mg/Ca ratio and limited volumes of burial-derived dolomitizing fluids, burial processes typically led to the formation of burial dolomite with a relatively coarse, sucrosic fabric. Usually, this evolves into nonplanar dolomite typified by poor to nonexistent porosity and permeability (Gregg et al., 1993). Sometimes, the burial evolution process was arrested before porosity was completely lost, often by the emplacement of hydrocarbons that shut down further cementation. In this case, burial dolomitization improves reservoir properties compared with adjacent limestones that would otherwise make poor reservoirs. Solution cavities, vugs, and intercrystalline porosity are commonly developed in local often structurally focused bathyphreatic sites, where there was an excess of dissolu-

tion over precipitation during replacement. Dissolution processes associated with burial dolomitization can be particularly intense in zones where hot, basin-derived, organic-entraining fluids moved updip along faults, fractures or unconformities.

7. Dolomite: the ore host

Dolomite formation has often played an integral part in the mineralization of ore deposits, many mineralized dolomites are more than passive hosts (Table 10). Certainly, some have acted as passive porous vessels allowing passage and mixing of metalliferous solutions, they did little more than hold the resulting mineralization. More often, the formation of late stage burial and hydrothermal dolomites was intimately related to basinal solutions that soon after were actively involved in the ore precipitation process. Because late-stage dolomitization extends beyond the zone of sulfide mineralization, these coarse-grained dolomites can sometimes be used as pointers to structurally focused sites of potential mineralization (Warren and Kempton, 1997). Although other, often diagenetically earlier, textures are occasionally present, most ore hosting dolomites are dominated by nonplanar (xenotopic) mosaics with crystals that range from 100 μm to more than 1 cm. These late stage associations typically include saddle-dolomite cements and show negative burial-related oxygen isotope signatures (Fig. 27).

Lower temperature (60°C–200°C) late-stage diagenetic or burial dolomites typically host MVT mineralization. Ore minerals are dominated by sphalerite and galena, with minor barite, pyrite and marcasite. Texturally, most ores are dominated by colloform-banded sphalerite with isolated crystals of galena dispersed within the sphalerite bands. Late-stage dolomites may form a substrate to mineralization, or an intermixed layering especially in the early stages of mineralization (e.g. Cadjebut, Gays River; Warren and Kempton, 1997; Kontak, 1998).

Nonmagmatic base metal mineralization typically occurs at redox interfaces where sulfate reduction is either by bacterial sulfate reduction (BSR) or thermochemical sulfate reduction (TSR; see Warren, 1999, Chaps. 8 and 9 for discussion). Anaerobic sulfate reducing bacteria can produce dolomite and isotopically light H_2S as they metabolize organic matter (or hydrocarbons) while utilizing sulfate as the oxidizing agent:

$$Ca^{2+} + Mg^{2+} + 4SO_4^- + 4CH_4 + 4H^+ \rightarrow 4H_2S + CaMg(CO_3)_2 + 6H_2O + 2CO_2$$

Sulfate-reducing bacteria commonly thrive within or near hydrocarbon–water contacts in situations varying from near surface methane seeps to depths of a few kilometers (Warren, 1999).

Bacterial sulfate reduction can occur at temperatures up to 110°C in some pressured hydrothermal environments, but at higher temperatures TSR comes to dominate. For example, in MVT deposits, a metal-sulfide phase typically coprecipitates with hydrothermal or saddle dolomite at temperatures of 60°C–200°C (Hill, 1995):

$$H_2S + CO_2 + MeCl^+ + Mg^{2+} + 2CaCO_3 + H_2O \rightarrow MeS + Ca^{2+} + CaMg(CO_3)_2 + HCO_3^- + Cl^- + 3H^+$$

Where Fe is abundant in the throughflushing waters, pyrite forms by reacting with the H_2S; where Pb and Zn are available, galena and sphalerite form. The acidic nature of both the BSR and TSR reaction environments means that carbonate dissolution is often associated. Hence, the ore is often hosted in vugs, secondary pores or interclast porosity in carbonate breccias. Sometimes, the required sulfate is carried by throughflushing basinal waters; at other times, it is derived from nearby dissolving evaporite beds, which may also act as hydrocarbon traps (Warren, 1999). The ability of dissolving anhydrites to act as sulfur sources explains the intimate relationship of some MVT deposits to evaporites (Table 10; Gays River, Cadjebut, some Knox Group deposits). However, others are associated with intervals of hydrocarbons within traps that are not evaporitic or they are precipitated in zones where metalliferous sulfur-depleted brines mix when sulfate-entraining waters and the organics come from hydrocarbons in the pore fluids (Table 10).

Some, but not all, MVT-associated late stage dolomite hosts are laterally limited masses of coarsely crystalline dolomite whose positions are controlled by major regional faults (Table 10). Such faults tend

to be steep and so cut across diverse thick sedimentary successions (e.g. Navan and Cadjebut Pb–Zn deposits; Fig. 35; Warren and Kempton, 1997). The relationship between major faults and dolomite distribution suggests the hot basinal fluids were part of a deeper circulating system that rose along and seeped from these faults, extending laterally where permeability was greater. These deep regional aquifers feeding the faults can also contain burial dolomites hosting Pb–Zn ores.

Table 10
Late stage dolomite acting as an ore host in MVT deposits. Mineralization typically emplaced at low temperatures and associated with hydrocarbons and dissolving evaporites

Pb–Zn ores, western Basque–Cantabrian region, northern Spain (Lower Cretaceous) (Bustillo and Ordonez, 1995)	Ore host dolomites are massive homogeneous burial dolomites that overprint primary structures. Most display textures consisting of geometric, xenotopic mosaics with crystals that range in size from 100 μm to 1 mm. They are fault-focused dolomitized masses in the partially dolomitized Urgonian Complex. Ores are related to the regional migration of Pb- and Zn-enriched brines that were expelled from adjacent basinal mudstones. Hydrocarbons were important in fixing sulphides and oil- and gas-fields of similar age are located near the Pb–Zn deposits.
Zn–Pb–Ba Iranuh District, Esfahan Area, Iran (Lower Cretaceous) (Ghazban et al., 1994)	Ore hosts are coarse-grained discordant, late diagenetic dolomites emplaced along the Irankuh fault. The ore-stage dolomites formed from warm (100°C) saline, ^{87}Sr-enriched fluids similar to oilfield brines. Host dolostones show extensive depletion $\delta^{18}O$ (−4.9‰ to −12.7‰) indicating increased temperatures. A progressive depletion in stable carbon isotope ratios of the host dolostone occurs as mineralization is approached. Overlap in $\delta^{18}O$ values and $^{87}Sr/^{86}S$ ratios between coarse-grained ore hosing dolomite and adjacent sucrosic and saddle dolomites implies that these rocks were isotopically modified by similar fluids.
Gays River Pb–Zn, Nova Scotia (Visean) (Kontak, 1998; Savard, 1996)	Paragenetically, constant volume dolomitization of the host rock is followed by euhedral, manganiferous dolomite cement, then sphalerite and galena. Syn- to postore calcite with trace amounts of barite, fluorite, and quartz, occlude the remaining porosity. Dolomitization by hot basinal brines, in a burial setting typified by red bed clastics overlain by thick halokinetic rift evaporites and marginward carbonate platforms. Overlying and capping evaporites, prior to their dissolution, focused and trapped escaping metalliferous basinal fluids into the platform. Evaporites probably supplied sulphate that helped fix the metals via thermochemical sulphate reduction.
Navan Zn–Pb, Ireland (Lower Carboniferous) (Rizzi and Braithwaite, 1997; Braithwaite and Rizzi, 1997; Hitzman et al., 1998)	Ore hosted principally (97%) by the Meath Formation (Navan Group). Most dolomitization at Navanis confined to the Meath Formation. Dolomite is linear trending NE–SW, with a flattened, laterally limited, tabular geometry in cross-section. Dolomitizing fluids initially rose vertically, cross-cutting stratigraphic and sedimentological boundaries, although fluid flow was subsequently controlled by these features. Metalliferous brines were fed from a deeper regional aquifer that was also forming widespread burial dolomite. Ores follows the dolomite trend and were precipitated during ongoing dolomite cementation. Three stages of dolomitization are indicated. Isotopic and fluid inclusion data suggest growth of successive stages from waters which became progressively hotter (60°C–160°C).
Cadjebut Pb–Zn, Canning Basin, Australia (Devonian) (Warren and Kempton, 1997; Tompkins et al., 1994)	Cadjebut MVT mineralization is hosted by carbonate-evaporite units in the Givetian lower dolomite sequence of the Pillara platform, occurs as two ore types: (1) an early Zn-rich, stratiform and rhythmically banded ore and its laterally equivalent halo of banded marcasite, barite ± calcite; and (2) a cross-cutting, breccia-fill, Pb-rich ore. Both ore types are intimately related to the bathyphreatic dissolution of stratiform anhydrite units which the ore replaces (sulphur source). There are two forms of dolomite in the region. An earlier brine reflux dolomite, with its lateral extent controlled by the distribution of platform ramp evaporites. A later coarser-grained burial/saddle dolomite that hosts the ore bodies. The distribution of this later dolomite is tied to basin-defining extensional/growth faults that acted as conduits and foci for the upward flow of metalliferous basinal fluids (Fig. 35). Isotopically, the oxygen isotope signature of this later burial dolomite is lighter than the reflux dolomite, reflecting focused upwelling of higher temperature basinal fluids (Fig. 27).

(continued on next page)

Table 2 (*continued*)

Polaris Pb–Zn, Canadian Arctic Archipelago (Upper Ordovician) (Randell, 1994; Heroux et al., 1996)	Coarsely recrystallized ore hosting dolomite, white dolospar, internal sediments, clayminerals and brown dolomitized limestone constitute the alteration halo at Polaris. Host-rock dissolution was synchronous with pre-folding ore precipitation. Synsedimentary faults and gravity-slump breccias in the host limestones probably afforded preferential permeability. Halokinesis driving much of the structural focusing of the mineralising fluids. Polaris lies in shelf carbonates of the Thumb Mountain Formation. Ore was deposited from tectonically driven bittern-derived 105° to 125°C basinal brines, while burial temperatures in the adjacent unaltered carbonates were around 60°C. The mineralized zone is characterized by a zone of pure illite above a kaolinite envelope surrounding the deposit. Faults and folds marking the culmination at Polaris of the late Devonian–Ellesmerian orogeny that ruptured the shale seal, terminating the mineralization.
Pb–Zn deposits, Knox Group and Shady Dolomite Formation carbonates, southern Appalachia, USA (Cambrian and Lower Ordovican) (Montañez, 1994; Haynes and Kesler, 1994; Jones et al., 1996)	Mineralization, consisting of sphalerite and sparry dolomite, fills interstices in the breccias that formed in limestone. These MVT deposits are found largely in two major paleoaquifers in the region, the Lower Cambrian Shady Dolomite and the Lower Ordovician Knox Group karst zone. Regionally extensive (approximately 70,000 km^2), late diagenetic dolomites that also hosts the ore consist of replacement dolomites and zoned dolomite cements. As much as 50% of the limestone in mineralized breccia sections is lost over enormous areas of paleoaquifer that extend far beyond significant mineralization. Late diagenetic dolomitization of the Upper Knox Group in the southern Appalachian basin was closely associated with widespread secondary porosity development, and hydrocarbon migration. Late diagenetic matrix dolomites served as long-lived aquifers that focused and channeled diagenetic fluids in the deep subsurface (2 to >5 km) driven by fluid migration that was a response to late Paleozoic Alleghenian tectonism (330 to 265 Ma). Thermochemical sulfate reduction is the main metal fixing mechanism with sulfate derived from dissolving Cambrian and Ordovician evaporates.
Pb–Zn deposits, southern Canadian Rockies (Cambro-Ordovician) (Yao and Demicco, 1995; Nesbitt and Muehlenbachs, 1994; Nesbitt and Prochaska, 1998; Qing and Mountjoy, 1994a,b,c)	Ore hosting dolomite, made up of white, sparry, hydrothermal, replacement, and open-space filling dolomite form strata-bound sheets over broad platforms, except near the margin, where they also form dikes that crosscut sedimentary bedding planes. Contained within the dolomites are occurrences of talc and MVT Pb–Zn (the former Kicking Horse and Monarch mines) mineralization and economic concentrations of magnesite (Mount Brussilof mine). Fluid inclusion data indicated that the primary dolomitizing fluids were warm to hot (100°C to 200°C) saline brines (13–25 wt.%). The high salinity brines were derived by the subsurface dissolution of thick salt sequences. Field evidence indicates that the two kinds of dolomite bodies were formed by pervasive, formation-parallel flow and fracture-channeled, cross-formational flow, respectively. The timing of dolomitization (Silurian to Late Devonian) coincided with the timing of the early Paleozoic contractional deformation in the west. Finite element modeling showed that the observed dolomite geometry and geochemistry are consistent with miogeocline-scale ground-water flow driven by west-to-east topographic relief.

The varying styles of burial and hydrothermal dolomite ore hosts can be clearly seen when temperatures of the deposit and the surrounding host rock are compared, as was done in a comparison study of 14 major MVT districts of Canada and the USA. There thermal alteration in deposit surrounds were compared to inclusion-derived temperatures in the ore zone interior (Sangster et al., 1994). This temperature comparison divided the various dolomite-hosted deposits into three groups. Group 1 deposits have ores that are in thermal equilibrium with their host rocks and encompasses the majority of the studied MVT deposits (Pine Point, Newfoundland Zinc, Mascot-Jefferson City, Copper Ridge, Sweetwater, Central Missouri, Northern Arkansas, and Tri-State). Group 2 deposits have ore zones that are significantly hotter than surrounding host rocks and, as such, define a positive thermal anomaly (Upper Mississippi Valley, Polaris, and central Tennessee). Group 3 deposits revealed the highest color alteration index values of the studied North American MVT districts, with host-rock temperatures greatly

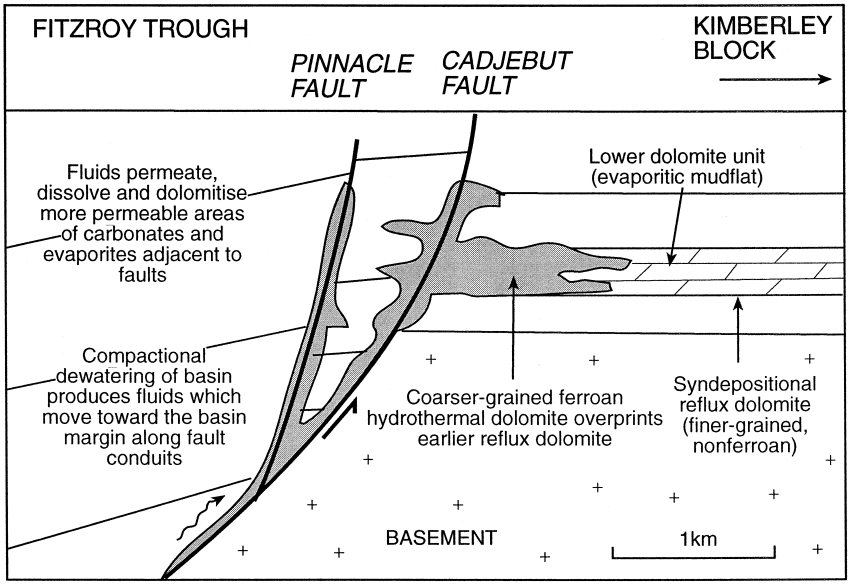

Fig. 35. Fault-focused burial dolomitization controls the distribution of coarse-grained dolomite in Devonian carbonates of the northern Canning Basin Margin, Australia. Dolomitizing fluids were expelled from the neighbouring Fitzroy trough and migrated up extensional fault conduits to penetrate further into the more permeable intervals in the carbonate. Evaporitic intervals and dissolution breccias facilitated greater volumes of fluid incursion (after Warren and Kempton, 1997).

exceeding ore mineral fluid inclusion temperatures, that is they show a negative thermal anomaly. They are the least common style (Austinville-Ivanhoe, northern Newfoundland, and Robb Lake deposits). Group 2 deposits (hot ore in cool rocks) all lie within the continental interior, some group 1 deposits (ore temperature = host-rock temperature) are well within the continental interior but others are adjacent to orogenic belts on the continental side, while group 3 deposits (cool ore in hot rocks) are all positioned within orogenic belts but on the continental side.

This is consistent with current hypotheses regarding the formation of many MVT deposits and their dolomite hosts via fluids squeezed cratonward from active orogenic belts (Fig. 24B; Sangster et al., 1994). Orogenic uplift at the craton edge induces heating of host rocks via the migration of hot brines driven cratonward by the hydraulic gradient. Once the ore-bearing fluids entered the foreland carbonate platforms, they traveled through sedimentary aquifers of the continental interior raising the temperature of the thinly covered carbonate rocks. The fluids left, as evidence of their passage, group 1 MVT deposits distributed with decreasing homogenization temperatures away from the orogenic front. The correspondence between host-rock and ore temperatures suggests that group 1 deposits were deposited essentially within their own aquifers. Group 2 deposits were formed when the same, or genetically similar, fluids rose from the regional aquifer(s) into structurally controlled conduits in the continental interior, possibly developed as a result of synorogenic doming and arching. This upward channeling of the fluids resulted in rapid and localized fluid flow, which precluded or at least inhibited widespread heating of the host rocks by ore fluids. Group 3 deposits formed when cooler ore carrying fluids are squeezed into hotter orogenic zones. But not all Pb–Zn deposits formed via compression-driven hydrologies, some provinces (e.g. Pb–Zn deposits along the Devonian margin of the Canning basin, Australia) formed via fault-focused escape of basinal fluids in a passive margin setting (McManus and Wallace, 1992; Warren and Kempton, 1997).

Permeability, which allowed penetration of dolomitizing solutions, and then sulfide mineralization, varies in origin. It may be a reactivated meteoric karst network, a synmineralization bathyphreatic

karst, an earlier permeable dolomite horizon, or an evaporite dissolution breccia. The dissolution breccia may be formed by the processes that promote the mineralization (as at Cadjebut), or may be an inherited dissolution horizon indicating earlier and shallower meteoric dissolution.

Ore hosting dolomites may also form at higher temperatures generated by igneous or metamorphic processes. These include mineralized contact haloes of dolomite skarn and dolomitic marbles in which the mineralization is associated with structural focusing within regional metamorphic settings. At these higher temperature ($>200°C–250°C$), and in regions of suitable source rock, the formation of coarsely crystalline dolomites can be associated with the precipitation of copper sulfides in addition to those of Pb and Zn. Some MVT areas exposed to warmer fluids can also contain copper sulfides in regions of hotter through flowing brines (e.g. southeast Missouri region).

In most large mineralized skarn systems the skarn and the ore come from the same hydraulic system, the association between hydrothermal dolomite and mineralization is not surprising. Skarns can form in both contact and regional metamorphic settings and typically, but not exclusively involve a carbonate protolith (Meinert, 1993). Some minerals, such as calcite and quartz are to be found in almost all skarn deposits with a carbonate protolith. Others, such as humite, periclase, phlogopite, talc, serpentine and brucite characterize magnesian skarns (often with a dolomite/evaporite protolith) and are absent from other types.

Dolomitic skarns form under the influence of a variety of metasomatic processes and involve fluids of magmatic, metamorphic, basinal, meteoric and marine origin. Skarns form over a wide range of temperatures that overlap with those of other mineralized deposits. It is only at the higher temperature end of the dolomite recrystallization spectrum that they are easily separated (Meinert, 1993). Dolomitic skarns can form adjacent to plutons, along major faults and shear zones, in seafloor mounds (black smokers), and in deeply buried metamorphic terranes. This group of settings is too broad and well documented to be adequately covered in this review, so we will restrict our discussion to a few examples illustrating this diversity.

In the Niccioleta ore deposit, Tuscany, Italy, metasomatic reactions have transformed anhydrites to garnet skarns, dolomites to pyroxene skarns and mica schists to epidote skarns (Dechomets, 1985). All transformations have involved pyrite formation via thermochemical sulfate reduction where acidic Fe-rich solutions have leached Na, K, CO_2, and parts of the Ca and Mg in the protolith and so created space for mineralization. As part of the transformation process, dolomites adjacent to the deposits were altered to coarsely crystalline high temperature xenotopic forms.

Recrystallization and reprecipitation of coarse dolomites also formed a halo around parts of the contact metamorphic magnesian skarns that formed during the magmatic and postmagmatic stages in the intracontinental paleorift zones of the Siberian Platform (Mazurov and Titov, 1999). Spinel-forsterite magnesian skarns of the magmatic stage are confined to the overdome parts of doleritic bodies and are the result of the interaction between massive sedimentary dolomites and fluids released from liquid magma. The magnesian skarns of the postmagmatic stage are typically localized in the margins and along the fronts (outwedges) of doleritic sills, apophyses, and the branches of intrusive bodies that crosscut the adjacent carbonate-evaporite series. These skarns have a banded structure and resemble gravel conglomerates with carbonate (often dolomitic) cement. The "clasts" are globules of disintegrated doleritic porphyrites that are completely or partially substituted by zonal magnesian skarns. Intrusion and solidification of basic magma within a highly reactive carbonate–evaporite sequence formed these unusual dolomitic rocks.

The Mount Bischoff tin deposit, Tasmania, is a more typical dolomite-hosted style of skarn mineralization. It occurs within a locally recrystallized dolomite unit in structurally complex, late-Precambrian rocks that were intruded by a swarm of narrow, vertical-to-steeply dipping, quartz–feldspar porphyry dikes of Devonian age (Halley and Walshe, 1995). The dikes are distributed in a crudely radial pattern and have undergone an early stage of potassic alteration, overprinted to a variable degree by greisening. The alteration is zoned along and across the dikes consistent with their acting as major fluid foci. Within the dolomite associated with this alter-

ation, replacement and recrystallization occurred in two distinct stages. During stage 1, serpentine and chondrodite assemblages formed at 400°C to 460°C from hydrothermal fluids with 30–36 wt.% NaCl. A zonation from serpentine to chondrodite to magnesite reflects the lowering of silica activity in the fluid as it reacted with the dolomite. During stage 2, quartz, talc, phlogopite, and carbonate formed at 320°C to 360°C from hydrothermal fluids with about 2 m NaCl, 1.5 m CO_2, and 0.3 m CH_4.

In the Kokomo mining district of Colorado, dolomite formed some 40 Ma as hydrothermal haloes or skarns about volcanic plugs, associated with manto ores in sedimentary carbonate hosts (Ag–Pb–Zn massive sulfide replacement deposits) (Thompson, 1998). The mantos are surrounded by halos of siderite-manganosiderite, coarsely crystalline hydrothermal dolomite, and/or jasperoid. The massive sulfide replacement ores show banded and tabular textures similar to those of ores at Leadville and Gilman, CO. Ore deposition occurred, in association with hydrothermal dolomitization, in the general sequence: jasperoid, iron sulfides (pyrrhotite, marcasite, and pyrite) + siderite, quartz, high iron sphalerite, ferroan dolomite, galena, chalcopyrite and sulfosalts, barite, ferroan calcite, and calcite. Fluid inclusion analyses of quartz and carbonate/dolomite minerals indicate that temperatures averaged 350°C during the early stages of ore deposition and decreased to about 160°C during the late stages. Ore fluid salinities also decreased from 4.6 to < 2 wt.% NaCl equiv.

Coarse-grained dolomite, magnesite and siderite are characteristic hydrothermal alteration minerals in Miocene hanging wall dacites about Kuroko orebodies (Shikazono et al., 1998). The $Mg/(Mg + Fe)$ ratios of the carbonates decrease from the central chlorite alteration zone to marginal zone and the $Mg/(Mg + Fe)$ ratios of carbonates and chlorite positively correlate. The $\delta^{18}O$ and $\delta^{13}C$ values also positively correlate with each other and lie between the igneous and marine carbonate values. The sparry dolomite and the magnesite formed in the central zone close to the orebodies via interaction of hydrothermal solutions with biogenic marine carbonates. Calcite formed further from the orebodies from hydrothermal fluids that did not entrain a biogenic marine carbon component.

8. Summary

We started off this review by asking the question, "What is Dolomite?" Let us see if we can answer that question with a summary of our most important observations and conclusions:

- Both dolomite the rock and dolomite the mineral encompass a wide range of Ca–Mg carbonates with similar, but not identical, Mg/Ca ratios.
- Sedimentary dolomite is a metastable mineral/rock that precipitates or replaces earlier more soluble phases a number of times as it approaches a more ideal stoichiometry. It undergoes Ostwald ripening or aging.
- As it moves through earth-space and time, a sedimentary dolomite evolves in response to changing conditions of burial, pore brine chemistry, temperature and pressure. As dolomite passes through various diagenetic settings its chemical and porosity characteristics are reset.
- A dolomite body may form for the first time at the surface or in the subsurface and it may generate or lose porosity a number of times in its burial history.
- Depositional settings include; sabkhas, salinas, salterns, humid subtidal mud shoals and evaporite-free schizohaline lakes. The resulting dolomites are typically fine-grained or mimetic with sedimentary structures indicative of their depositional setting. Bacterial mediation is significant in precipitating dolomite in most earth surface and some shallow subsurface settings.
- Diagenetic settings include the shallow seafloor, shallow burial marine (connate) settings, the interiors of atolls, mixing zones between waters of differing salinities, zones of brine reflux, and deep burial settings. Later formed diagenetic dolomites are coarser-grained than depositional dolomites and the geometries of the various bodies reflect the formative subsurface hydrologies.
- Dolomites with well-developed intercrystalline porosity make excellent hydrocarbon reservoirs. Many such reservoirs have an intimate association with evaporites. This reflects both the likelihood of the dolomite forming by brine reflux (platform, strand-zone and basin-center evaporite hydrologies) and the ability of evaporites to form effective seals to permeable intervals. Nonevaporitic dolomite reser-

voirs typically formed via fracturing or karstification. Many dolomite reservoirs can be related to regional unconformities.

• Late diagenetic dolomite (burial and hydrothermal) can act as an ore host. Many MVT deposits are hosted in such dolomites. Typically, the same solutions that formed the burial dolomite host were also capable of carrying metals. Where a suitable structural focus and redox system coincide, ore deposits form in a burial dolomite host. Dolomite hosts also form as skarns, mantos and during metamorphism.

In summary, dolomite is a complex mineral that evolves throughout its burial history. It does so by a series of dissolution–reprecipitation reactions that favor the retention of intergranular porosity. Hence, it is often an excellent reservoir for hydrocarbons or a host rock to base metal ores.

Acknowledgements

This paper benefited greatly from the helpful suggestions of the two reviewers, Professors C.J.R. Braithwaite and G.M. Friedman.

References

Adams, J.F., Rhodes, M.L., 1960. Dolomitization by seepage refluxion. Am. Assoc. Petrol. Geol. Bull. 44, 1912–1920.

Aharon, P., Kolodny, Y., Sass, E., 1977. Recent hot brine dolomitization in the "Solar Lake", Gulf of Elat; isotopic, chemical, and mineralogical study. J. Geol. 85 (1), 27–48.

Aharon, P., Socki, R.A., Chan, L., 1987. Dolomitization of atolls by sea water convective flow: test of a hypothesis at Niue, South Pacific. J. Geol. 95, 187–203.

Alderman, A.R., Skinner, H.C., 1957. Dolomite sedimentation in the southeast of South Australia. Am. J. Sci. 255, 561–567.

Alderman, A.R., von der Borch, C.C., 1963. Dolomite reaction series. Nature 198 (4879), 465–466.

Alsharhan, A.S., 1993. Facies and sedimentary environment of the Permian carbonate (Khuff Formation) in the United Arab Emirates. Sediment. Geol. 84 (1–4), 89–99.

Amthor, J.E., Mountjoy, E.W., Machel, H.G., 1993. Subsurface dolomites in Upper Devonian Leduc Formation buildups, central part of Rimbey-Meadowbrook reef trend, Alberta, Canada. Bull. Can. Petrol. Geol. 41 (2), 164–185.

Amthor, J.E., Mountjoy, E.W., Machel, H.G., 1994. Regional-scale porosity and permeability variations in Upper Devonian Leduc buildups; implications for reservoir development and prediction in carbonates. Am. Assoc. Petrol. Geol. Bull. 78 (10), 1541–1559.

Andreason, M.W., 1992. Coastal siliciclastic sabkhas and related evaporative environments of the Permian Yates Formation, North Ward-Estes field, Ward County, Texas. Am. Assoc. Petrol. Geol. Bull. 76 (11), 1735–1759.

Aulstead, K.L., Spencer, R.J., Krouse, H.R., 1988. Fluid inclusions and isotopic evidence on dolomitization, Devonian of Western Canada. Geochim. Cosmochim. Acta 52, 1027–1035.

Ayalon, A., Longstaffe, F.J., 1995. Stable isotope evidence for the origin of diagenetic carbonate minerals from the Lower Jurassic Inmar Formation, southern Israel. Sedimentology 42 (1), 147–160.

Back, W., Hanshaw, B.B., Plummer, L.N., Rahn, P.H., Rightmire, C.T., Rubin, M., 1983. Process and rate of dedolomitization; mass transfer and ^{14}C dating in a regional carbonate aquifer. Geol. Soc. Am. Bull. 94 (12), 1415–1429.

Badiozamani, K., 1973. The dorag dolomitization model — application to the middle Ordovician of Wisconsin. J. Sediment. Petrol. 43, 965–984.

Baker, P.A., Kastner, M., 1981. Constraints on the formation of sedimentary dolomite. Science 213, 214–216.

Baker, P.A., Burns, S.J., 1985. Occurrence and formation of dolomite in organic-rich continental margin sediments. Am. Assoc. Petrol. Geol. Bull. 69, 1917–1930.

Banner, J.L., 1995. Applications of the trace element and isotope geochemisty of strontium to studies of carbonate diagenesis. Sedimentology 45 (2), 805–824.

Banner, J.L., Hanson, G.N., Meyers, W.J., 1988. Water–rock interaction history of regionally extensive dolomites of the Burlington-Keokuk Formation (Mississippian); isotopic evidence. In: Shukla, V., Baker, P.A. (Eds.), Sedimentology and Geochemistry of Dolostones, Based on a Symposium. Spec. Publ.-SEPM vol. 43, pp. 97–113.

Baron, G., 1960. Sur la synthese de la dolomie. Application au phenomene de dolomitization. Rev. Inst. Fr. Pet. Ann. Combust. Liq. 15 (1), 3–68.

Baudouy, S., LeGorjus, C., 1991. Sendji field — People's Republic of Congo, Congo Basin. In: Beaumont, E.A., Foster, N.H. (Eds.), Structural Traps V: AAPG Treatise of Petroleum Geology, Atlas of Oil and Gas Fields. pp. 121–149.

Bebout, D.G., Maiklem, W.R., 1973. Ancient anhydrite facies and environments; their role in reconstructing geologic history of middle Devonian Elk Point Basin, Alberta. Am. Assoc. Petrol. Geol. Bull. 57 (4), 769–770.

Behre, C.H. Jr., 1947. Geochemistry and localization of dolomitization. J. Geol. 42, 540–542.

Behrens, E.W., Land, L.S., 1972. Subtidal Holocene dolomite, Baffin Bay, Texas. J. Sediment. Petrol. 42, 155–161.

Bein, A., Land, L.S., 1983. Carbonate sedimentation and diagenesis associated with Mg–Ca-chloride brines; the Permian San Andres Formation in the Texas Panhandle. J. Sediment. Petrol. 53, 243–260.

Bentley, J., 1984. Petroleum geology of the central Broome Platform. In: Purcell, P.G. (Ed.), The Canning Basin, Western Australia. Proceedings Geological Society of Australia and Petroleum Exploration Society of Australia, Canning Basin Symposium, Perth, WA, pp. 157–168.

Berner, R.A., Westrich, J.T., 1985. Bioturbation and the early diagenesis of carbon and sulfur. Am. J. Sci. 285, 193–206.

Blatt, H., 1992. Sedimentary Petrology. W.H. Freeman, New York, 514 pp.

Boles, J.R., 1978. Active ankeritic cementation in the subsurface Eocene of southwest Texas. Contrib. Mineral. Petrol. 68, 13–22.

Boles, J.R., Franks, S.G., 1979. Clay diagenesis in Wilcox Sandstones of southwest Texas: implications of smectite diagenesis on sandstone cementation. J. Sediment. Petrol. 49, 59–70.

Boni, M., Parente, G., Bechstadt, T., De Vivo, B., Iannace, A., 2000. Hydrothermal dolomites in SW Sardinia (Italy): evidence for a widespread late-Variscan fluid flow event. Sediment. Geol. 131 (3–4), 181–200.

Bos, C.F.M., 1989. Planning of an appraisal/development program for the complex Khuff carbonate reservoir in the Yibal field, north Oman. Proceedings 6th Society of Petroleum Engineers Middle East Oil Show, Bahrain, SPE 17988. pp. 631–640.

Bourrouilh-Le Jan, F.G., 2000. Deodat Gratet de Dolomieu. Life and works of a European geologist, naturalist and lithologist. C. R. Acad. Sci., Ser. IIa: Sci. Terre Planetes 330 (1), 83–95, French.

Braithwaite, C.J.R., 1991. Dolomites; a review of origins, geometry and textures. Trans. R. Soc. Edinburgh: Earth Sci. 82 (2), 99–112.

Braithwaite, C.J.R., Heath, R.A., 1996. Regional geometry, petrographic variation, and origins of Upper Ordovician dolomites in Hadeland, Norway. Nor. Geol. Tidsskr. 76, 63–74.

Braithwaite, C.J.R., Rizzi, G., 1997. The geometry and petrogenesis of hydrothermal dolomites at Navan, Ireland. Sedimentology 44 (3), 421–440.

Brognon, G.P., Verrier, G.R., 1966. Oil and geology in Cuanza basin of Angola. Am. Assoc. Petrol. Geol. Bull. 50, 108–158.

Budd, D.A., 1997. Cenozoic dolomites of carbonate islands; their attributes and origin. Earth Sci. Rev. 42 (1–2), 1–47.

Burns, S.J., McKenzie, J.A., Vasconcelos, C., 2000. Dolomite formation and biogeochemical cycles in the Phanerozoic. Sedimentology 1, 49–61, Suppl.

Bush, P., 1973. Some aspects of the diagenetic history of the sabkha in Abu Dhabi, Persian Gulf. In: Purser, B.H. (Ed.), The Persian Gulf, Holocene Carbonate Sedimentation and Diagenesis in a Shallow Epicontinental Sea. Springer, New York, pp. 395–407.

Bustillo, M., Ordonez, S., 1995. Lower Cretaceous Pb–Zn ores of Cantabria, Northern Spain — new considerations based on petrological and geochemical evidence. Trans.-Inst. Min. Metall., Sect. B 104, B55–B65.

Butler, G.P., 1969. Modern evaporite deposition and geochemistry of coexisting brines, the Sabkha, Trucial coast, Arabian Gulf. J. Sediment. Petrol. 39, 70–89.

Butler, R.W.H., Lickorish, W.H., Grasso, M., Pedley, H.M., Ramberti, L., 1995. Tectonics and sequence stratigraphy in Messinian basins, Sicily; constraints on the initiation and termination of the Mediterranean salinity crisis. Geol. Soc. Am. Bull. 107 (4), 425–439.

Camoin, G., Maurin, A.F., 1988. Roles des micro-organismes (bacteries, cyanobacteries) dans la genese des “Mud Mounds”, exemples du Turonien des Jebels Bireno et Mrhila (Tunisie) (Roles of micro-organisms, bacteria, cyanobacteria, in the formation of mud mounds, examples from the Turonian strata of jebels Bireno and Mrhila, Tunisia. C. R. Acad. Sci., Ser. II: Mec., Phys., Chim., Sci. Terre Univers 307 (4), 401–407.

Camoin, G., Debrenne, F., Gandin, A., 1989. Premieres images des communautes microbiennes dans les ecosystemes cambriens (first images of microbial communities in Cambrian ecosystems). C. R. Acad. Sci., Ser. II: Mec., Phys., Chim., Sci. Terre Univers 308 (16), 1451–1458.

Cander, H.S., 1994. An example of mixing-zone dolomite, middle Eocene Avon Park Formation, Floridan Aquifer system. J. Sediment. Res., Sect. A 64 (3), 615–629.

Carballo, J.B., Land, L.S., Miser, D.E., 1987. Holocene dolomitization of supratidal sediments by active tidal pumping, Sugarloaf Key, Florida. J. Sediment. Petrol. 57 (1), 153–165.

Carozzi, A.V., 1993. Sedimentary Petrography. Prentice-Hall, Englewood Cliffs, NJ, 263 pp.

Chafetz, H.S., Folk, R.L., 1984. Travertines: depositional morphology and the bacterially constructed constituents. J. Sediment. Petrol. 54 (1), 289–316.

Chafetz, H.S., Rush, P.F., 1994. Diagenetically altered sabkha-type Pleistocene dolomite from the Arabian Gulf. Sedimentology 41 (3), 409–421.

Chafetz, H.S., Imerito-Tetzlaff, A.A., Zhang, J.L., 1999. Stable-isotope and elemental trends in Pleistocene sabkha dolomites: Descending meteoric water vs. sulfate reduction. J. Sediment. Res., Sect. A 69 (1A), 256–266.

Chave, K.E., 1952. A solid solution between calcite and dolomite. J. Geol. 60, 190–192.

Chai, L., Navrotsky, A., Reeder, R.J., 1995. Energetics of calcium-rich dolomite. Geochim. Cosmochim. Acta 59 (5), 939–944.

Choquette, P.W., Pray, L.C., 1970. Geologic nomenclature and classification of porosity in sedimentary carbonates. Am. Assoc. Petrol. Geol. Bull. 54, 207–250.

Choquette, P.W., Steinen, R.P., 1980. Mississippian nonsupratidal dolomite, Ste. Genevieve Limestone, Illinois Basin: evidence for mixed water dolomititzation. In: Zenger, D.H., Dunham, J.B., Ethington, R.L. (Eds.), Concepts and Models of Dolomitization. Spec. Publ.-SEPM 28, pp. 168–196.

Choquette, P.W., Cox, A., Meyers, W.J., 1992. Characteristics, distribution and origin of porosity in shelf dolostones; Burlington-Keokuk Formation (Mississippian), U.S. Mid-Continent. J. Sediment. Petrol. 62 (2), 167–189.

Choquette, P.W., Steinen, R.P., 1985. Mississippian oolite and non-supratidal dolomite reservoirs in the Ste. Genevieve Formation, North Bridgeport Field, Illinois basin. In: Roehl, P.O., Choquette, P.W. (Eds.), Carbonate Petroleum Reservoirs. Springer, New York, pp. 207–225.

Chuber, S., Pusey, W.C., 1985. Productive Permian carbonate cycles, San Andres Formation, Reeves field, West Texas. In: Roehl, P.O., Choquette, P.W. (Eds.), Carbonate Petroleum Reservoirs. Springer, New York, pp. 289–307.

Clark, D.N., 1980. The diagenesis of Zechstein carbonate sediments. In: Fuchtbauer, H., Peryt, T. (Eds.), The Zechstein Basin with Emphasis on Carbonate Sequences, E. Schweizerbart’sche VbH. Contrib. Sediment. vol. 9, pp. 167–203.

Clement, J.H., 1985. Depositional sequences and characteristics of Ordovician Red River reservoirs, Pennel field, Williston basin, Montana. In: Roehl, P.O., Choquette, P.W. (Eds.), Carbonate Petroleum Reservoirs. Springer, New York, pp. 71–84.

Clayton, R.N., Skinner, H.C.W., Berner, R.A., Rubinson, M., 1968. Isotopic compositions of recent South Australian lagoonal carbonates. Geochim. Cosmochim. Acta 32, 983–988.

Compton, J.S., Siever, R., 1986. Diffusion and mass balance of Mg during early dolomite formation, Monterey Formation. Geochim. Cosmochim. Acta 50 (1), 125–135.

Compton, J.S., 1988. Degree of supersaturation and precipitation of organogenic dolomite. Geology 16 (4), 318–321.

Cook, T.D., 1979. Exploration history of South Texas Lower Cretaceous carbonate platform. Am. Assoc. Petrol. Geol. Bull. 70, 32–49.

Cowan, P.E., Harris, P.M., 1986. Porosity in the San Andres Formation (Permian), Cochran and Hockley counties, Texas. Am. Assoc. Petrol. Geol. Bull. 70, 888–897.

Craig, D.H., 1988. Caves and other features of Permian karst in San Andres dolomite, Yates field reservoirs, west Texas. In: James, N.P., Choquette, P.W. (Eds.), Paleokarst. Springer, New York, pp. 342–363.

Danielli, H.M.C., 1988. The Eocene reservoirs of Wafra field, Kuwait/Saudi Arabia partitioned neutral zone. In: Lomando, A.J., Harris, P.M. (Eds.), Giant Oil and Gas Fields. SEPM Core Workshop, pp. 119–154.

Davies, G.R., Ludlam, S.D., 1973. Origin of Laminated and Graded Sediments, Middle Devonian of Western Canada. Geol. Soc. Am. Bull. 84 (11), 3527–3546.

Dechomets, R., 1985. Sur l'origine de la pyrite et des skarns du gisement, en contexte evaporitique, de Niccioleta (Toscane, Italie). Miner. Deposita 20 (3), 201–210.

Deffeyes, K.S., Lucia, F.J., Weyl, P.K., 1965. Dolomitization of recent and Plio-Pleistocene sediments by marine evaporite waters on Bonaire, Netherlands Antilles. In: Pray, L.C., Murray, R.C. (Eds.), Dolomitization and Limestone Diagenesis. Spec. Publ.-SEPM vol. 13, pp. 71–88.

DeMis, W.D., 1992. Elkhorn Ranch field — USA Williston Basin. In: Foster, N.H., Beaumont, E.A. (Eds.), Stratigraphic Traps II: AAPG Treatise of Petroleum Geology, Atlas of Oil and Gas Fields. pp. 369–388.

Dix, G.R., 1993. Patterns of burial and tectonically controlled dolomitization in an Upper Devonian fringing-reef complex — Leduc Formation, Peace River Arch area, Alberta, Canada. J. Sediment. Petrol. 63, 628–640.

Dravis, J., Yurewicz, D.A., 1985. Enhanced carbonate petrography using fluorescence microscopy. J. Sediment. Petrol. 55, 795–804.

Dunham, R.J., 1962. Classification of carbonate rocks according to depositional texture. AAPG Mem. 1, 108–121.

Durocher, S., Alaasm, I.S., 1997. Dolomitization and neomorphism of Mississippian (Visean) upper Debolt Formation, Blueberry Field, northeastern British Columbia; geologic, petrologic, and chemical evidence. Am. Assoc. Petrol. Geol. Bull. 81 (6), 954–977.

Ebanks, W.J., 1991. Bindley field — USA Anadarko Basin, Kansas. In: Beaumont, E.A., Foster, N.H. (Eds.), Stratigraphic Traps II: AAPG Treatise of Petroleum Geology, Atlas of Oil and Gas Fields. pp. 117–133.

Ehrets, J.R., Kissling, D.L., 1985. Deposition, diagenesis and paleostructural control of Duperow and Birdbear (Nisku) reservoirs, Williston Basin. In: Longman, M.W., Shanley, K.W., Lindsay, R.F., Eby, D.E. (Eds.), Rocky Mountain Carbonate Reservoirs. SEPM Core Workshop, pp. 183–216.

El-Sayed, M.I., Fairchild, I.J., Spiro, B., 1991. Kuwaiti dolocrete; petrology, geochemistry and groundwater origin. Sediment. Geol. 73 (1–2), 59–75.

Elliott, L.A., Warren, J.K., 1989. Stratigraphy and depositional environment of lower San Andres Formation in subsurface and equivalent outcrops; Chaves, Lincoln, and Roosevelt counties, New Mexico. Am. Assoc. Petrol. Geol. Bull. 73 (11), 1307–1325.

Epting, M., 1980. Sedimentology of Miocene carbonate buildups, central Luconia, offshore Sarawak. Geol. Soc. Malays. Bull. 12, 17–30.

Eriksson, K.A., Warren, J.K., 1983. A paleohydrologic model for Early Proterozoic dolomitization and silicification. Precambrian Res. 21 (3–4), 299–321.

Eugster, H.P., Hardie, L.A., 1978. Saline Lakes. In: Lerman, A. (Ed.), Lakes; Chemistry, Geology, Physics. Springer, New York, pp. 237–293.

Fairbridge, R.W., 1957. The dolomite question. In: LeBlanc, R.J., Breeding, J.G. (Eds.), Regional Aspects of Carbonate Deposition. Spec. Publ.-SEPM vol. 5, pp. 125–178.

Fairchild, I.J., 1983. Chemical controls of cathodoluminescence of natural dolomites and calcite: new data and review. Sedimentology 30, 579–583.

Feazel, C.T., 1985. Diagenesis of Jurassic grainstone reservoirs in Smackover Formation, Chatom field, Alabama. In: Roehl, P.O., Choquette, P.W. (Eds.), Carbonate Petroleum Reservoirs. Springer, New York, pp. 357–367.

Fischer, D., Heck, T., Gerhard, L.C., 1990. Medicine Pole Hills field — USA Williston Basin. In: Beaumont, E.A., Foster, N.H. (Eds.), Stratigraphic Traps I: AAPG Treatise of Petroleum Geology, Atlas of Oil and Gas Fields, Tulsa, OK. pp. 229–251.

Fisher, W.L., Rodda, P.U., 1969. Edwards Formation (lower Cretaceous) Texas: dolomitization in a carbonate platform system. Am. Assoc. Petrol. Geol. Bull. 52, 55–72.

Folk, R.L., Land, L.S., 1975. Mg/Ca ratio and salinity: two controls on crystallization of dolomite. Am. Assoc. Petrol. Geol. Bull. 59, 60–68.

Folk, R.L., 1987. Detection of organic matter in thin sections of carbonate rocks using a white card. Sediment. Geol. 54, 193–200.

Folk, R.L., 1993. SEM imaging of bacteria and nannobacteria in carbonate sediments and rocks. J. Sediment. Petrol. 63 (5), 990–999.

Folk, R.L., 1994. Nannobacteria: major participants in the precipitation of carbonates and other minerals. In: Sasowsky, I.D., Palmer, M.V. (Eds.), Breakthroughs in Karst Geomicrobiology and Redox Geochemistry; Abstracts and Field-Trip Guide vol. 1. Karst Waters Institute, Charles Town, WV, pp. 17–18.

Fookes, E., 1995. Development and eustatic control of an Upper Jurassic reef complex (Saint Germain-de-Joux, eartern France). Facies 33, 129–149.

Fouke, B.W., Beets, C.J., Meyers, W.J., Hanson, G.N., Melillo, A.J., 1996. Sr-87/Sr-86 chronostratigraphy and dolomitization history of the Seroe Domi Formation, Curacao (Netherlands Antilles). Facies 35, 293–320.

Freeze, R.A., Cherry, J.A., 1979. Groundwater. Prentice-Hall, Englewood Cliffs, NJ, 604 pp.

Friedman, G.M., 1965. Terminology of crystallization textures and fabrics in sedimentary rocks. J. Sediment. Petrol. 35, 643–655.

Friedman, G.M., 1980. Dolomite is an evaporite mineral: evidence from the rock record and from sea-marginal ponds of the Red Sea. In: Zenger, E.H., Dunham, J.B., Ethington, R.L. (Eds.), Concepts and Models of Dolomitization. Spec. Publ.-SEPM vol. 28, pp. 69–80.

Friedman, G.M., Sanders, J.E., 1967. Origin and occurrence of dolostones. In: Chilingar, G.V., Bissell, H.J., Fairbridge, R.W. (Eds.), Carbonate Rocks, Origin, Occurrence, and Classification. Elsevier, Amsterdam, pp. 267–348.

Gao, G.Q., Land, L.S., 1991. Early Ordovician Cool Creek dolomite, Middle Arbuckle Group, Slick Hills, SW Oklahoma, USA. J. Sediment. Petrol. 61, 161–173.

Gao, G., Land, L.S., Folk, R.L., 1992. Meteoric modification of early dolomite and late dolomitization by basinal fluids, upper Arbuckle Group, Slick Hills, Southwestern Oklahoma. Am. Assoc. Petrol. Geol. Bull. 76, 1649–1664.

Gao, G., Land, L.S., Elmore, R.D., 1995. Multiple episodes of dolomitization in the Arbuckle Group, Arbuckle Mountains, south-central Oklahoma; field, petrographic, and geochemical evidence. J. Sediment. Res., Sect. A 65 (2), 321–331.

Garber, R.A., Harris, P.M., Borer, J.M., 1990. Occurrence and significance of magnesite in Upper Permian (Guadalupian) Tansill and Yates formations, Delaware Basin, New Mexico. Am. Assoc. Petrol. Geol. Bull. 74 (2), 119–134.

Garea, B.B., Braithwaite, C.J.R., 1996. Geochemistry, isotopic composition and origin of the Beda dolomites, block NC74F, SW Sirt Basin, Libya. J. Petrol. Geol. 19 (3), 289–304.

Garrison, R.E., Graham, S.A., 1984. Early diagenetic dolomites and the origin of dolomite-bearing breccias, lower Monterey formation, Arroyo Seco, Monterey County, California. In: Garrison, R.E., Kastner, M., Zenger, D.H. (Eds.), Dolomites of the Monterey Formation and Other Organic-Rich Units. Spec. Publ.-SEPM (Pacific Section, Los Angeles) vol. 41, pp. 87–101.

Garven, G., Appold, M.S., Toptygina, V.I., Hazlett, T.J., 1999. Hydrogeologic modeling of the genesis of carbonate-hosted lead–zinc ores. Hydrogeol. J. 7, 108–126.

Gawthorpe, R.L., 1987. Burial dolomitization and porosity development in a mixed carbonate-clastic sequence: an example from Bowland Basin, northern England. Sedimentology 34, 533–558.

Gebelein, C.D., Hoffman, P., 1973. Algal origin of dolomite lamination in stromatolitic limestone. J. Sediment. Petrol. 43, 603–611.

Ghazban, F., McNutt, R., Schwarcz, H., 1994. Genesis of sediment-hosted Zn–Pb–Ba deposits in the Iranuh District, Esfahan Area, west-central Iran. Econ. Geol. 89 (6), 1262–1278.

Ghosh, S.K., Friedman, G.M., 1989. Petrophysics of a dolostone reservoir; San Andres Formation (Permian), West Texas. Carbonates Evaporites 4 (1), 45–119.

Gill, D., 1985. Depositional facies of Middle Silurian (Niagaran) pinnacle reefs, Belle River Mills Gas field, Michigan Basin, southeastern Michigan. In: Roehl, P.O., Choquette, P.W. (Eds.), Carbonate Petroleum Reservoirs. Springer, New York, pp. 121–139.

Gill, I.P., Moore, C.H., Aharon, P., 1995. Evaporitic mixed-water dolomitization on St. Croix, U.S.V.I. J. Sediment. Res., Sect. A 65 (4), 591–604.

Given, R.K., Wilkinson, B.H., 1987. Dolomite abundance and stratigraphic age, constraints on rates and mechanisms of dolostone formation. J. Sediment. Petrol. 57, 1068–1078.

Graf, D.L., Goldsmith, G.R., 1956. Some hydrothermal syntheses of dolomite and protodolomite. J. Geol. 64, 173–186.

Gregg, J.M., Sibley, D.F., 1984. Epigenetic dolomitization the origin of xenotopic dolomite texture. J. Sediment. Petrol. 54, 907–931.

Gregg, J.M., Shelton, K.L., 1990. Dolomitization and dolomite neomorphism in the back reef facies of the Bonneterre and Davis formations (Cambrian), Southeastern Missouri. J. Sediment. Petrol. 60 (4), 549–562.

Gregg, J.M., Howard, S.A., Mazzullo, S.J., 1992. Early diagenetic recrystallization of Holocene (< 3000 years old) peritidal dolomites, Ambergis Cay, Belize. Sedimentology 39, 143–160.

Gregg, J.M., Laudon, P.R., Woody, R.E., Shelton, K.L., 1993. Porosity evolution of the Cambrian Bonneterre Dolomite, southeastern Missouri. Sedimentology 40 (6), 1153–1169.

Gunatilaka, A., 1989. Spheroidal dolomites; origin by hydrocarbon seepage? Sedimentology 36 (4), 701–710.

Gunatilaka, A., Mwango, S., 1987. Continental sabkha pans and associated nebkhas in southern Kuwait, Arabian Gulf. In: Frostrick, L., Reid, I. (Eds.), Desert Sediments: Ancient and Modern. Geol. Soc. Spec. Publ. vol. 35, pp. 187–203.

Gunatilaka, A., Saleh, A., Al-Temeemi, A., Nassar, N., 1987. Calcium-poor dolomite from the sabkhas of Kuwait. Sedimentology 34, 999–1006.

Halley, R.B., Schmoker, J.W., 1983. High porosity Cenozoic rocks of South Florida: progressive loss of porosity with depth. Am. Assoc. Petrol. Geol. Bull. 67, 191–200.

Halley, S.W., Walshe, J.L., 1995. A reexamination of the Mount Bischoff cassiterite sulphide skarn, Western Tasmania. Econ. Geol. 90 (6), 1676–1693.

Hanshow, B.B., Back, W., Deike, R.G., 1971. A geochemical hypothesis of dolomitization by ground water. Econ. Geol. 66, 710–724.

Hardie, L.A., 1987. Dolomitization; a critical view of some current views. J. Sediment. Petrol. 57 (1), 166–183.

Hardie, L.A., 1991. On the significance of evaporites. Annu. Rev. Earth Planetary Sci. 19, 131–168.

Hardie, L.A., 1996. Secular variation in seawater chemistry: an explanation for the coupled secular variation in the mineralo-

gies of marine limestones and potash evaporites over the past 600 m.y. Geology 24 (3), 279–283.
Harris, P.M., Walker, S.D., 1990. McElroy field — USA Central Basin platform Permian basin, Texas. In: Beaumont, E.A., Foster, N.H. (Eds.), Stratigraphic Traps I: AAPG Treatise of Petroleum Geology, Atlas of Oil and Gas Fields, Tulsa, OK. pp. 195–223.
Haynes, F.M., Kesler, S.E., 1994. Relation of mineralization to wall-rock alteration and brecciation, Mascot Jefferson City Mississippi Valley Type district, Tennessee. Econ. Geol. 89 (1), 51–66.
Heroux, Y., Chagnon, A., Savard, M., 1996. Organic matter and clay anomalies associated with base-metal sulphide deposits. Ore Geol. Rev. 11 (1–3), 157–173.
Hewett, D.F., 1928. Dolomitization and ore deposition. Econ. Geol. 23, 821–863.
Hill, C.A., 1995. H_2S-related porosity and sulfuric acid oil-field karst. In: Budd, D.A., Saller, A.H., Harris, P.M. (Eds.), Unconformities and Porosity in Carbonate Strata. AAPG Mem. vol. 63, pp. 301–306.
Hitzman, M.W., Allan, J.R., Beaty, D.W., 1998. Regional dolomitization of the Waulsortian limestone in southeastern Ireland: evidence of large scale fluid flow driven by the Hercynian orogeny. Geology 26 (6), 547–550.
Holland, H.D., Horita, J., Seyfried, W., 1996. On the secular variations in the composition of Phanerozoic marine potash evaporites. Geology 24 (11), 993–996.
Horn, M.K., 1990. Renqui field. In: Beaumont, E.A., Foster, N.H. (Eds.), Structural Traps II: AAPG Treatise of Petroleum Geology, Atlas of Oil and Gas Fields. pp. 227–252.
Hsu, K.J., 1967. Chemistry of dolomite formation. Elsevier Dev. Sediment. 9b, 169–191.
Hsu, K.J., Siegenthaler, C., 1969. Preliminary experiments on hydrodynamic movement induced by evaporation and their bearing on the dolomite problem. Sedimentology 12, 448–453.
Hsu, K.J., Schneider, J., 1973. Progress report on dolomitization-hydrology of Abu Dhabi Sabkhas, Arabian Gulf. The Persian Gulf. Springer, New York, pp. 409–422.
Hu, B.L., 1992. Petroleum geology and prospects of the Tarim basin, China. In: Halbouty, M.T. (Ed.), Giant Oil and Gas Fields of the Decade 1978–1988. AAPG Mem. vol. 54, pp. 493–510.
Hull, C.E., Warman, H.R., 1979. Asmari oil fields of Iran. Am. Assoc. Petrol. Geol. Bull. 54, 428–437.
Humphrey, J.D., Quinn, T.M., 1989. Coastal mixing zone dolomite, forward modeling, and massive dolomitization of platform-margin carbonates. J. Sediment. Petrol. 59, 438–454.
Hurley, N.F., Budros, R., 1990. Albion-Scipio and Stoney Point fields, U.S.A., Michigan Basin. In: Beaumont, E.A., Foster, N.H. (Eds.), Stratigraphic Traps I: AAPG Treatise of Petroleum Geology, Atlas of Oil and Gas Fields, Tulsa, OK. pp. 1–37.
Illing, L.V., Wells, A.J., Taylor, J.C.M., 1965. Penecontemporaneous dolomite in the Persian Gulf. In: Pray, L.C., Murray, R.C. (Eds.), Dolomitization and Limestone Diagenesis. Spec. Publ.-Soc. Econ. Paleont. Mineral. vol. 13, pp. 89–111.
Illing, L.V., Taylor, J.C.M., 1993. Penecontemporaneous dolomitization in Sabkha Faishakh, Qatar — evidence from changes in the chemistry of the interstitial brines. J. Sediment. Petrol. 63 (6), 1042–1048.
James, N.P., Bone, Y., Kyser, T.K., 1993. Shallow burial dolomitization and dedolomitization of mid-Cenozoic, cool-water, calcitic, deep-shelf limestones, southern Australia. J. Sediment. Petrol. 63, 528–538.
Jodry, R.L., 1969. Growth and dolomitization of Silurian reefs, St. Clair County, Michigan. Am. Assoc. Petrol. Geol. Bull. 53, 957–981.
Johnson, R.A., Budd, D.A., 1994. The utility of continued reservoir description: an example from Bindley field, western Kansas. Am. Assoc. Petrol. Geol. Bull. 78, 722–743.
Jones, H.D., Kesler, S.E., Furman, F.C., Kyle, J.R., 1996. Sulfur isotope geochemistry of southern Appalachian Mississippi Valley-Type deposits. Econ. Geol. 91 (2), 355–367.
Kahle, C.F., 1965. Possible roles of clay minerals in the formation of dolomite. J. Sediment. Petrol. 35, 448–453.
Kaldi, J., Gidman, J., 1982. Early diagenetic dolomite cements: examples from the Permian Lower Magnesian Limestone of England and the Pleistocene carbonates of the Bahamas. J. Sediment. Petrol. 52, 1073–1085.
Kamali, M.R., Lemon, N.M., Apak, S.N., 1995. Porosity generation and reservoir potential of Ouldburra Formation carbonates, Officer Basin, South Australia. APEA J. 35, 106–120.
Karajas, J., Kernick, N., 1984. A prospective Nita Formation reservoir trend on the Broome Platform. In: Purcell, P.G. (Ed.), The Canning Basin, Western Australia. Proceedings Geological Society of Australia and Petroleum Exploration Society of Australia, Canning Basin Symposium, Perth, WA, pp. 169–177.
Kastner, M., 1984. Control of dolomite formation. Nature 311 (5985), 410–411.
Kaufman, J., 1994. Numerical models of fluid flow in carbonate platforms — implications for dolomitization. J. Sediment. Res., Sect. A 64 (1), 128–139.
Kaufman, J., Harrison, G.N., Meyers, W.J., 1991. Dolomitization of the Swan Hills Formation, Rosevear field, Alberta, Canada. Sedimentology 38, 41–66.
Kelts, K.R., Mackenzie, J.A., 1982. Diagenetic dolomite formation in Quaternary anoxic diatomaceous muds of Deep Sea Drilling Project Leg 64, Gulf of California. Initial Rep. Deep Sea Drill. Proj. 64 (2), 553–569.
Kendall, A.C., 1988. Aspects of evaporite basin stratigraphy. In: Schreiber, B.C. (Ed.), Evaporites and Hydrocarbons. Columbia University Press, New York, pp. 11–65.
Kendall, A.C., 1989. Brine mixing in the Middle Devonian of Western Canada and its possible significance to regional dolomitization. Sediment. Geol. 64, 271–285.
Kendall, A.C., 1992. Evaporites. In: Walker, R.G., James, N.P. (Eds.), Facies Models: Responses to Sea Level Change. Geological Association of Canada, pp. 375–409.
Kerans, C., 1988. Karst-controlled reservoir heterogeneity in Ellenberger Group carbonates of west Texas. Am. Assoc. Petrol. Geol. Bull. 72, 1160–1183.
Khalaf, F.I., 1990. Occurrence of phreatic dolocrete within Ter-

tiary clastic deposits of Kuwait, Arabian Gulf. Sediment. Geol. 68 (3), 223–239.

Kinsman, D.J.J., 1965. Dolomitization and evaporite development, including anhydrite, Lagoonal Sediments, Persian Gulf. Geological Society of America.

Kocurko, M.J., 1979. Dolomitization by spray-zone brine seepage, San Andres, Colombia. J. Sediment. Petrol. 49, 209–214.

Kontak, D.J., 1998. A study of fluid inclusions in sulphide and nonsulphide mineral phases from a carbonate-hosted Zn–Pb deposit, Gays River, Nova Scotia, Canada. Econ. Geol. 93 (6), 793–816.

Kopaska-Merkel, D.C., Friedman, G.M., 1989. Petrofacies analysis of carbonate rocks; example from lower Paleozoic Hunton Group of Oklahoma and Texas. Am. Assoc. Petrol. Geol. Bull. 73 (11), 1289–1306.

Kretz, R., 1992. Carousel model for the crystallization of saddle dolomite. J. Sediment. Petrol. 62, 190–195.

Krumbein, W.E., 1979. Calcification by bacteria and algae. In: Trudinger, P.A., Swaine, D.J. (Eds.), Biogeochemical Cycling of Mineral-Forming Elements. Elsevier, Amsterdam, pp. 47–62.

Kupecz, J.A., Land, L.S., 1994. Progressive recrystallization and stabilization of early-stage dolomite: lower Ordovician Ellenburger Group, west Texas. In: Purser, B., Tucker, M., Zenger, D. (Eds.), Dolomites — A Volume in Honor of Dolomieu. Spec. Publ. Int. Assoc. Sedimentol. vol. 21. Blackwell Scientific Publications, Cambridge, pp. 255–279.

Land, L.S., 1973. Holocene meteoric dolomitization of Pleistocene limestones, North Jamaica. Sedimentology 20, 411–424.

Land, L.S., 1980. The isotopic and trace element geochemistry of dolomite: the state of the art. In: Zenger, D.H., Dunham, J.B., Ethington, R.L. (Eds.), Concepts and Models of Dolomitization. Spec. Publ.-SEPM vol. 28, pp. 87–110.

Land, L.S., 1984. Frio Sandstone diagenesis, Texas Gulf Coast. In: McDonald, D.A., Surdam, R.C. (Eds.), Clastic Diagenesis. AAPG Mem. vol. 37, pp. 47–62.

Land, L.S., 1985. The origin of massive dolomite. J. Geol. Educ. 33, 112–125.

Land, L.S., 1991. Dolomitization of the Hope Gate Formation (North Jamaica) by seawater: reassessment of mixing zone dolomite. In: Taylor, H.P., O'Neil, J.R., Kaplan, I.R. (Eds.), Stable Isotope Geochemistry: A Tribute to Samuel Epstein. Geochem. Soc. Spec. Publ. vol. 3, pp. 121–133.

Land, L.S., 1998. Failure to precipitate dolomite at 25 degrees C from dilute solution despite 1000-fold oversaturation after 32 years. Aquat. Geochem. 4 (3–4), 361–368.

Land, L.S., Hoops, G.K., 1973. Sodium in carbonate sediments and rocks: a possible index to the salinity of diagenetic solutions. J. Sediment. Petrol. 43, 614–617.

Land, L.S., Salem, M., Morrow, D., 1975. Paleohydrology of ancient dolomites: geochemical evidence. Am. Assoc. Petrol. Geol. Bull. 59, 1602–1625.

Landes, K.K., 1946. Porosity through dolomitization. Am. Assoc. Petrol. Geol. Bull. 30, 305–318.

Last, W.M., 1990. Lacustrine dolomite — an overview of modern, Holocene, and Pleistocene occurrences. Earth Sci. Rev. 27 (3), 221–263.

Leary, D.A., Vogt, J.N., 1986. Diagenesis of the San Andres Formation (Guadalupian), Central Basin Platform, Permian Basin. In: Bebout, D.G., Harris, P.M. (Eds.), Hydrocarbon Reservoir Studies San Andres/Grayburg Formations, Permian Basin. Spec. Publ.-SEPM vol. 26, pp. 67–68.

Lee, Y.I., Friedman, G.M., 1987. Deep-burial dolomitization in the Ordovician Ellenberger Group carbonates, west Texas and southeastern New Mexico. J. Sediment. Petrol. 57, 544–577.

Lee, Y.I., Friedman, G.M., 1988. Deep-burial dolomitization in the Ordovician Ellenberger Group carbonates, west Texas and southeastern New Mexico — reply. J. Sediment. Petrol. 58, 910–913.

Leighton, M.W., Pendexter, C., 1962. Carbonate rock types. AAPG Mem. 33–61.

Lindsay, R.F., Kendall, C.G.St.C., 1985. Depositional facies, diagenesis and reservoir character of Mississippian cyclic carbonates in the Mission Canyon Formation, Little Knife field, Williston Basin, North Dakota. In: Roehl, P.O., Choquette, P.W. (Eds.), Carbonate Petroleum Reservoirs. Springer, New York, pp. 175–190.

Lippmann, F., 1973. Sedimentary Carbonate Minerals. Springer, New York.

Lippmann, F., 1982. Stable and metastable solubility diagrams for the system $CaCO_3$–$MgCO_3$–H_2O at ordinary temperatures. Bull. Mineral. 105, 273–279.

Lopez-Gomez, J., Mas, R., Arche, A., 1993. The evolution of the Middle Triassic (Muschelkalk) carbonate ramp in the SE Iberian Ranges, eastern Spain: sequence stratigraphy, dolomitization processes and dynamic controls. Sediment. Geol. 87 (3–4), 165–193.

Longman, M.W., Schnidtman, K.H., 1985. Deposition and diagenesis of Mississippian Charles "C" (Ratcliffe) reservoir in Lustre field, Valley County, Montana. In: Longman, M.W., Shanley, K.W., Lindsay, R.F., Eby, D.E. (Eds.), Rocky Mountain Carbonate Reservoirs. SEPM Core Workshop, pp. 265–310.

Longman, M.W., Fertal, T.G., Stell, J.R., 1992. Reservoir performance in Ordovician Red River Formation, Horse Creek and South Horse Creek fields, Bowman County, North Dakota. Am. Assoc. Petrol. Geol. Bull. 76, 449–467.

Loucks, R.G., Anderson, J.H., 1985. Depositional facies, diagenetic terranes and porosity development in Lower Ordovician Ellenberger Dolomite, Puckett field, west Texas. In: Roehl, P.O., Choquette, P.W. (Eds.), Carbonate Petroleum Reservoirs. Springer, New York, pp. 19–37.

Lucia, F.J., 1968. Recent sediments and diagenesis of south Bonaire, Netherlands Antilles. J. Sediment. Petrol. 845–858.

Lucia, F.J., 1972. Recognition of evaporite–carbonate shoreline sedimentation. In: Rigby, J.K., Hamblin, W.K. (Eds.), Recognition of Ancient Sedimentary Environments. Spec. Publ.-Soc. Econ. Paleontol. Mineral. vol. 16, pp. 190–191.

Lucia, F.J., 1983. Petrophysical parameters estimated from visual description of carbonate rocks: a field classification of pore space. J. Petrol. Technol. 35, 626–637, (March).

Lucia, F.J., 1995. Rock-fabric/petrophysical classification of carbonate pore space for reservoir characterization. Am. Assoc. Petrol. Geol. Bull. 79, 1275–1300.

Lucia, F.J., 1999. Carbonate Reservoir Characterization. Springer, Berlin, 226 pp.

Lucia, F.J., Major, R.P., 1994. Porosity evolution through hypersaline reflux dolomitization. In: Purser, B., Tucker, M., Zenger, D. (Eds.), Dolomites — A Volume in Honor of Dolomieu. Spec. Publ.-Int. Assoc. Sedimentol. vol. 21. Blackwell Scientific Publications, Cambridge, pp. 325–341.

Lumsden, D.N., 1988. Characteristics of deep marine dolomite. J. Sediment. Petrol. 58, 1023–1051.

Lumsden, D.N., Chimahusky, J.S., 1980. Relationship between dolomite nonstoichiometry and carbonate facies parameters. Spec. Publ.-SEPM 28, 123–138.

Machel, H.G., 1987. Saddle dolomite as a by-product of chemical compaction and thermochemical sulfate reduction. Geology 15 (10), 936–940.

Machel, H.G., Anderson, J.H., 1989. Pervasive subsurface dolomitization of the Nisku Formation in central Alberta. J. Sediment. Petrol. 59, 891–911.

Machel, H.G., Burton, E.A., 1991. Burial-diagenetic sabkha-like gypsum and anhydrite nodules. Chem. Geol. 90, 211–231.

Machel, H.G., Burton, E.A., 1994. Golden Grove Dolomite, Barbados; origin from modified seawater. J. Sediment. Res., Sect. A 64 (4), 741–751.

Machel, H.G., Mountjoy, E.W., 1986. Chemistry and environments of dolomitization — a reappraisal. Earth Sci. Rev. 23, 175–222.

Mackenzie, J., 1981. Holocene dolomitzation of calcium carbonate sediments from the coastal sabkhas of Abu Dhabi, U.A.E. J. Geol. 89, 185–198.

Mackenzie, J., Hsu, K.J., Schneider, J.F., 1980. Movement of subsurface waters under the sabkha, Abu Dhabi, UAE and its relation to evaporative dolomite genesis. Spec. Publ.-SEPM 28, 11–30.

Magaritz, M., Goldenberg, L., Kafri, U., Arad, A., 1980. Dolomite formation in the seawater–freshwater interface. Nature 287, 622–624.

Magaritz, M., Peryt, T.M., 1994. Mixed evaporative and meteoric water dolomitization; isotope study of the Zechstein Limestone (Upper Permian), southwestern Poland. Sediment. Geol. 92, 257–272.

Maiklem, W.R., 1971. Evaporative drawdown — a mechanism for water level lowering and diagenesis in the Elk Point Basin. Bull. Can. Assoc. Petrol. Geol. 19, 487–503.

Malone, M.J., Baker, P.A., Burns, S.J., 1994. Recrystallization of dolomite — evidence from the Monterey Formation (Miocene). Sedimentology 41 (6), 1223–1239.

Mattavelli, L., Margarucci, V., 1990. Malossa field, Italy Po basin. In: Beaumont, E.A., Foster, N.H. (Eds.), Structural Traps VII: AAPG Treatise of Petroleum Geology, Atlas of Oil and Gas Fields. pp. 119–137.

Mattes, B.W., Conway, M.S., 1990. Carbonate/evaporite deposition in the Late Precambrian–Early Cambrian Ara Formation of southern Oman. In: Robertson, A.H.F., Searle, M.P., Ries, A.C. (Eds.), The Geology and Tectonics of the Oman Region. Geol. Soc. Spec. Publ. vol. 49, pp. 617–636.

Mawson, S.D., 1929. Some South Australian limestones in the process of formation. Q. J. Geol. Soc. London 85, 613–623.

Mazurov, M.P., Titov, A.T., 1999. Magnesian skarns from the sites of layer-by-layer injections of basic magma into the evaporites of the platform's sedimentary cover. Geol. Geofiz. 40 (1), 82–89, Russian.

Mazzullo, S.J., Reid, A.M., Gregg, J.M., 1987. Dolomitization of Holocene supratidal deposits, Ambergis Cay, Belize. Geol. Soc. Am. Bull. 98, 224–231.

Mazzullo, S.J., Bischoff, W.D., Teal, C.S., 1995. Holocene shallow-subtidal dolomitization by near-normal seawater, northern Belize. Geology 23 (4), 341–344.

McCullough, M.L., Land, L.S., 1992. Diagenetic history of a submerged Pleistocene Jamaican fringing reef. Carbonates Evaporites 7, 2–10.

McManus, A., Wallace, M.W., 1992. Age of Mississippi Valley type sulfides determined using cathodoluminesence cement stratigraphy, Lennard Shelf, Canning Basin, Western Australia. Econ. Geol. 87, 189–193.

McQuillan, H., 1985. Fracture-controlled production from the Oligo-Miocene Asmari Formation in Gachsaran and Bibi Hakimeh fields, southwest Iran. In: Roehl, P.O., Choquette, P.W. (Eds.), Carbonate Petroleum Reservoirs. Springer, New York, pp. 511–523.

Medlin, W.L., 1959. Preparation of synthetic dolomite. Am. Mineral. 44, 979–986.

Meinert, L.D., 1993. Igneous petrogenesis and skarn deposits. In: Kirkham, R.V., Sinclair, W.D., Thorpe, R.I., Duke, J.M. (Eds.), Mineral Deposit Modeling. Geol. Assoc. Can. Spec. Paper vol. 40, pp. 569–583.

Metherell, R.G., Workman, L.E., 1969. Geology of Crossfield East and Lone Pine Creek gas field, Alberta. Can. Soc. Petrol. Geol. Bull. 17, 92–108.

Meyers, W.J., Lu, F.H., Zachariah, J.K., 1997. Dolomitization by mixed evaporative brines and freshwater, upper Miocene carbonates, Nijar, Spain. J. Sediment. Res., Sect. A 67 (5), 898–912.

Middleburg, J.J., de Lange, G.J., Kreulen, R., 1990. Dolomite formation in anoxic sediments of Kau Bay, Indonesia. Geology 18, 399–402.

Middleton, K., Coniglio, M., Sherlock, R., Frape, S.K., 1993. Dolomitization of Middle Ordovician carbonate reservoirs, southwestern Ontario. Bull. Can. Petrol. Geol. 41 (2), 150–163.

Miller, J.A., 1985. Depositional and reservoir facies of the Mississippian Leadville Formation, Northwest Lisbon field, Utah. In: Roehl, P.O., Choquette, P.W. (Eds.), Carbonate Petroleum Reservoirs. Springer, New York, pp. 161–173.

Milliken, K.L., Land, L.S., Loucks, R.G., 1981. History of burial diagenesis determined from isotopic geochemistry, Brazoria County, Texas. Am. Assoc. Petrol. Geol. Bull. 65, 1397–1413.

Miser, D.E., Swinnea, J.S., Steinfink, H., 1987. TEM observations and X-ray structure refinement of a twinned dolomite microstructure. Am. Mineral. 72, 188–193.

Mitchell, J.T., Land, L.S., Miser, D.E., 1987. Modern marine dolomite cement in a north Jamaican fringing reef. Geology 15, 557–560.

Montañez, I.P., 1994. Late diagenetic dolomitization of Lower Ordovician, Upper Knox carbonates: a record of the hydrody-

namic evolution of the south Appalachian Basin. Am. Assoc. Petrol. Geol. Bull. 78 (8), 1210–1239.
Monty, C.L.V., Rouchy, J.M., Maurin, A., Bernet-Rollande, M.C., Perthuisot, J.P., 1987. Reef-stromatolites-evaporites facies relationships from middle Miocene examples of the Gulf of Suez and the Red Sea. In: Peryt, T.M. (Ed.), Evaporite Basins. Lect. Notes Earth Sci. vol. 13. Springer, Berlin, pp. 133–188.
Moore, C.H., Chowdhury, A., Chan, L., 1988. Upper Jurassic Smackover dolomitization, Gulf of Mexico; a tale of two waters. In: Skula, V., Baker, P.A. (Eds.), Sedimentology and Geochemistry of Dolostones. Spec. Publ.-SEPM vol. 43.
Morgan, W.A., 1985. Silurian reservoirs in upward-shoaling cycles of the Hunton Group, Mt. Everette and southwest Reeding fields, Kingfisher County, Oklahoma. In: Roehl, P.O., Choquette, P.W. (Eds.), Carbonate Petroleum Reservoirs. Springer, New York, pp. 107–120.
Morrow, D.W., 1982. Diagenesis 2; Dolomite: Part 2. Dolomitization models and ancient dolostones. Geosci. Can. 9 (2), 95–107.
Morrow, D., 1998. Regional subsurface dolomitization: models and constraints. Geosci. Can. 25 (2), 57–70.
Morrow, D.W., Ricketts, B.D., 1988. Experimental investigation of sulfate inhibition of dolomite and its mineral analogues. In: Shukla, V., Baker, P.A. (Eds.), Sedimentology and Geochemistry of Dolostones. Spec. Publ.-SEPM vol. 43, pp. 27–38.
Morse, J.W., Casey, W.H., 1988. Ostwald processes and mineral paragenesis in sediments. Am. J. Sci. 288, 537–560.
Morse, J.W., Mackenzie, F.T., 1990. Geochemistry of Sedimentary Carbonates. Elsevier, Amsterdam, 707 pp.
Mountjoy, E.W., Halim-Dihardja, M.K., 1991. Multiple phase fracture and fault controlled burial dolomitization, Upper Devonian Wabamum Group, Alberta. J. Sediment. Petrol. 61, 590–612.
Mountjoy, E.W., Amthor, J.E., 1994. Has burial dolomitization come of age? Some answers from the West Canada Sedimentary Basin. In: Purser, B., Tucker, M., Zenger, D. (Eds.), Dolomites — A Volume in Honor of Dolomieu. Spec. Publ.-Int. Assoc. Sedimentol. vol. 21, pp. 203–229.
Mountjoy, E.W., Machel, H.G., Green, D., Duggan, J., Williams-Jones, A.E., 2000. Devonian matrix dolomites and deep burial carbonate cements: a comparison between the Rimbey-Meadowbrook reef trend and the deep basin of west-central Alberta. Bull. Can. Petrol. Geol. 47 (4), 487–509.
Mriheel, I.Y., Anketell, J.M., 1995. Origin of the mid-Ypresian Jirani Dolomite; a major reservoir rock in the NW Libya offshore. J. Petrol. Geol. 18 (4), 439–451.
Muchez, P., Viaene, W., 1994. Dolomitization caused by water circulation near the mixing zone: an example from the Lower Viséan of the Campine Basin (northern Belgium). In: Purser, B., Tucker, M., Zenger, D. (Eds.), Dolomites — A Volume in Honor of Dolomieu. Spec. Publ.-Int. Assoc. Sedimentol. vol. 21. Blackwell Scientific Publications, Cambridge, pp. 155–166.
Mullins, H.T., Dix, G.R., Gardulski, A.F., Land, L.S., 1988. Neogene deep-water dolomite from the Florida–Bahamas Platform. In: Shukla, V., Baker, P.A. (Eds.), Sedimentology and Geochemistry of Dolostones, Based on a Symposium. Spec. Publ.-SEPM vol. 43, pp. 235–243.
Murray, R.C., 1960. Origin of porosity in carbonate rocks. J. Sediment. Petrol. 30, 59–84.
Murray, R.C., 1969. Hydrology of South Bonaire, Netherlands Antilles; a rock selective dolomitization model. J. Sediment. Petrol. 39, 1007–1013.
Müller, S., Teitz, G., 1971. Dolomite replacing “cement A” in biocalcarenites from Fuerteventura, Canary Islands, Spain. In: Bricker, D.P. (Ed.), Carbonate Cements. John Hopkins Press, Baltimore, 376.
Nesbitt, B.E., Muehlenbachs, K., 1994. Paleohydrology of the Canadian Rockies and origins of brines, Pb–Zn deposits and dolomitization in the Western Canada Sedimentary Basin. Geology 22, 243–246.
Nesbitt, B.E., Prochaska, W., 1998. Solute chemistry of inclusion fluids from sparry dolomites and magnesites in Middle Cambrian carbonat rocks of the southern Canadian Rocky Mountains. Can. J. Earth Sci. 35 (5), 546–555.
Nicolaides, S., 1995. Origin and modification of Cambrian dolomites (Red Heart Dolomite and Arthur Creek Formation), Georgina Basin, central Australia. Sedimentology 42 (2), 249–266.
Nielsen, P., Swennen, R., Dickson, J.A.D., Fallick, A.E., Keppens, E., 1997. Spheroidal dolomites in a Visean karst system — bacterial induced origin. Sedimentology 44 (1), 177–195.
Ohde, S., Kitano, Y., 1981. Protodolomite in Daito-jima, Okinawa. Geochem. J. 15, 199–207.
Oliver, J., 1986. Fluids expelled tectonically from orogenic belts: their role in hydrocarbon migration and other geologic phenomena. Geology 14, 99–102.
Patterson, R.J., Kinsman, D.J.J., 1981. Hydrologic framework of a sabkha along the Arabian Gulf. Am. Assoc. Petrol. Geol. Bull. 65, 1457–1475.
Patterson, R.J., Kinsman, D.J.J., 1982. Formation of diagenetic dolomite in coastal sabkhas along the Arabian (Persian) Gulf. Am. Assoc. Petrol. Geol. Bull. 66, 28–43.
Peryt, T.M., Scholle, P.A., 1996. Regional setting and role of meteoric water in dolomite formation and diagenesis in an evaporite basin; studies in the Zechstein (Permian) deposits of Poland. Sedimentology 43 (6), 1005–1023.
Peterson, J.A., 1983. Petroleum geology and resources of southeastern Mexico, northern Guatemala, and Belize. Geol. Surv. Circ. (U. S.) 760, 44 pp.
Peterson, J.A., 1992. Aneth field — USA Paradox basin, Utah. In: Foster, N.H., Beaumont, E.A. (Eds.), Stratigraphic Traps III: AAPG Treatise of Petroleum Geology, Atlas of Oil and Gas Fields. pp. 41–81.
Petta, T.J., Rapp, S.D., 1990. Appleton field — USA Gulf of Mexico basin, Alabama. In: Beaumont, E.A., Foster, N.H. (Eds.), Structural Traps IV: AAPG Treatise of Petroleum Geology, Atlas of Oil and Gas Fields. pp. 299–318.
Pilkey, O.H., 1966. Carbonate and clay mineralogy of the Persian Gulf. Deep Sea Res. 13, 1–16.
Phipps, G.G., 1989. Exploring for dolomitized Slave Point carbonates in northeastern British Columbia. Geophysics 54, 806–814.
Powers, R.W., 1962. Arabian Upper Jurassic carbonate reservoirs. In: Ham, W.E. (Ed.), Classification of Carbonate Rocks. AAPG Mem. pp. 122–192.

Purvis, K., 1989. Zoned authigenic magnesites in the Rotliegend Lower Permian, southern North Sea. Sediment. Geol. 65 (3–4), 307–318.

Qing, H., Mountjoy, E.W., 1994a. Formation of coarsely crystalline, hydrothermal dolomite reservoirs in the Presquile Barrier, Western Canada Sedimentary Basin. Am. Assoc. Petrol. Geol. Bull. 78 (1), 55–77.

Qing, H.U., Mountjoy, E.W., 1994b. Rare earth element geochemistry of dolomites in the Middle Devonian Presqu'ile barrier, Western Canada Sedimentary Basin: implications for fluid-rock ratios during dolomitization. Sedimentology 41 (4), 787–804.

Qing, H., Mountjoy, E.W., 1994c. Origin of dissolution vugs, caverns, and breccias in the Middle Devonian Presqu'ile barrier, host of Pine Point Mississippi Valley-type deposits. Econ. Geol. 89 (4), 858–876.

QGPC (Qatar General Petroleum Corporation and Amoco Qatar Petroleum Company), 1991. Dukhan field. In: Foster, N.H., Beaumont, E.A. (Eds.), Structural Traps V: AAPG Treatise of Petroleum Geology, Atlas of Oil and Gas Fields. pp. 103–120.

Radke, B.M., Mathis, R.L., 1980. On the formation and occurrence of saddle dolomite. J. Sediment. Petrol. 50 (4), 1149–1168.

Raiswell, R., 1982. Pyrite texture, isotopic composition and the availability of iron. Am. J. Sci. 282 (8), 1244–1263.

Ramsey, D.W., Onasch, C.M., 1999. Fluid migration in a cratonic setting: the fluid histories of two fault zones in the eastern midcontinent. Tectonophysics 305 (1–3), 307–323.

Randell, M.W., 1994. Geology of the Polaris Pb–Zn Mississippi Valley-Type deposit, Canadian Arctic Archipelago. Doctoral thesis, University of Toronto (Canada).

Reeder, R.J., 1981. Electron optical investigation of sedimentary dolomites. Contrib. Mineral. Petrol. 76, 148–157.

Reeder, R.J., 1983. Crystal chemistry of rhombohedral carbonates. Mineral. Soc. Am.: Rev. Mineral. 11, 1–48.

Reeder, R.J., Prosky, J.L., 1986. Compositional sector zoning in dolomite. J. Sediment. Petrol. 56, 237–247.

Reeder, R.J., Sheppard, C.E., 1982. Variation of lattice parameters in some sedimentary dolomite. Am. Mineral. 69, 520–527.

Reinhold, C., 1998. Multiple episodes of dolomitization and dolomite recrystallization during shallow burial in Upper Jurassic shelf carbonates: eastern Swabian Alb, southern Germany. Sediment. Geol. 121 (1–2), 71–95.

Riviere, A., 1939. Sur la dolomitization des sediments calcaires. Comptes Rendus 209, 597–599.

Rizzi, G., Braithwaite, C.J.R., 1997. Sedimentary cycles and selective dolomitization in limestones hosting the giant Navan Pb–Zn ore deposit, Ireland. Explor. Min. Geol. 6 (1), 63–77.

Rodgers, K.A., Easton, A.J., Downes, C.J., 1982. The chemistry of carbonate rocks of Niue Island, South Pacific. J. Geol. 90, 645–662.

Roedder, E.S., 1984. Fluid inclusions. Mineral. Soc. Am.: Rev. Mineral. 12, 646 pp.

Roehl, P.O., 1985. Depositional and diagenetic controls on reservoir rock development and petrophysics in Silurian tidalites, Interlake Formation, Cabin Creek field area, Montana. In: Roehl, P.O., Choquette, P.W. (Eds.), Carbonate Petroleum Reservoirs. Springer, New York, pp. 85–105.

Roehl, P.O., Weinbrandt, R.M., 1985. West Cat Canyon Field. In: Roehl, P.O., Choquette, P.W. (Eds.), Carbonate Petroleum Reservoirs. Springer, New York, pp. 525–545.

Rosen, M.R., Miser, D.E., Warren, J.K., 1988. Sedimentology, mineralogy and isotopic analysis of Pellet Lake, Coorong region, South Australia. Sedimentology 35 (1), 105–122.

Rosen, M.R., Miser, D.E., Starcher, M.A., Warren, J.K., 1989. Formation of dolomite in the Coorong region, South Australia. Geochim. Cosmochim. Acta 53 (3), 661–669.

Rougerie, F., Wauthy, B., 1988. The endo-upwelling concept: a new paradigm for solving an old paradox. Proceedings of the Sixth International Reef Symposium — Australia. pp. 1–6.

Runnells, D.D., 1969. Diagenesis, chemical sediments, and the mixing of natural waters. J. Sediment. Petrol. 39, 1188–1201.

Ruppel, S.C., Cander, H.S., 1988. Dolomitization of shallow water carbonates by seawater and seawater-derived brines, San Andres Formation (Guadalupian), West Texas. In: Shukla, V.J., Baker, P.A. (Eds.), Sedimentology and Geochemistry of Dolostones. Spec. Publ.-SEPM vol. 43, pp. 245–262.

Ruzla, K., Friedman, G.M., 1985. Factors controlling porosity in dolomite reservoirs of the Ordovician Red River Formation, Cabin Creek field, Montana. In: Roehl, P.O., Choquette, P.W. (Eds.), Carbonate Petroleum Reservoirs. Springer, New York, pp. 39–58.

Saller, A.H., 1984. Petrologic and geochemical constraints on the origin of subsurface dolomite, Enewetak Atoll; an example of dolomitization by normal seawater. Geology 12 (4), 217–220.

Saller, A.H., Van Hoorn, D., Miller, J.A., Guy, B.T., 1991. Reservoir geology of Devonian carbonates and chert — implications for Tertiary recovery, Dollarhide field, Andrews County, Texas. Am. Assoc. Petrol. Geol. Bull. 75, 86–107.

Saller, A.H., Henderson, N., 1998. Distribution of porosity and permeability in platform dolomites — insight from the Permian of west Texas. Am. Assoc. Petrol. Geol. Bull. 82 (8), 1528–1550.

Sangster, D.F., Nowlan, G.S., McCracken, A.D., 1994. Thermal comparison of Mississippi Valley-Type lead–zinc deposits and their host rocks using fluid inclusion and conodont alteration index data. Econ. Geol. 89 (3), 493–514.

Santiago, J., Baro, A., 1992. Mexico's giant fields, 1978–1988 decade. In: Halbouty, M.T. (Ed.), Giant Oil and Gas Fields of the Decade 1978–1988. AAPG Mem. pp. 73–99.

Sass, E., Bein, A., 1988. Dolomites and salinity; a comparative geochemical study. In: Shukla, V., Baker, P.A. (Eds.), Sedimentology and geochemistry of dolostones, based on a symposium. Spec. Publ.-SEPM vol. 43, pp. 223–233.

Savard, M.M., 1996. Pre-ore burial dolomitization adjacent to the carbonate-hosted Gays River Zn–Pb deposit, Nova Scotia. Can. J. Earth Sci. 33 (2), 302–315.

Schmidt, V., McIlreath, I.A., Budwill, A.E., 1985. Origin and diagenesis of Middle Devonian pinnacle reefs encased in evaporites, "A" and "E" pools, Rainbow field, Alberta. In: Roehl, P.O., Choquette, P.W. (Eds.), Carbonate Petroleum Reservoirs. Springer, New York, pp. 141–160.

Schmoker, J.W., Krystinik, K.B., Halley, R.B., 1985. Selected characteristics of limestone and dolomite reservoirs in the United States. Am. Assoc. Petrol. Geol. Bull. 69 (5), 733–741.

Schramm, M.W., Livraga, G., 1986. Vega field and the potential of the Ragusa Basin, offshore Sicily. In: Halbouty, M.T. (Ed.), Future Petroleum Provinces of the World. AAPG Mem. pp. 559–566.

Schreiber, B.C., 1988. Evaporites and Hydrocarbons. Columbia University Press, New York, 475 pp.

Sears, S.O., Lucia, F.J., 1980. Dolomitization of Northern Michigan Niagara Reefs by Brine Refluxion and Freshwater/Seawater Mixing. Spec. Publ.-SEPM vol. 28, pp. 215–235.

Shields, M.J., Brady, P.V., 1995. Mass balance and fluid flow constraints on regional-scale dolomitization, Late Devonian, Western Canada Sedimentary Basin. Bull. Can. Petrol. Geol. 43 (4), 371–392.

Shikazono, N., Hoshino, M., Utada, M., Nakata, M., Ueda, A., 1998. Hydrothermal carbonates in altered wall rocks at the Uwamuki Kuroko deposits, Japan. Mineral. Deposita 33 (4), 346–358.

Shinn, E.A., 1983. Tidal flat environment. AAPG Mem. 33, 173–310.

Sibley, D.F., 1980. Climatic control of dolomitization, Seroe Domi Formation (Pliocene), Bonaire, N.A. In: Zenfger, D.H., Dunham, J.B., Ethington, R.L. (Eds.), Concepts and Models of Dolomitization. Spec. Publ.-SEPM vol. 28, pp. 247–258.

Sibley, D.F., Gregg, J.M., 1987. Classification of dolomite rock textures. J. Sediment. Petrol. 57, 967–975.

Sibley, D.F., Nordeng, S.H., Borkowski, M.L., 1994. Dolomitization kinetics in hydrothermal bombs and natural settings. J. Sediment. Res., Sect. A 64 (3), 630–637.

Sieverding, J.L., Royse, F., 1990. Whitney Canyon — Carter Creek field — USA western Wyoming thrust belt, Wyoming. In: Beaumont, E.A., Foster, N.H. (Eds.), Stratigraphic Traps III: AAPG Treatise of Petroleum Geology, Atlas of Oil and Gas Fields. pp. 1–29.

Simms, M., 1984. Dolomitization by groundwater — flow systems in carbonate platforms. Trans. Gulf Coast Assoc. Geol. Soc. XXXIV, 411–420.

Skall, H., 1975. The paleoenvironment of the Pine Point lead–zinc district. Econ. Geol. 70 (1), 22–47.

Skeats, E.W., 1905. The chemical and mineralogical evidence as to the origin of dolomites of southern Tyrol. Q. J. Geol. Soc. London 61, 97–141.

Skinner, H.C.W., 1963. Precipitation of calcian dolomites and magnesian calcites in the southeast of South Australia. Am. J. Sci. 261, 449–472.

Smith, D.B., 1981. The magnesian Limestone (Upper Permian) reef complex of northeastern England. Spec. Publ.-SEPM 30, 187–202.

Spencer, R.J., Hardie, L.A., 1990. Contol of seawater composition by mixing of river waters and mid-ocean ridge hydrothermal brines. In: Spencer, R.J., Chou, I.M. (Eds.), Fluid Mineral Interactions: A Tribute to H.P. Eugster. Geochem. Soc. Spec. Publ. vol. 2, pp. 409–419.

Sperber, C.M., Wilkinson, B.H., Peacor, D.R., 1984. Rock composition, dolomite stoichiometry and rock/water reactions in dolomitic carbonate rocks. J. Geol. 92, 609–622.

Spotl, C., Wright, V.P., 1992. Groundwater Dolocretes from the Upper Triassic of the Paris Basin, France — a case study of an arid, continental diagenetic facies. Sedimentology 39 (6), 1119–1136.

Steidtmann, E., 1926. The origin of dolomites. In: Twenhofel, W.H. (Ed.), Treatise on Sedimentation. Williams and Wilkins, Baltimore, MD, pp. 256–265.

Strakhov, N.M., 1958. Facts and hypotheses in the problem of the formation of dolomite rocks. Izv. Akad. Nauk S.S.S.R. Ser. Geol. 6, 3–22.

Suchy, V., Rozkosny, I., Zak, K., Francu, J., 1996. Epigenetic dolomitization of the Pridoli Formation (Upper Silurian), the Barrandian Basin, Czech Republic — implications for burial history of Lower Palaeozoic strata. Geol. Rundsch. 85 (2), 264–277.

Suess, E., von Huene, R., Emeis, K.-C., Bourgois, J., Cruzado Castaneda, J.d.C., De Wever, P., Eglinton, G., Fernandez, A.W.S., Garrison, R., Greenberg, M., Hill, P.R., Ibaraki, M., Kastner, M., Kemp, A.E.S., Kvenvolden, K.A., Langridge, R., Lindsley-Griffin, N., McCabe, R., Marsters, J., Martini, E., Ocola, L., Paz, E.H., Resig, J., Schrader, H.-J., Thornburg, T.M., Yamano, M., 1988. Ocean Drilling Program Leg 112, Peru continental margin: Part 2. Sedimentary history and diagenesis in a coastal upwelling environment. Geology 16 (10), 939–943.

Sun, S.Q., 1994. A reappraisal of dolomite abundance and occurrence in the Phanerozoic. J. Sediment. Res., Sect. A 64 (2), 396–404.

Sun, S.Q., 1995. Dolomite reservoirs; porosity evolution and reservoir characteristics. Am. Assoc. Petrol. Geol. Bull. 79 (2), 186–204.

Sun, S.Q., Esteban, M., 1994. Paleoclimatic controls on sedimentation, diagenesis, and reservoir quality — lessons from Miocene carbonates. Am. Assoc. Petrol. Geol. Bull. 78 (4), 519–543.

Taylor, T.R., Sibley, D.F., 1986. Petrographic and geochemical characteristics of dolomite in the Trenton Formation, Ordovician, Michigan Basin. Sedimentology 33, 61–86.

Teisserene, P., Villemin, J., 1989. Sedimentary basin of Gabon — geology and oil systems. In: Edwards, J.D., Santogrossi, P.A. (Eds.), Divergant/Passive Margin Basins. AAPG Mem. vol. 48, pp. 117–199.

Thompson, T.B., 1998. Geology and geochemistry of the Kokomo Mining District, Colorado. Econ. Geol. 93 (5), 617–638.

Tompkins, L.A., Rayner, M.J., Groves, D.I., Roche, M.T., 1994. Evaporites; in situ sulfur source for rhythmically banded ore in the Cadjebut Mississippi Valley-type Zn–Pb deposit, Western Australia. Econ. Geol. 89 (3), 467–492.

Tucker, M., Wright, V.P., 1990. Carbonate Sedimentology. Blackwell Scientific Publications, Oxford, 482 pp.

Vahrenkamp, V.C., Swart, P.K., 1994. Late Cenozoic dolomites of the Bahamas: metastable analogues for the genesis of ancient platform dolomites. In: Purser, B., Tucker, M., Zenger, D. (Eds.), Dolomites — A Volume in Honor of Dolomieu. Spec. Publ.-Int. Assoc. Sedimentol. vol. 21, pp. 133–153.

Vasconcelos, C., Mackenzie, J.A., 1997. Microbial mediation of modern dolomite precipitation and diagenesis under anoxic conditions (Lagoa Vermelha, Rio de Janeiro, Brazil). J. Sediment. Res., Sect. A 67 (3), 378–390, (Part A).

Vasconcelos, C., Mackenzie, J.A., Bernasconi, S., Grujic, D., Tien, A.J., 1995. Microbial mediation as a possible mechanism for natural dolomite formation at low temperatures. Nature 377 (6546), 220–222.

Veizer, J., 1983. Trace elements and isotopes in sedimentary carbonates. In: Reeder, R.J. (Ed.), Carbonates: Mineralogy and Chemistry. Mineral. Soc. Am.: Rev. Mineral. vol. 11, pp. 265–300.

Van Tuyl, F.M., 1918. Depth of dolomitization. Science 48, 350–352.

von der Borch, C.C., 1965. Source of ions for Coorong dolomite formation. Am. J. Sci. 684–688.

Von der Borch, C.C., 1976. Stratigraphy and formation of Holocene dolomitic carbonate deposits of the Coorong area, South Australia. J. Sediment. Petrol. 46 (4), 952–966.

Von der Borch, C.C., Lock, D., 1979. Geological significance of the Coorong dolomites. Sedimentology 26, 813–824.

Von der Borch, C.C., Lock, D., Schwebel, D., 1975. Ground-water formation of dolomite in the Coorong region of South Australia. Geology 3, 283–285.

Von Morlot, A., 1847. Uber die dolomit und seine kunstliche darstellung aus kalkstein. Haidinger Naturwiss, Abhandl. 1, 305.

Wallace, M.W., 1990. Origin of dolomitization on the Barbwire Terrace, Canning Basin, Western Australia. Sedimentology 37, 105–122.

Ward, W.C., Halley, R.B., 1985. Dolomitization in a mixing zone of near-seawater composition, Late Pleistocene, Northeastern Yucatan Peninsula. J. Sediment. Petrol. 55, 407–420.

Wardlaw, N.C., 1976. Pore geometry of carbonate rocks as revealed by pore casts and capillary pressure. Am. Assoc. Petrol. Geol. Bull. 60 (2), 245–257.

Wardlaw, N.C., Cassan, J.P., 1978. Estimation of recovery efficiency by visual observation of pore systems in reservoir rocks. Bull. Can. Petrol. Geol. 26 (4), 572–585.

Wardlaw, N.C., Taylor, R.P., 1976. Mercury capillary pressure curves and the interpretation of pore structure and capillary behaviour in reservoir rocks. Bull. Can. Petrol. Geol. 24 (2), 225–262.

Wardlaw, N.C., McKellar, M., Yu, L., 1988. Pore and throat size distributions determined by mercury porosimetry and by direct observation. Carbonates Evaporites 3 (1), 1–15.

Warren, J.K., 1988. Sedimentology of Coorong dolomite in the Salt Creek region, South Australia. Carbonates Evaporites 3 (2), 175–199.

Warren, J.K., 1989. Evaporite Sedimentology: Importance in Hydrocarbon Accumulation. Prentice-Hall, Englewood Cliffs, NJ, 285 pp.

Warren, J.K., 1990. Sedimentology and mineralogy of dolomitic Coorong lakes, South Australia. J. Sediment. Petrol. 60 (6), 843–858.

Warren, J.K., 1991. Sulfate dominated sea-marginal and platform evaporative settings. In: Melvin, J.L. (Ed.), Evaporites, Petroleum and Mineral Resources. Dev. Sedimentol. vol. 50. Elsevier, Amsterdam, pp. 477–533.

Warren, J.K., 1999. Evaporites: Their Evolution and Economics. Blackwell Scientific Publications, Oxford, 438 pp.

Warren, J.K., Kendall, C.G.St.C., 1985. Comparison of sequences formed in marine sabkha (subaerial) and salina (subaqueous) settings; modern and ancient. Am. Assoc. Petrol. Geol. Bull. 69 (6), 1013–1023.

Warren, J.K., Kempton, R.H., 1997. Evaporite Sedimentology and the Origin of Evaporite-Associated Mississippi Valley-type Sulfides in the Cadjebut Mine Area, Lennard Shelf, Canning Basin, Western Australia. In: Montanez, I.P., Gregg, J.M., Shelton, K.L. (Eds.), Basinwide Diagenetic Patterns: Integrated Petrologic, Geochemical, and Hydrologic Considerations. Spec. Publ.-SEPM vol. 57, pp. 183–205.

Watson, H.J., 1982. Casablanca field offshore Spain: a paleogeographic trap. In: Halbouty, M.T. (Ed.), The Deliberate Search for the Subtle Trap. AAPG Mem. vol. 32, pp. 237–250.

Watts, N.R., Coppold, M.P., Douglas, J.L., 1994. Application of reservoir geology to enhanced oil recovery from Upper Devonian Nisku Reefs, Alberta, Canada. Am. Assoc. Petrol. Geol. Bull. 78 (1), 78–101.

Wells, A.J., 1962. Recent dolomite in the Persian Gulf. Nature 194, 274–275.

Wenk, H.R., Barber, D.J., Reeder, R.J., 1983. Microstructures in carbonates. Mineral. Soc. Am.: Rev. Mineral. 11, 261–301.

Wenk, H.R., Hu, M., Frisia, S., 1993. Partially disordered dolomite: microstructural characterization of Abu Dhabi sabkha carbonates. Am. Mineral. 78 (7–8), 769–774.

Weyl, P.K., 1960. Porosity through dolomitization:conservation of mass requirements. J. Sediment. Petrol. 30, 85–90.

Whitaker, F.F., Smart, P.L., Vahrenkamp, V.C., Nicholson, H., Wogelius, R.A., 1994. Dolomitization by near-normal seawater? Field evidence from the Bahamas. In: Purser, B., Tucker, M., Zenger, D. (Eds.), Dolomites — A Volume in Honor of Dolomieu. Spec. Publ.-Int. Assoc. Sedimentol. vol. 21. Blackwell Scientific Publications, Cambridge, pp. 111–132.

Whittaker, S.G., Mountjoy, E.W., 1996. Diagenesis of an Upper Devonian carbonate–evaporite sequence: Birdbear Formation, southern Interior Plains, Canada. J. Sediment. Res., Sect. A 66 (5), 965–975.

Wilson, A.O., 1985. Depositional and diagenetic facies in the Arab-C and -D reservoirs, Qatif field, Saudi Arabia. In: Roehl, P.O., Choquette, P.W. (Eds.), Carbonate Petroleum Reservoirs. Springer, New York, pp. 319–340.

Wilson, J.L., 1975. Carbonate Facies in Geologic History. Springer, Berlin, 471 pp.

Wilson, E.N., Hardie, L.A., Philips, O.M., 1990. Dolomitization from geometry, flow patterns, and the origin of massive dolomite: the Triassic Latemar buildup, northern Italy. Am. J. Sci. 290, 741–796.

Wojcik, K.M., Goldstein, R.H., Walton, A.W., 1994. History of diagenetic fluids in a distant foreland area, Middle and Upper Pennsylvanian, Cherokee Basin, Kansas, USA — Fluid inclusion evidence. Geochim. Cosmochim. Acta 58 (3), 1175–1191.

Wolfbauer, C.A., Surdam, R.C., 1974. Origin of non-marine dolomites Eocene Lake Gosiute, Green River Basin, Wyoming. Geol. Soc. Am. Bull. 85, 1733–1740.

Woody, R.E., Gregg, J.M., Koederitz, L.F., 1996. Effect of texture on the petrophysical properties of dolomite — evidence from the Cambrian–Ordovician of southeastern Missouri. Am. Assoc. Petrol. Geol. Bull. 80 (1), 119–132.

Wright, D.T., 1999. The role of sulphate-reducing bacteria and

cyanobacteria in dolomite formation in distal ephemeral lakes of the Coorong region, South Australia. Sediment. Geol. 126 (1–4), 147–157.

Xun, Z., Fairchild, I.J., 1987. Mixing zone dolomitization of Devonian carbonates, Guangxi, south China. In: Marshall, J.D. (Ed.), Diagenesis of Sedimentary Sequences. Spec. Publ.-Geol. Soc. London vol. 36, pp. 157–170.

Yang, B.X., 1986. Diagenetic history and reservoir characteristics of a Middle Carboniferous dolomite reservoir, eastern Sichuan, China. Sediment. Geol. 46, 275–291.

Yao, Q.J., Demicco, R.V., 1995. Paleoflow patterns of dolomitizing fluids and paleohydrology of the southern Canadian Rocky mountains — evidence from dolomite geometry and numerical modelling. Geology 23 (9), 7691–7694.

Ye, Q.C., Mazzullo, S.J., 1993. Dolomitization of Lower Permian platform facies, Wichita Formation, North Platform, Midland Basin. Carbonates Evaporites 8 (1), 55–70.

Yie, D.S., 1991. Diagenesis and reservoir characteristics of Cambrian through Early Ordovician dolomite in the northern Tarim basin. In: Jia, R.X. (Ed.), Petroleum Research in the Northern Tarim Basin, China: Part I. Stratigraphy and Sedimentology. China University Geosciences Press, Beijing, pp. 263–273.

Yie, D.S., Liu, S.H., 1991. Diagenesis and reservoir property of the Sinian Qigebulake Formation dolomite in northeast Tarim basin. In: Jia, R.X. (Ed.), Petroleum Research in the Northern Tarim Basin, China: Part I. Stratigraphy and Sedimentology. China University Geosciences Press, Beijing, pp. 247–255.

Yoo, C.M., Gregg, J.M., Shelton, K.L., 2000. Dolomitization and dolomite neomorphism: Trenton and Black River Limestones (Middle Ordovician) northern Indiana, USA. J. Sediment. Res., Sect. A 70 (1), 265–274.

Young, R.B., 1933. Conditions of deposition of the Dolomite Series. Trans. Geol. Soc. S. Afr. 36, 135–1221.

Zenger, D.H., 1996. Dolomitization patterns in the widespread Bighorn Formation (Upper Odovician), Western Craton, USA. Carbonates Evaporites 11 (2), 219–225.

Zenger, D.H., Dunham, J.B., Ethington, R.L., 1980. Concepts and models of dolomitization. Spec. Publ.-SEPM 28, 320 pp.

Zhai, G.M., Zha, Q.H., 1982. Buried hill oil and gas pools in the North China basin. In: Halbouty, M.T. (Ed.), The Deliberate Search for the Subtle Trap. AAPG Mem. vol. 32, pp. 317–335.

Zimmermann, H., 2000. On the origin of fluid inclusions in ancient halite — basic interpretation strategies. In: Geertmann, R.M. (Ed.), Salt 2000 — 8th World Salt Symposium vol. 1. Elsevier, Amsterdam, pp. 199–203.